

Characterization of a Ca^{2+} -activated K^+ channel
from skeletal muscle membranes in artificial
bilayers

A Thesis Presented

by

Cecilia Vergara

to

The Department of Physiology and Biophysics
in partial fulfillment of the requirements

for the degree of
Doctor of Philosophy

in the subject of

Physiology

Harvard University
Cambridge, Massachusetts

May, 1983

TABLE OF CONTENTS

Acknowledgements.....	i
List of Illustrations.....	ii
List of Tables.....	iv
Abbreviations.....	v
Summary.....	vi
Chapter 1 Introduction.....	1
Chapter 2 Materials and Methods.....	45
Chapter 3 Results: Channel Gating.....	53
Chapter 4 Results: Channel Selectivity.....	79
Chapter 5 Results: Channel Conduction.....	89
Chapter 6 Results: Channel Blockade.....	95
Chapter 7 General Discussion.....	149
References.....	160

ACKNOWLEDGEMENTS

I thank very very specially Ramon Latorre and Juan Bacigalupo for their patience, help and support during all these years. Also I thank Juan Reyes, Dale Benos, Magdalena Tosteson, Martin Kushmerick, Elwood Henneman, Edward Moczydlowski, Roberto Coronado, Christopher Miller, Cecilia Hidalgo, Mario Roseblatt, Elena Gonzales and so many others for their support and help during different stages of this project.

I also thank the Division of Medical Sciences for financial support and Marianita Sanchez for her invaluable help on typing this thesis.

List of Illustrations

Figure	page
1 Diagram of a skeletal muscle cell.....	10
2 S kematic energy profiles for transmembrane ion permeation...	21 /ch
3 Relationship between applied voltage, energy profiles and current-voltage curve.....	22
4 Experimental protocol.....	49
5 Channel incorporation.....	51
6 Macroscopic current-voltage curve.....	54
7 Ca^{2+} dependence of macroscopic current.....	56
8 Effect of Ca^{2+} and Mg^{2+} on the macroscopic current-voltage curve.....	57
9 Effect of Ca^{2+} and Mg^{2+} on the macroscopic conductance-voltage curve	59
10 Single channel current fluctuations: fast and slow kinetics.....	61
11 Single channel current-voltage curve.....	62
12 Single channel current fluctuations at different membrane potentials	63
13 Single channel current fluctuations at different $[Ca^{2+}]$	65
14 Fraction of open time as a function of potential and $[Ca^{2+}]$.	66
15 Open-closed equilibrium as a function of $[Ca^{2+}]$	68
16 Mean open and mean closed times as a function of potential and $[Ca^{2+}]$	69
17 Channel activation by Cd^{2+}	71
18 Effect of K^+ on channel gating.....	73
19 K^+ over Cl^- selectivity determined by reversal potentials....	80
20 Single channel current-voltage curves under biionic conditions between K^+ and Li^+ , Na^+ , Rb^+ and NH_4^+	82

Figure	page
21 Current-voltage curves for two different channels under biionic conditions between K^+ and Tl^+	84
22 Conductance-activity curve.....	91
23 Effect of <u>cis</u> and <u>trans</u> TEA on macroscopic currents.....	97
24 Effect of <u>cis</u> and <u>trans</u> TEA on single channel conductance..	98
25 Voltage dependence of <u>cis</u> and <u>trans</u> TEA block.....	100
26 Channel blockade by C_9	103
27 Effect of Tris on single channel conductance.....	106
28 Effect of Ca^{2+} and potential on slow channel kinetics.....	108
29 Burst and "slow" closed dwell time distributions.....	113
30 Potential and $[Ca^{2+}]$ dependence of the slow kinetics induced by Ca^{2+}	115
31 Frequency of slow closing events as a function of $[K^+]$	119
32 Effect of <u>cis</u> Ba^{2+} and potential on the slow channel kinetics.....	122
33 Effect of <u>trans</u> Ba^{2+} on the slow channel kinetics.....	124
34 Dependence of the unconditional mean burst and mean slow closed times on $[Ba^{2+}]$	129
35 Potential dependence of the unconditional mean burst and mean slow closed times.....	130
36 Competition of <u>cis</u> Ba^{2+} and K^+ ions for the blocking site..	134
37 K^+ and Ba^{2+} acts as competitive inhibitors.....	135
38 Effect of symmetric $[K^+]$ on the Ba^{2+} induced slow kinetics.	137
39 Effect of <u>trans</u> $[K^+]$ and potential on the Ba^{2+} induced slow kinetics.....	138
40 Open state probability for channels inserted into PE or PS membranes.....	152
41 Approximate energy profile for the interaction of Ba^{2+} and Ca^{2+} with the channel.....	158

List of Tables

Table		page
1	Mean dwell times for the different Ca^{2+} activated channel kinetic processes.	114
2	Kinetic and equilibrium characteristics of the Ca^{2+} and Ba^{2+} induced "slow" process.	118

ABBREVIATIONS

Ach	:	acetylcholine
ATP	:	adenosinetriphosphate
C ₉	:	triethylnonylammonium
EGTA	:	ethyleneglycol-bis-(γ -amino-ethyl ether)N,N' tetraacetic acid
I _A	:	inactivating potassium currents
I _{Ca}	:	calcium currents
I _K	:	potassium currents
I _{K,Ca}	:	calcium activated potassium currents
I _{Na}	:	sodium currents
I-V	:	current-voltage
MOPS	:	4-morpholinepropanesulfonic acid
PE	:	phosphatidylethanolamine
PS	:	phosphatidylserine
QA	:	quaternary ammonium
SDS	:	sodium dodecylsulfate
SR	:	sarcoplasmic reticulum
STX	:	saxotoxin
TEA	:	tetraethylammonium
TT	:	transverse tubule
TTX	:	tetrodotoxin

SUMMARY

Ca^{2+} -activated K^+ channels of large unitary conductance have been identified in several different types of cells. These channels play an important role in widely different physiological functions ranging from repetitive activity to hormone secretion. In order to study this channel in a simplified, cell free system, I have incorporated it into planar lipid bilayer membranes. Incorporation occurs after the interaction of striated rabbit muscle membrane vesicles of transverse tubule (TT) origin with the planar bilayer. After addition of TT vesicles, the membrane conductance increases in steps of 230 pS in 0.1 M KCl. Each step corresponds to the incorporation of one channel.

The many-channel conductance is both voltage and $[\text{Ca}^{2+}]$ dependent. At 1 mM Ca^{2+} , the steady state conductance is maximal at voltages higher than +20 mV and decreases for more negative voltages. (Voltages refer to the side to which the vesicles are added, cis side. Trans side is virtual ground.) Decreasing the $[\text{Ca}^{2+}]$ reversibly shifts the macroscopic conductance-voltage curve towards the right along the voltage axis. Furthermore, Ca^{2+} activates the conductance only if added to the cis side. Single channel activity appears in bursts followed by periods when the channel remains quiescent. Ca^{2+} and voltage modify the fraction of time that the channel remains open in a manner that parallels the voltage and Ca^{2+} dependence of the multi-channel membrane. The Ca^{2+} dependence of the open-closed equilibrium indicates that at least two Ca^{2+} are necessary to fully activate a channel. Furthermore, the fact that both the mean open

and mean closed times are $[Ca^{2+}]$ dependent indicates that the minimal kinetic scheme able to explain the channel gating kinetics must consist of two closed and two open states. The channels are also activated by Cd^{2+} , but not by Mg^{2+} , Ba^{2+} or Sr^{2+} .

The channel completely excludes anions and shows a selectivity sequence $Tl^+ > K^+ > Rb^+$, Cs^+ , NH_4^+ , Na^+ , Li^+ . Actually Rb^+ , Cs^+ , Na^+ , and Li^+ block the channel. In neutral bilayers, the channel conductance saturates with K^+ ion activity. However it markedly deviates from a Langmuir isotherm expected for single ion channels. The data can be fitted by assuming the existence of two binding sites in the ion conduction pathway. A high affinity binding site with an apparent dissociation constant (K_d) of 3 mM and a low affinity site with a K_d of 80 mM. At low (50 mM) K^+ activities, channel conductance is higher in negatively charged membranes. This result suggests that the ion conduction pathway senses part of the surface potential induced by the negatively charged phospholipids.

The Ca^{2+} -activated K^+ channel is blocked by addition of tetraethylammonium (TEA) ions either to the cis or trans side. In both cases TEA block induces a reduction in channel conductance suggesting that the blocking process is much faster than the gating process. Trans and cis TEA blockade have different characteristics. Trans blockade is characterized by a K_d of 0.29 mM and is voltage independent whereas cis blockade is voltage dependent and the K_d at zero volts is 45 mM. Conversely, triethylnonylammonium (C_9) blocks the channel more efficiently from the cis than from the

trans side. The K_d for cis blockade is about $4 \mu\text{M}$, whereas from the trans side $300 \mu\text{M}$ Ca^{2+} only reduces the channel conductance by about 12%. Ba^{2+} and Ca^{2+} induce a voltage-dependent blockade that is slower than channel gating and is competitive with K^+ . This slow Ca^{2+} blockade gives origin to the quiescent periods mentioned above.

From these results I conclude that the channel incorporates asymmetrically into the planar lipid bilayer. The cis side corresponds to the cytoplasmic channel side. The TEA results together with the selectivity and conductance characteristics of the channel suggest that it has a wide "mouth" at the cis and trans side connected by a narrow region where selectivity and probably Ba^{2+} and Ca^{2+} blockade takes place. I also discuss several alternative models that may account for the channel activation by Ca^{2+} .

CHAPTER I

INTRODUCTION

General

Many cells respond to external stimuli with a change in membrane potential. Depending on the cell type, the response can be a propagated action potential, a receptor potential, a synaptic potential, a fertilization potential, a pacemaker potential or the response can be coupled to the release of neurotransmitter and/or hormones. All of these cellular signals play an important role in the integrated responses of the whole cell or organism. For example, a fertilization potential in the oocyte signals the initiation of many different biochemical changes that prevent the entry of more sperms as well as trigger the metabolic activity required for subsequent development. Therefore, the understanding of how these electrical signals are generated and how they can be modulated become important issues in physiology.

The mechanism of conduction of action potentials in squid giant axons was the first of these processes studied and understood in some detail (Hodgkin and Huxley, 1952d). The studies of Hodgkin, Huxley and Katz (Hodgkin and Katz, 1949; Hodgkin et al., 1952; Hodgkin and Huxley, 1952a-d) clearly demonstrated that voltage dependent changes in membrane permeability for Na^+ and K^+ ions are responsible for the generation of the action potential. With the help of the voltage clamp technique developed by Cole and Marmont (Cole, 1949; Marmont, 1949), they showed that depolarizing potentials turn on two different currents: first, an

inward (depolarizing) current carried mainly by Na^+ ions that inactivates with time, and second, with some delay after the turn on of the depolarization, an outward (repolarizing) current carried mainly by K^+ ions. They proposed that the Na^+ and K^+ voltage dependent permeabilities originated from two independent and highly selective conductance pathways. This suggestion was later supported by pharmacological means. Thus, Narahashi et al. (1964) showed that the drug tetrodotoxin (TTX) was able to block completely the sodium currents while leaving the potassium currents untouched. On the other hand, Armstrong and Binstock (1965) demonstrated that tetraethylammonium (TEA) ions, when applied to the internal surface of an axon membrane, block the outward K^+ currents with no effect on inward Na^+ currents.

The excitable properties of different types of cells were modeled according to Hodgkin and Huxley kinetic schemes for several years after the origin of the action potential mechanism in squid axons was elucidated. Only Na^+ and K^+ conductance pathways with the general characteristics of those of squid were considered, and their kinetics were modified until the right shape for the action potential from each cell type was obtained. However, Hagiwara et al. (1961) discovered a kinetically different type of K^+ conductance in the neurones of the mollusc Onchidium. They found that under voltage clamp conditions these cells presented Na^+ and K^+ currents (I_{Na} and I_{K}) of the Hodgkin and Huxley type but in addition there was an early outward K^+ current that became inactivated soon after a depolarizing step. Later, inactivating K^+ currents have been described in many different cell types including vertebrate and invertebrate neurones; they have an important role in determining repetitive firing in all those cells where it has been found

(see review by Connor, 1980). In 1970, a third type of K^+ conductance was described by Meech and Strumwasser in Aplysia neurons. This K^+ conductance is activated by an increase in the intracellular $[Ca^{++}]$ and depolarizing membrane potentials and has been named $I_{K,Ca}$. In neurons and in myotubes, $I_{K,Ca}$ is probably involved in the regulation of repetitive activity (Meech and Standen, 1975; Barret et al., 1981).

Different types of depolarizing currents have also been discovered. Oomura et al. (1961) found that Ca^{++} ions carry the inward currents in the cell body of a snail neuron (see also Hagiwara et al., 1961). Later work has shown that many different cells present Ca^{++} or combinations of Ca^{++} and Na^+ depolarizing currents. From their voltage dependence, kinetics of activation and pharmacology, it has become clear that different kinds of Ca^{++} conductance pathways exist (Hagiwara, 1980; Hagiwara and Byerly, 1981). All the conductances that I have mentioned display one common characteristic, namely, they are turned on by changes in membrane potential, although the exact dependence on voltage and kinetics of activation are peculiar to each type of conductance pathway.

Simultaneous to the discovery of the voltage dependent mechanism of action potential generation, Fatt and Katz (1951) proposed a different mechanism for triggering changes in membrane permeability. They studied the changes in post synaptic membrane potential triggered by the release of acetylcholine (ACh) in the frog neuromuscular junction. To explain their findings they proposed that the post synaptic membrane became permeable to Na^+ , K^+ , Cl^- and possibly other ions after the binding of ACh independent of the value of the membrane potential. Later work by Takeuchi and Takeuchi (1960) using the same preparation established that the conductance increase produced by ACh is specific for cations.

It soon became evident that increases in cation permeabilities were not the only response to neurotransmitter binding. The inhibitory potentials observed in some nerve cells and crustacean muscle fibers were shown to be produced by changes in the permeability of the post synaptic membrane to K^+ and/or Cl^- ions (Kuffler, 1960). Moreover, neurotransmitters can close conductance pathways that are open in resting conditions (Weight and Votava, 1970; Sigelbaum et al., 1982).

The Need For Channels

The original description of the action potential and synaptic potential mechanisms did not specify the nature of the conductance pathways. For some time ion movement was described as though the membrane were a homogeneous media; i.e., ion fluxes through the membrane were described by the general flux equations describing ion movement along a concentration gradient and a constant electric field (Mullins, 1961). Nevertheless, a major difficulty in considering the membrane as a homogeneous medium is the large amount of energy needed to transfer an ion from the aqueous solution surrounding the membrane into the core of the lipid bilayer, a region of low dielectric constant (Bokris and Reddy, 1970). Parsegian (1969) calculated that approximately 40 kcal/mol are needed to transfer an ion of 2 \AA in radius from an aqueous solution with a dielectric constant of 80 into a 70 \AA thick hydrocarbon slab with a dielectric constant of 2 (for comparison, the energy involved in the breaking of the terminal phosphate in an ATP molecule is of the order of 10 kcal/mol). This energy of transfer translates into a partition coefficient for ions on the order of 10^{-30} . (Partition

coefficient = membrane ion concentration/solution ion concentration).

This value is much too low to account for the membrane resistance values measured in resting cells (Ehrenstein and Lecar, 1972). The passage of ions then must occur through specialized conducting regions existing within the membrane. These specialized regions are pores or ion channels formed by integral membrane proteins that span the lipid bilayer. They can open and close, a process called gating, and, once open, allow a large number of ions (10^6 - 10^9 ions/sec) to move down their electrochemical gradients (Armstrong, 1975a).

The protein nature of ion channels was first suggested by the effect of proteases on membrane excitability. In early experiments, perfusion of squid giant axons with different proteases resulted in either complete loss of excitability or changes in duration of the action potential (Rojas and Luxoro, 1963; Takenaka and Yamagishi, 1969). Later, the clear demonstration of the specific destruction of the Na^+ inactivation mechanism in axons perfused with pronase (Armstrong et al., 1973) left little doubt about the protein nature of the Na^+ channel. More recently, the saxotoxin (STX) and bungarotoxin binding peptides from the Na^+ and ACh channel respectively have been successfully purified and reconstituted in liposomes and bilayers (Weigele and Barochi, 1982; Hartshorne and Catterall, 1981; Haganir et al., 1979; Krueger et al., 1983; Schindler and Quast, 1980). Also, the genes coding for some of the subunits of the Na^+ and ACh channel proteins have been cloned and sequenced (Noda et al., 1982).

The ion flow through a channel can be measured as an electric current (I). The current flowing through a single class of channels in the membrane is described by:

$$I = GN f(V_m - E) \quad (1)$$

In this expression, G is the single channel conductance or the number of ions flowing per unit time through a single channel; N is the number of channels per unit membrane area; f is a function that represents the fraction of open channels at V_m ; V_m is the applied membrane potential; and E is the potential at which no net current flows through the channel (reversal potential). When only one ionic species move through this pathway, we have:

$$E_{(in-out)} = \frac{RT}{zF} \ln \frac{[ion]_{out}}{[ion]_{in}} \quad (2)$$

where R , T , z and F have their usual meaning. The difference $(V_m - E)$ represents then the electrochemical driving force for ion movement through the channel.

For a complete characterization of the current flowing through a channel, then, we need to understand each parameter in equation (1). The single channel conductance reflects the permeability and selectivity properties of the channel and the function, f , depends on the channel gating mechanism.

How To Study Membrane Currents

For voltage gated channels, the fraction of open channels in the membrane is a function of membrane potential. Because the process of channel opening is voltage dependent, a device to control the voltage

across the membrane (voltage clamp) becomes an indispensable tool in the study of this process. To obtain good control of the membrane potential, several conditions have to be met. These conditions include spatial uniformity of the controlled potential (space clamp) and fast settling of the command potential across the membrane (Bezanilla et al., 1982a). The current measured under voltage clamp is the algebraic sum of all the currents flowing through the membrane at any time. To find out which type of ion(s) is(are) contributing to this net current, one has to either do ion replacement experiments or find specific blockers that would selectively eliminate one or more conductance pathways leaving the other(s) unaffected. Another possible way of separating currents is by making use of the inherent differences in the activation or relaxation times of the channels studied (Noble and Tsien, 1968). Even though an enormous amount of information on the conductance mechanisms of many different types of cells has emerged using the voltage clamp, the technique has some limitations. First, there are some cells that because of their size or geometry cannot be properly voltage clamped. Second, given that one measures total current, it is always possible to have a component arising from channels different from the one of interest. Third, because voltage clamp measurements only give information about the average behavior of a population of channels, it is not always possible to relate this macroscopic behavior to the properties of the individual channels responsible for it.

Considering these limitations new methods for studying the properties of single channels were developed. There are currently three different approaches: noise analysis, patch clamp recording, and channel reconstitution.

Noise analysis is a technique useful for obtaining information about the value of single channel conductance and under some circumstances the mean time a channel stays in the open state. This is accomplished by studying the fluctuations of the macroscopic membrane current around its mean value (noise) due to the random opening and closing of individual channels (Neher and Stevens, 1977).

The patch clamp technique consists in recording extracellular currents from a very small membrane area ($1-10 \mu^2$) by using a glass electrode with a small tip diameter ($\sim 0.5 \mu$) closely apposed to the membrane. Under appropriate conditions, the resistance to current flow between the pipette electrode and the bath can become so high that the main path for current flow is through the membrane patch. Under these conditions, currents flowing through individual channels can be directly recorded (Neher and Sakman, 1976; Hamill et al., 1981).

The third technique to study single channel properties is channel reconstitution. The rationale behind this technique is to transfer a channel from its native membrane into an artificial membrane system over which one has a higher degree of experimental control than over the native membrane (Miller, 1983a, b). The most widely used model membrane system for ion channels studies has been the planar bilayer introduced by Mueller et al. (1963). Recently, patch clamp recording (see above) from liposomes containing reconstituted ionic channels has also been successful (Tank et al., 1982).

Different methods for forming bilayers and incorporating the channels into them have been described and used successfully to characterize the properties of several types of channels, mainly the Na⁺ channel, a K⁺ channel from sarcoplasmic reticulum, a Cl⁻ channel from

Torpedo electroplax, bacterial and mitochondrial porins, Ca^{++} -activated K^+ channels, the delayed rectifier from lobster axons, channels from cardiac sarcolemma, the Na^+ channel, and Ca^{++} channels from paramecium membranes (Mueller et al., 1963; Montal and Mueller, 1972; Schindler, 1979; Miller and Racker, 1976; Boehm et al., 1980; Coronado and Latorne, 1983; Wilmsen et al., 1983; Miller, 1983a, b; Schindler and Rosenbusch, 1978; Schein et al., 1976; Ehlrich et al., 1983; Latorre et al., 1982; White and Miller, 1981; Krueger et al., 1983).

The techniques for studying single channel properties, especially patch clamp and the reconstitution technique are important also because they can be used to study the properties of membranes not accessible to conventional microelectrode voltage clamp. Some examples are chromaffin cells (Hamil et al., 1981) and the membranes of the transverse tubule (TT) system in skeletal muscle fibers, the system utilized in the present study.

Characteristics Of The TT System

The TT system is a network of tubules that invaginate from the surface membrane perpendicular to the long axis of a muscle fiber. As was suggested by Huxley and Taylor (1958), they are involved in the inward conduction of the surface membrane depolarization allowing the almost simultaneous contraction of the whole cross section of a muscle fiber. Figure 1 is a schematic diagram of a skeletal muscle fiber showing the relationships between surface membrane, TT and sarcoplasmic reticulum (SR).

Indirect biochemical and electrophysiological evidences suggest that

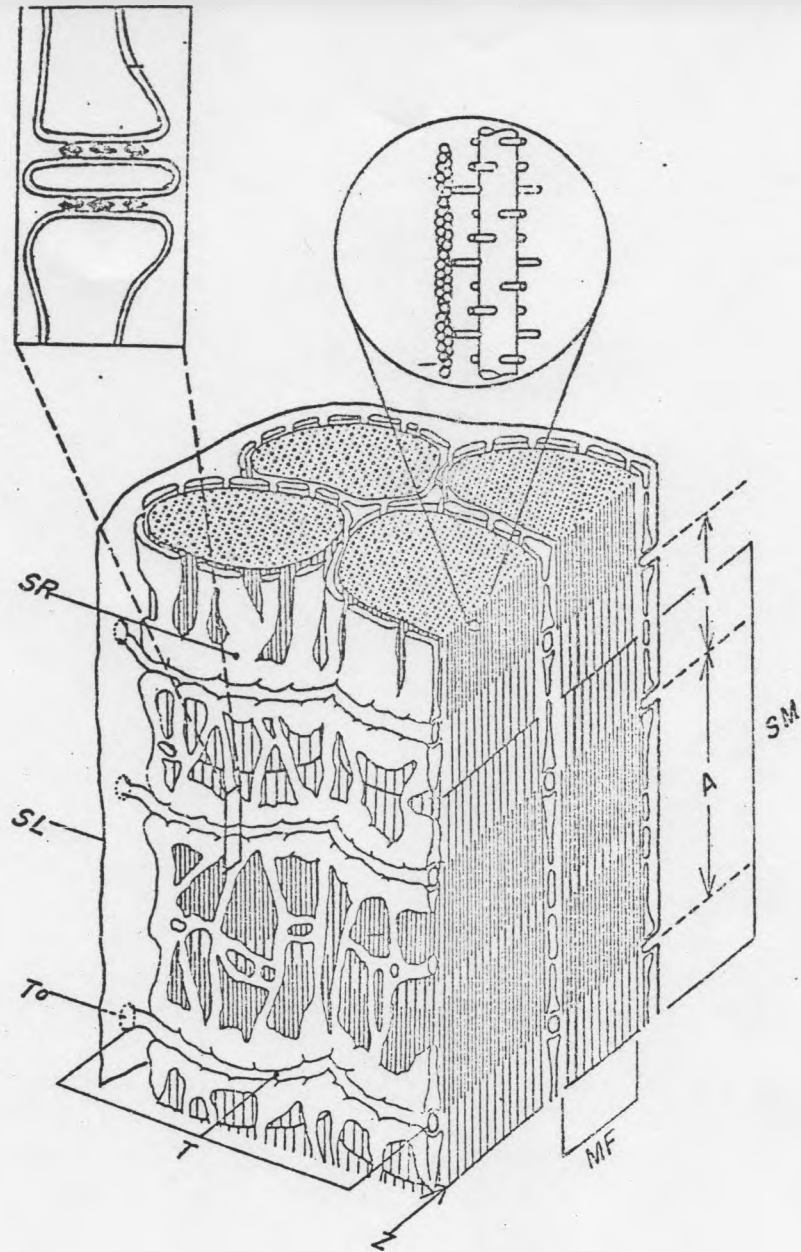


Fig. 1. Schematic representation of a muscle cell. The diagram shows the spacial relationship between surface membrane (SL), transverse tubules (T) and the sarcoplasmic reticulum membranes (SR). To = transverse tubule entrance, SM = sarcomere, MF = microfibril, A = A band, I = I band, Z = z line. Inset: Section showing the relationship between the terminal sarcoplasmic reticulum cisternae and transverse tubule.

even though the surface membrane and the TT membrane are continuous, they present different functional properties. Jaimovich et al. (1976) and Venösa and Hörowicz (1981) studied TTX and ouabain binding to intact and detubulated frog sartorius muscles. They found that the density of TTX binding sites on surface sarcolemma is about four-fold higher than that on the TT system, while the density of ouabain binding sites is about 25-fold higher in surface sarcolemma than in TT. This indicates the differential distribution of some membrane components in the two systems of membranes. Also from the studies on action potentials in intact and detubulated frog muscle cells, Adrian et al. (1970) proposed that the distribution of delayed rectifier, slow delayed rectifier and inward rectifier channels in these cells was not homogeneous. In detubulated cells, these authors did not observe the late after potentials or slow hyperpolarizations that had been attributed to the slow delayed rectifier and inward rectifier channels, respectively (Gage and Eisenberg, 1969). Accordingly, they proposed that these last two types of channels were localized mainly on the TT membrane.

Studies of the resting Cl^- and K^+ conductances on normal (Hodgkin and Hörowicz, 1960) and detubulated frog muscle fibers (Eisenberg and Gage, 1969) led to the conclusion that the K^+ conductance system is distributed on the surface and TT membranes while the Cl^- conductance is almost exclusively located on the surface membrane in these fibers. On the other hand, from the same type of measurements, Palade and Barzhi (1977) found that in rat diaphragm at least 80% of the Cl^- conductance is associated with the TT.

Also, Ca^{++} -dependent K^+ currents have been studied in rat myotubes. Barret et al. (1981) have proposed that Ca^{++} -dependent K^+ channels exist

in the TT system of adult muscle cells. Ca^{++} -activated K^+ currents have recently been measured in adult rat muscle cells by Chiarandini and Stefani (1983) without discussing their possible localization. The rationale for undertaking the experiments that will be described was that the geometry of the TT system (Fig. 1) does not allow the use of other techniques to study its electrical properties. On the other hand, at this stage of the work on channel reconstitution, it is important to characterize the properties that channels display in bilayers and compare them with the properties displayed on the native systems in order to be sure that the technique is a valid one. Once the technique is validated, its advantages over the native system can be exploited to advance in the understanding of ion permeation through channels. The advantages of this technique are mainly the relative ease with which one can study a single type of channel, the accessibility to both sides of the membrane, and the possibility of manipulating the lipid environment as a tool for answering questions about the permeation process.

This thesis work presents the characterization of a Ca^{++} -activated, voltage-dependent, K^+ -selective channel from TT membrane vesicles reconstituted in artificial lipid bilayers. I present data on the mechanism of Ca^{++} and voltage activation (channel gating) and on the properties of the open channel (conductance, selectivity and channel blockage by tetraethylammonium, triethylindylammonium (C_9), Ca^{++} and Ba^{++} ions). Next, I will describe channel selectivity, gating, conductance and blockage in some detail, emphasizing the properties displayed by single channels.

CHANNEL SELECTIVITY

I earlier emphasized the existence of different channel types that under normal circumstances allow either Na^+ , K^+ , Ca^{++} , or Cl^- ions to move across different types of membranes in a selective manner. However, these channels are not perfectly selective to a given ionic species. In this regard, channels are "leaky" with a degree of leakiness that varies from channel to channel. For example, Na^+ ions pass only 10-fold faster than K^+ through the Na^+ channels, and K^+ about 100-fold faster than Na^+ through the delayed rectifier (Hille, 1972, 1973, 1975). Further, in the absence of external Ca^{++} , Na^+ ions can move through Ca^{++} channels in molluscan neurones (Kostyuk and Krishtal, 1977). In squid axons, Li^+ ions can carry depolarizing currents and support action potentials in the absence of external Na^+ . Also in the absence of external Na^+ , K^+ ions can carry inward currents through the Na^+ channel (Hodgkin, 1951).

Most of the advances toward the formulation of a theory to explain selectivity in ion channels are based on studies done in model systems, namely, cation selective glass electrodes, ion carriers, and solvents of known structure (Eisenman, 1962; Krasne and Eisenman, 1973). Most of the work has been done for alkali monovalent cations but the conclusions from these studies can be extended to monovalent and polyvalent anions and cations as well (Diamond and Wright, 1969).

An important observation that led to an understanding of the origin of ion selectivity was that out of the 120 possible combinations of selectivity sequences for the group Ia alkali metal cations only a few (eleven) are seen experimentally (see Krasne, 1978 for review).

Furthermore, out of the eleven observed sequences, only I and XI are monotonic functions of hydrated and naked ion size, respectively. All other sequences show a non monotonic dependence on ion size. From his work on the selectivity displayed by glass electrodes, Eisenman (1962) proposed that the observed sequences in this system can be explained by considering the balance between the equilibrium energies of interaction of the cation and water and the energy of interaction of the cation and an anionic binding site in the electrode. He considered the coulombic forces that can be generated by the interaction of the cation and the anionic binding site as a function of their radii, and called the force generated at a particular distance from the anion site the field strength. A high field strength site is one of small radius, more charge or larger dipole moment so that the bound cation will be closer to the center of charge of the anion group. For a high field strength site, the ion is attracted more strongly by the site than by its hydration water molecules. Thus, the preferred cations would be those of smaller radius generating the sequence $\text{Li}^+ > \text{Na}^+ > \text{K}^+ > \text{Rb}^{++} > \text{Cs}^{++}$ for the group Ia cations. On the other hand, for a low field strength site, the energy necessary to dehydrate the cation will be the determinant factor for selectivity and the sequence $\text{Cs}^{++} > \text{Rb}^{++} > \text{K}^+ > \text{Na}^+ > \text{Li}^+$ is generated. For intermediate field strengths, intermediate sequences result.

Further studies on the ionic selectivity displayed by different chemical groups including uncharged dipolar groups in solvents and ion carriers have confirmed that the selectivity displayed by a binding site arises from differences in the electrostatic interactions between ions and the ligand group compared to those between the ion and water molecules. Furthermore, the selectivities displayed by known groups on

carriers and solvents can be compared with that of channels in order to obtain some hints about the sites determining selectivity in ion channels (Krasne and Eisenman, 1973).

How can we relate these concepts of ion binding affinity to the selectivity displayed by ion channels and to the permeation of the different ions? Let us first consider the methods used to measure selectivity of ion channels.

Conductance

Inasmuch as selectivity refers to the ability of an ion to move through a channel, a way to measure this ability is to measure the channel conductance for different ions under comparable conditions; i.e., equivalent membrane potentials and ion concentrations.

Reversal Potentials

A different approach is to measure permeability ratios for different ions using the Goldman Hodgkin and Katz formulation for zero current or reversal potentials as a function of the concentrations of the current carrying ions (Hodgkin and Katz, 1949). This can be done under several experimental conditions, the two most common are dilution potentials and biionic potentials.

Dilution potentials refer to measurements where only one type of salt is present across the membrane but the concentrations on both sides are different. This measurement allows the determination of the relative permeabilities of cations vs anions.

Biionic potentials refer to measurements where different salts with a common anion or cation are present across the membrane at the same

concentration. These measurements allow the determination of the relative permeabilities of the two cations (or anions).

In all cases, the relationship between the zero current or reversal potential (E) and permeabilities (P) is given by:

$$E_{(1-2)} = \frac{RT}{F} \ln \frac{\sum A_{a_1} P_{a_1} + \sum A_{c_2} P_{c_2}}{\sum A_{a_2} P_{a_2} + \sum A_{c_1} P_{c_1}} \quad (3)$$

where 1 and 2 refer to the two sides of the membrane. A stands for activity and a and c for anions and cations respectively. R, T and F have their usual meaning. Several assumptions are involved in the derivation of this equation: (i) the ionic concentrations at the membrane solution interfaces are related by a linear partition coefficient to the bulk ionic concentration; (ii) ions move independently of each other, (iii) the diffusion coefficient and the electric field are constant in the membrane. Because of these assumptions, the Goldman, Hodgkin, and Katz formulation considers the ion permeation process as a continuum.

If the assumption of independent movement of ions holds, then the selectivity measured either by reversal potentials or channel conductance is expected to be the same. On the other hand, if the movement of an ion is influenced by the presence of other ions (of the same or of a different kind), then the permeabilities obtained by the two methods need not be the same (Hille, 1975; Krasne, 1978).

The study of Na^+ and K^+ channels from nerve and muscle has shown several phenomena that cannot be explained by the continuum electrodiffusion theory, such as ion competition and saturation of channel conductance with ion activity (Hille, 1975). For this reason, a

different view to ion permeation was adopted based on a kinetic approach to diffusion using the reaction rate theory introduced by Eyring and coworkers (Eyring et al., 1949; Zwolinski et al., 1949). According to this view, the permeation pathway (channel) can be considered as a series of energy peaks and wells that an ion must cross in order to go through the membrane. Energy peaks represent the minimum amount of energy that an ion has to possess in order to overcome electrostatic or steric constraints. Energy wells represent favorable residence regions that the ion has to escape from in order to advance further. Using Eyring's approach, Lauger (1973) developed a description of the transport of an ion through a pore as a function of ion concentration and membrane potential for a channel that can only be empty or singly occupied (single ion channel). The number of barriers and wells, their heights and locations being arbitrarily chosen. He showed that irrespective of the number of barriers, the permeability for two different ions measured under biionic conditions is determined by the height of the energy barriers with respect to the outside solution and is independent of the depth of the energy wells or binding sites. However, for channels that contain more than one ion at a time or even for singly occupied channels whose selectivity is being measured not by zero current potentials (e.g., conductance), selectivity becomes a function of the energy peaks and wells. For multiple occupancy the problem becomes even more complicated because it is possible that the position and/or heights of the energy peaks and valleys are modified by the presence of different ions (Hille, 1975).

Having a barrier model for the channel, one can now apply Eisenman's selectivity theory to the binding sites or energy peaks along a channel.

The validity for applying Eisenman's theory (equilibrium measurements) to the energy peaks has been considered by Hille (1975). He realized that an ion at the peak of an energy barrier is, according to rate theory, in a quasi equilibrium condition so it is possible to apply Eisenman's principles to the energy barriers. Also, as discussed by Eisenman and Horn (1983), an ion at an energy peak is only at a slightly less favorable energy level as compared to a binding site. An energy barrier higher than 10 kT should slow down ion movement to values much slower than those observed for ion channels (10^6 - 10^9 ions/sec); therefore, even at the highest energy peak an ion must have interaction with channel sites favorable enough (quasi equilibrium) to allow for the observed transport rates.

Now we are faced with the specific problem of finding out how the energy profile for a particular channel looks like. How many barriers are there? Where in the electric field are they located? Which barrier is the rate limiting step for the process? Once we know the answers to these questions, we can ask what the individual selectivities of the barriers are. Also, we need to know about channel occupancy, or the number of ions that can be found simultaneously inside the channel.

With respect to the number of ions occupying the channel, the first example of multi occupancy was worked out for the delayed rectifier of squid axons (Hodgkin and Keynes, 1955). Studying K^+ ion fluxes, they found that inward and outward K^+ movements were not independent since, at constant membrane potential, an increase in external $[K^+]$ reduced K^+ efflux; the K^+ influx at constant membrane potential was not proportional to the external $[K^+]$ but increased more steeply so the variations of flux

ratios (influx/efflux) with driving force they found were much greater than expected assuming independent ion movement. They explained all these findings considering the channels as long narrow pores holding several K^+ ions moving in single file (i.e., the ions are not able to pass each other).

The shape of the channel conductance vs ion concentration curve is another way of deciding about channel occupancy. Lauger (1973) showed that singly occupied channels show saturation of conductance with ion activity in a manner totally equivalent to the saturation of an enzymatic reaction with substrate concentration. For a multiply occupied channel, however, the conductance decreases at higher ionic concentrations, because at a sufficiently high ion concentration outside, a vacant site in the channel is replaced faster by an ion coming from the solution than by the other ion inside the channel, and no net movement of ions occurs.

Complicated functions of conductance vs ion concentration can also be obtained for single ion channels under special circumstances. The interactions of an ion with its binding site may affect the energy level of the site due to conformational changes induced on the protein by coulombic forces generated between the ion and charged groups on the protein. If the rate of the conformational change on the protein induced by the ion is comparable or smaller than the ion jumping rate, then the simple saturation of conductance with ion concentration found for single ion channels with fixed barrier structure does not hold (Lauger et al., 1980).

In order to characterize the energy profile for a channel, it is useful to divide the transport process into two steps, a complexation step that considers the barriers for association and dissociation of the

ion and the channel and a translocation step that represents the barrier for ion movement through the channel. Fig. (2) is a diagram showing the energy profiles for ion permeation when the complexation step is rate limiting [Fig. (2A)] or when translocation is rate limiting [Fig. (2B)].

Because the movement of an ion in a particular direction depends on the difference between its energy at the highest barrier for permeation and its energy in the aqueous phase, we can obtain information about the location of the rate limiting barrier by observing the effect of an applied membrane potential on the ion movement (current) (see Krasne, 1978). If the total ion concentration on the two sides of the membrane is the same, then the electric field within the membrane is constant (Sten-Knudsen, 1978) and the potential difference inside the membrane will vary linearly as a function of distance. The energy barriers located at different distances into the membrane will feel different fractions of the voltage drop across the membrane (Krasne, 1978). This is illustrated in Fig. (3A) for the two energy profiles of Fig. (2).

For a process where the translocation step is rate limiting (in symmetric conditions), one will find a hyperbolic I-V curve, while for a process where complexation is rate limiting, a saturating I-V curve is obtained [Fig. (3B)] (Krasne, 1978).

Obviously, location along the membrane field of the binding sites and the shape of the energy barriers involved can also be obtained by using channel blockers and studying the voltage dependence of the blockage (Woddhull, 1973; Armstrong, 1975b; Neher and Steinbach, 1978; Coronado and Miller, 1982; Miller, 1982; Vergara and Latorne, 1983).

The selectivity related to each process (complexation and translocation) need not be the same and most probably are not, since it

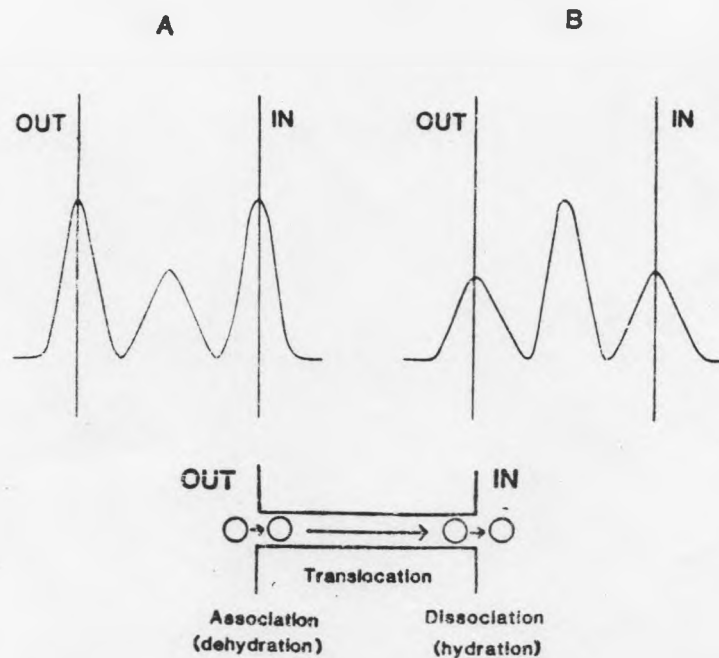


Fig. 2. Schematic energy profiles for ion permeation through the membrane. (A) The rate limiting steps of the transport reaction are association and dissociation reactions between the ion and the channel. (B) The rate limiting step of the transport reaction is ion translocation through the channel. Inset: Fanciful picture of the association, translocation and dissociation steps between an ion and the channel.

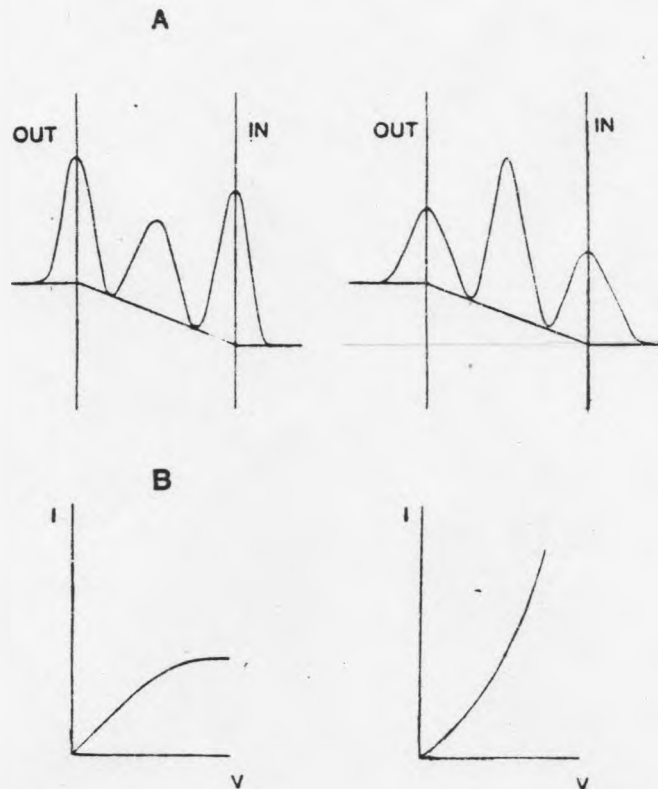


Fig. 3. Relationship between applied voltage, energy profiles and current-voltage curves. A. Effect of membrane potential on the energy profiles shown on Fig. 2. The potential difference is shown as varying linearly with distance into the membrane. Energy barriers and wells located at different distances into the membrane feel different fractions of the total voltage drop across the membrane. B. On the left, the current-voltage relationship for ion translocation through a channel when the rate limiting steps are association and dissociation of the ion with the channel. On the right, the current-voltage relationship for ion translocation through a channel when the rate limiting step is ion translocation through the channel.

is easy to imagine that different chemical groups are related with each process. A clear example of this has been worked out in a model system using the carrier tetraoctin (Krasne and Eisenman, 1976). By changing the lipid environment into which the carrier was studied, they were able to alter the rate limiting step of the process and also the measured selectivity sequences.

The major energy barrier for permeation has been called the "selectivity filter" by Hille (1971; 1972; 1973; 1975), the filter being the narrowest cross section inside the channel through which an ion totally or partially dehydrated can physically move. When an ion enters a channel but cannot go through the selectivity filter, this ion becomes a blocker. It is easy to imagine how selectivity for ions bigger than the cross section of the filter occurs, they are simply excluded by a "sieve mechanism." On the other hand, Bezanilla and Armstrong (1972) realized that the selectivity filter can also exclude ions smaller than an optimum size because of poor interactions of the "small ion" with the chemical groups forming the filter. If the ion-water interactions cannot be properly replaced by ion-selectivity filter interactions, then the potential energy of the small ion at the filter site will be greater than in solution and so the small ion is effectively excluded from the channel (see also Hille, 1975). This is an important observation inasmuch as most channels seem to select ions not by binding more tightly the preferred ions but by selectively excluding the non permeant ions (Bezanilla and Armstrong, 1972). If the selectivity of a channel would be governed by selective binding, then the net transport rate (channel conductance) will be low because tight binding is equivalent to a deep

energy well from where the ion has to escape in order to permeate through the channel. This seems to be the case for the Ca^{++} channel that indeed has a low conductance (1-2 pS; Kostyuk, 1981; Tsien, 1983). Kostyuk and collaborators (Kostyuk et al., 1980; Kostyuk, 1981) have proposed a model for the molluscan neuron Ca^{++} channel consisting of three barriers and two binding sites. From conductance measurements, he finds that the depth of the binding site at the outer mouth of the channel regulates selectivity. They propose that the higher conductance displayed by Ba^{++} and Sr^{++} ions on Ca^{++} channels [Ba^{++} (2.8) > Sr^{++} (2.6) > Ca^{++} (1.0) > Mg^{++} (0.2)] can be explained by a less tight binding of these ions to the outer energy well (Kostyuk et al., 1980; 1982).

A final goal in the study of ion permeation is to relate channel structure and function; i.e., relate the properties displayed by different channels to the structure of chemical groups in the channel protein. Although at this moment we are far from reaching this goal, some insight on channel structure has been gained from selectivity studies. For example, selectivity for the Na^+ channel in node of Ranvier, squid axon and skeletal muscle is governed by a site that behaves as a high field strength site; i.e., it has characteristics like small effective radius, high density of charge, and all the other properties related with a high field strength site (Chandler and Meves, 1965; Hille, 1972; Campbell, 1976). On the other hand, the selectivity displayed by the K^+ channel from these same preparations, together with the K^+ inward rectifier from egg cells, is consistent with a low field strength site having opposite properties than the selectivity filter of Na^+ channels (Hille, 1973; 1975; Binstock and Lecar, 1969; Hagiwara and Takahashi, 1974).

Ca^{++} -activated K^+ channels from myotubes and adult muscle, on the other hand, display an extreme selectivity to K^+ ions over the other group I_a monovalent cations; moreover, all monovalent cations seem to block this channel (Pallota et al., 1981; Methfessel and Boehm, 1982; and experiments to be described under Results). Because most ions block the Ca^{++} -activated K^+ channel, ionic selectivity has been difficult to study.

While Na^+ and K^+ channels show different degrees of selectivity, the permeability sequence displayed by Ach channels for monovalent cations is the same as their aqueous mobility sequence, suggesting little interaction of these ions with channel groups as they move through (Adams et al., 1980).

CHANNEL GATING

Ion channels are pores formed by integral membrane proteins that span the lipid bilayer (Armstrong, 1975a). Channels can be either open or closed and we define the kinetic process of opening and closing as channel gating. Two basic modes of gating have been described, chemical gating in which channel opening or closing is triggered by the binding of an agonist, and voltage dependent gating in which the open-closed transitions are triggered by changes in membrane potential. Chemically- and voltage-gated channels were thought of as mutually exclusive types (i.e., no effect of voltage on chemically-gated channels and no effect of transmitters on voltage-gated channels). However, recent work has shown that this is not the case. For example, Magleby and Stevens (1972a, b) showed that voltage affects some properties of the ACh channel and Mudge et al. (1979) have shown that transmitters can modulate voltage-dependent channels.

Chemical or Neurotransmitter Mediated Gating

Early electrophysiological experiments established that in a chemical synapse, the interaction of the presynaptically released neurotransmitter with a receptor in the postsynaptic membrane causes a change in the ionic permeability of the postsynaptic membrane (Fatt and Katz, 1951; Takeuchi and Takeuchi, 1960). The most studied synapse is the frog neuromuscular junction. In this case, the neurotransmitter is ACh and the postsynaptic receptor is the ACh receptor that upon binding of ACh allows the movement of cations down their electrochemical

gradients. Ideally, one would like to know from a molecular point of view how Ach triggers the opening of a channel. This question has been approached using tools from electrophysiology, biochemistry and pharmacology.

The electrophysiological approach to study the Ach channel activation kinetics has been based mainly on the study of the dose-response curves; i.e., on the relationship between the agonist concentration and the equilibrium number of open channels at that particular agonist concentration. The dose-response curves provide information on the number of agonist molecules that must bind to a receptor to cause channel opening. They also indicate how tightly the agonist binds and, under some conditions, indicate what is the probability that a channel will open given that the receptor has agonist bound to it (Dionne et al., 1978). The predictions of theoretically possible reaction schemes are compared with the experimentally obtained dose response curves with the aim of identifying the correct reaction sequence. Several theoretically possible reaction schemes have been proposed. In some of them, the closed/open transition is triggered by the binding of agonist (occupancy models), while in others the open and closed conformations exist in equilibrium irrespective of the binding of a drug (two-state models). In this case, a molecule acts as agonist or antagonist according to its selective affinity for the open or closed conformations, respectively. Although in principle it is possible to distinguish between the different models because their predictions are different, in practice this is not easy. The main reasons for this are that accurate dose-response curves are experimentally difficult to obtain (Dionne and Stevens, 1975) and in some cases the experimental data can be

fitted equally well to several models (Colquhoun, 1979; Peper et al., 1982).

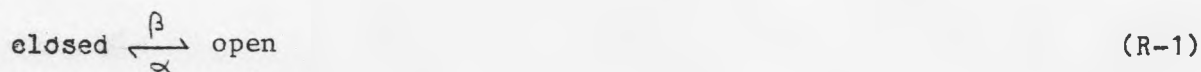
Voltage-Dependent Gating

In order to explain voltage-dependent gating the existence of charged groups or dipoles that change their orientation according to the membrane field have been postulated. The voltage dependent conformational change induces, in turn, the open/closed transitions (Hodgkin and Huxley, 1952d). The open/closed transitions can occur randomly but their probability of occurrence is modulated by voltage. The experimental approach to study channel gating has been through the study of macroscopic and gating currents under voltage clamp conditions and, more recently, through single channel currents (Bezanilla and White, 1983). Again, as in the case of chemically-activated channels, the experimental results are compared and fitted to the predictions made by different theoretical kinetic models. Gating currents reflect the charge movement associated with the opening and closing of voltage gated channels in response to changes in the membrane field. Because the charge displacement occurs within the membrane, they behave as capacitative currents. The existence of these currents was predicted by Hodgkin and Huxley (1952d), but it was not until much later that Armstrong and Bezanilla (1974) could measure the gating currents associated with the Na^+ channel activation process. Recently, the gating currents associated with K^+ channel activation have also been measured (Gilly and Armstrong, 1980; Bezanilla et al., 1982b).

To explain the gating properties of the EIM channel (EIM stands for Excitability Inducing Material--a protein of bacterial origin that

incorporates in artificial bilayers forming cation-selective channels; Bean et al., 1969), Ehrenstein et al. (1974) proposed a two-state model that has been used as the basic model of gating for most, if not all, other voltage dependent channels. Although most channels show gating behaviors more complicated than the model, it has provided a framework for the development of more elaborated reaction schemes (Bezanilla and White, 1983).

The model proposes that the gating of each individual channel in the membrane can be described by the reaction:



where α and β are the rate constants of transition between the open and closed states, and they are in general a function of membrane potential. Assuming that the channels are independent of each other, that their conductance is independent of voltage, and that switching between the open and closed conformation requires the rearrangement of charged groups in the protein, it is possible to predict the macroscopic and single channel kinetic and equilibrium behavior.

Macroscopic Equilibrium Behavior

If switching between the open and closed conformations requires the rearrangement of charges, the equilibrium between these two states must be voltage dependent and reflect the free energy difference between them. The relative number of channels in the open (n_o) and in the closed (n_c) state is given by the Boltzman distribution:

$$\frac{n_d}{n_c} = \frac{n_o}{N-n_o} = \exp(-G^*(V)/RT) \quad (4)$$

where N is the total number of channels and $G^*(V)$ is the voltage dependent free energy difference between the two states. If n equivalent charges move across the whole transmembrane field during the open/closed transition, then

$$G^*(V) = nF(V - V_o) \quad (5)$$

where F is Faraday, V the applied potential, and V_o the potential at which the number of open channels is equal to the number of closed channels. Accordingly, we can rearrange equation (5) as:

$$\frac{n_o}{N-n_o} = \exp(-nF(V-V_o)/RT) \quad (6)$$

If the single channel conductance is G , then the maximal conductance for a membrane having N channels is:

$$G_{max} = NG \quad (7)$$

and the voltage dependent conductance is

$$G(V) = n_o(V)G \quad (8)$$

then equation (5) becomes (Ehrenstein et al., 1974):

$$\frac{G(V)}{G_{\max} - G(V)} = \exp(-nF(V-V_0)/RT) \quad (9)$$

Single Channel Behavior

From reaction scheme 1, the ratio of the number of open and closed channels is

$$\frac{n_o}{n_c} = \frac{\beta}{\alpha} \quad (10)$$

and the average fraction of open channels,

$$f(V) = \frac{n_o}{n_o + n_c} = \frac{\beta}{\alpha + \beta} = (1 + \exp(-nF(V-V_0)/RT))^{-1} \quad (11)$$

If channels are independent of each other, the average fraction of time that a single channel stays open at a given potential must be equal to $f(V)$ (Ehrenstein et al., 1970).

Kinetic Behavior

For a two-state model, after a step in voltage, the macroscopic conductance relaxes from its initial value to a new equilibrium value and does so with an exponential time course with a relaxation time constant (τ) given by:

$$\tau = \frac{1}{\alpha + \beta} \quad (12)$$

For a fixed membrane potential, the open and closed dwell times are exponentially distributed in time because the transition between the two states is a random process. Accordingly, the opening and closing rate constants k_{12} and k_{21} can be determined from the reciprocal of the mean times spent in the closed ($\bar{\tau}_c$) and open ($\bar{\tau}_o$) configurations, respectively, or from the time constant of the exponential dwell time distributions (Ehrenstein et al., 1974).

What do the macroscopic and gating current together with single channel data reveal about possible models of channel activation?

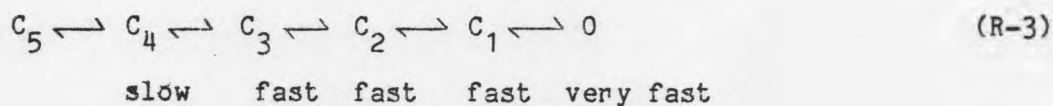
The two channels which have been studied most are the Na^+ and K^+ channels of the squid axon. As I mentioned above, the predictions of the simple two state model with respect to kinetics of channel activation, gating currents time course, and other parameters are not in accord with the experimental findings (Bezanilla and White, 1983).

For both Na^+ and K^+ channels, it has been found that more than one closed state must exist in order to account for some experimental results. Mainly, the delay of current development in response to a depolarizing potential and the different kinetics of current development depending on the initial and final values of the test potential pulses (Armstrong and Gilly, 1979; Gilly and Armstrong, 1982). For the Na^+ channel a reaction sequence that fits the activation conductance data is the following:



where C and O stand for closed and open, respectively, and α_1 and β_1 are the rate constants for the forward and backward reactions. Good fits to

the data are obtained considering that all transitions have equal rate constants except the last step (leading directly to channel opening) which is rate limiting for the whole sequence. For the K^+ channel macroscopic and single channel data suggest the existence of several closed and open states with the transition between the last closed and the open state being much faster than the other transitions between closed states (Gilly and Armstrong, 1982; Conti and Nener, 1980). Gating current data indicates that the first transition between closed states is a slow process (Bezanilla and White, 1983). The best fit to the available data is given by the following reaction sequence:

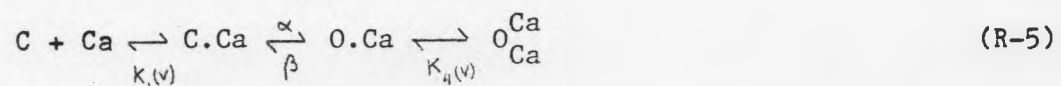
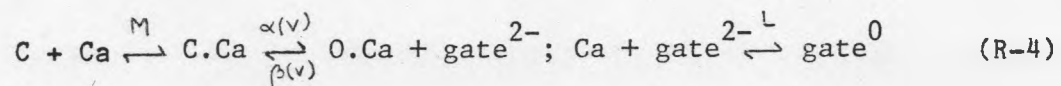


Ca⁺⁺-Activated K⁺ Channels

The activation of Ca⁺⁺-dependent K⁺ currents ($I_{K,Ca}$) is not only a function of intracellular [Ca⁺⁺] but also of membrane potential. Originally, Meech (1978) proposed that the voltage dependence of $I_{K,Ca}$ was indirect and reflected the voltage dependence of Ca⁺⁺ ion movement through voltage dependent Ca⁺⁺ channels and, therefore, Ca⁺⁺-activated K⁺ channels could be considered as agonist gated. Further studies have shown clearly that this is not the case inasmuch as membrane potential has a direct effect on the gating reaction (Latorre et al., 1982; Methfessel and Boehm, 1982; Mozdykowski and Latorre, 1983b; Hermann and Hartung, 1982). Ca⁺⁺-activated K⁺ channels then can be considered both chemical- and voltage-activated channels. An interesting problem is to

find out the nature of the voltage dependence. Single channel studies have revealed that, with respect to single channel conductance, two groups of Ca^{++} -activated K^+ channels exist. One group has conductance values ranging from 100-200 pS while the other has conductances between 10-20 pS (Adams et al., 1982; Krueger et al., 1982; Latorre et al., 1982; Marty, 1981; Methfessel and Boheim, 1982; Moczydlowski and Latorre, 1983; Pallota et al., 1981; Wöng et al., 1982; Walsh and Singer, 1983; Hermann and Hartung, 1982; Lux et al., 1981). For the high conductance group, the single channel activity presents complicated kinetics. Single channel currents show openings and closings of durations in the msec range (bursts of activity) interrupted by quiescent periods that last several hundred msec. Depolarizing membrane potentials and increases in intracellular $[\text{Ca}^{++}]$ increase the fraction of time that the channel is in the open state within a burst of activity. Also within bursts of activity very fast openings and closings (flickers) occur (Barret et al., 1982; Methfessel and Boheim, 1982; Moczydlowski and Latorre, 1983; Pallota and Magleby, 1983).

After an analysis of the effect of membrane potential and $[\text{Ca}^{++}]$ on bursts of activity (having excluded the flickers) Methfessel and Boheim (1982) in myoballs and Moczydlowski and Latorre (1983) in lipid bilayers proposed the following reaction schemes where two Ca^{++} ions are involved:



where the gate in reaction scheme 4 is postulated to normally block the

channel. Although these two reaction schemes are formally equivalent with respect to the $[Ca^{++}]$ dependence of the reaction, for reaction scheme 4 it was assumed that the voltage dependence of the gating reaction resides in the open/closed conformational change having voltage independent Ca^{++} binding reactions (M, L). Activation results from the binding of Ca^{++} to the blocking gate (Methfessel and Boheim, 1982). On the other hand, Moczydlowski and Latorre (1983) found that the mean open and mean closed times at the zero and infinite $[Ca^{++}]$ limits at all voltages converged to $1/\alpha$ and $1/\beta$, respectively, indicating voltage independent transition rates. Furthermore, they found that the slopes of the linear functions of mean open time vs $[Ca^{++}]$ and mean closed time vs $1/[Ca^{++}]$ are exponential functions of voltage indicating a voltage dependent binding reaction. Activation results in scheme 5 from the voltage modulated binding of Ca^{++} to the channel.

Also, in myotubes Pallota and Magleby (1983) analyzed the activation kinetics including the flickers at a constant membrane potential. They suggest that at least three closed and two open states are needed to explain the data.

For the low conductance channel, Hermann and Hartung (1982) have proposed as a minimal model a reaction sequence involving two closed and one open state and only one Ca^{++} ion involved.

In conclusion, then, the gating of neurotransmitter and voltage dependent channels consists of multi-step reactions that have not yet been completely characterized.

SINGLE CHANNEL CONDUCTANCE AND A CHANNEL BLOCKADE MODEL

The transport rate (conductance) for an ion is determined by the height of energy barriers as well as the depth of the wells on binding sites. For a single ion channel, regardless of the number of barriers, the channel conductance (G), shows saturation with ion activity in the same way that the velocity of an enzymatic reaction saturates with substrate concentration (e.g., Lauger, 1973):

$$G = \frac{G_{\max} a}{K_d + a} \quad (13)$$

where G_{\max} is the maximal conductance, a is ion activity and K_d the dissociation constant.

The relationship of G_{\max} and K_d with the energy values of the peaks (p) and wells (w) for a channel having n equal barriers and n^{-1} wells (measured at zero volt and considering the external solutions as zero energy) has been given by Coronado et al. (1980):

$$G_m \propto \frac{\sum_{i=1}^n \exp(-p/RT)}{\sum_{i=1}^n \exp(-w/RT)} \quad (14)$$

$$K_d \propto \sum_{i=1}^n \exp(-w/RT) \quad (15)$$

According to these expressions, the maximal channel conductance is a function of both the energy peaks and energy wells while the dissociation constant depends only on the depth of the energy wells.

The first computation of single channel conductances were based on estimates of the number of TTX binding sites (for the squid Na^+ channel) and from the rate of TEA blocking (for the squid K^+ channel) (Moore et al., 1967; Armstrong, 1966). These estimations clearly showed that the rate of ion movement was too high to be carrier mediated inasmuch as values of the order of 10^8 ions/sec) were obtained for these two channels. Later, single channel conductance data coming from noise analysis and single channel recordings have been obtained for a wide variety of channels. The range of conductance values found for different channels is enormous. As some examples, the estimated single channel conductance (noise analysis) of the Ca^{++} channel from snail neurons and chromaffin cells ranges from 0.06 to 0.5 pS when extracellular Ca^{++} is 1 mM, while a 400 pS Cl^- channel has been described from patch clamp recordings in rat myotubes (Tsien, 1983; Kostyuk, 1981; Blatz and Magleby, 1983; Latorre and Miller, 1983).

Very different energy barriers must underlie these very different rates of ion permeation. The very small conductance of Ca^{++} channels could be explained by the existence of a very deep well for Ca^{++} ions along the channel as discussed in the section on channel selectivity (Kostyuk, 1981; Kostyuk et al., 1980). On the other hand, the very high conductance, together with the high selectivity displayed by some K^+ channels will be discussed later in relation to the results presented in the following chapters.

Channel conductance can, in principle, be affected by membrane surface charge. Cell membranes bear a net negative surface charge (Ebel, 1967) and, accordingly, cations are accumulated while anions are depleted near the surface of the membrane. Thus, if the mouth of a channel lies at the membrane solution/interface, one can expect that the actual ion concentration felt by the channel is not the bulk ionic concentration but that determined by the presence of fixed surface charges in the membrane. Accordingly, in order to describe channel conductance using eq. (12), the activity term has to be modified to describe the actual ion concentration available to the channel. Effects of surface charge have been observed in artificial lipid bilayers for the conductance of the gramicidin channel and the K^+ channel from sarcoplasmic reticulum (Apell et al., 1979; Bell and Miller, 1983). On the other hand, for several channels studied on intact cells or bilayers, it has been found that surface charge affects the channel gating properties but not the channel conductance (Begenisich, 1975; Hille et al., 1975; Horn and Patlak, 1980; White and Miller, 1981; Föhlmeister and Adelman, 1982). As an explanation of the differential effect of surface charge on channel gating vs channel conduction, Hille et al. (1975) and Begenisich (1975) have proposed that the entrance of the channel is sufficiently away from the membrane surface so as not to be affected by the membrane surface charge. Possible physical models consider that channels can protrude from the surface of the membrane into the aqueous phase or that the conducting pore could be surrounded by a disk of protein devoid of charge (Hille et al., 1975; White and Miller, 1981; Cecchi et al., 1981; Apell et al., 1979).

The quantitative expression for surface potential (ψ) as a function of charge density (σ) and bulk ionic concentration (C) is given by the Gouy-Chapman theory for univalent electrolytes (McLaughlin, 1977).

$$\sinh \left(\frac{F\psi}{2RT} \right) = \frac{136\sigma}{\sqrt{C}} \quad (16)$$

where σ is expressed in charges/ \AA^2 , C in M and ψ in mV; F , R , and T have their usual meaning.

The value of the surface potential is a function of the distance (x) from the membrane and this relationship is given by (McLaughlin, 1977):

$$\psi(x) = \frac{2RT}{F} \ln \left(\frac{1 + \alpha \exp(-Kx)}{1 - \alpha \exp(-Kx)} \right) \quad (17)$$

where K is the reciprocal Debye length given by:

$$K = \left(\frac{2F^2 K_b}{\epsilon_0 \epsilon RT} \right)^{1/2} \quad (18)$$

and

$$\alpha = \frac{\exp\left(\frac{F\psi_0}{2RT}\right) - 1}{\exp\left(\frac{F\psi_0}{2RT}\right) + 1} \quad (19)$$

where ϵ and ϵ_0 are the dielectric constant and permittivity of the free space and K_b the bulk $[K^+]$. Inasmuch as the surface potential varies with distance from the membrane, the $[K^+]$ also becomes a function of

distance and can be described by a Boltzman distribution

$$K(x) = K_b \exp (-F\psi(x)/RT) \quad (20)$$

where $K(x)$ is the $[k]$ at distance x from the membrane and $\psi(x)$ is defined by eq. (17).

Thus, knowing the charge density and the bulk ionic concentration, it is possible to obtain values for the surface potential and $[K^+]$ at different distances from the plane of the membrane. In a bilayer system where these parameters (charge density and bulk ionic concentration) are under experimental control, it is possible to quantitate the effect of surface charge on channel conductance (Bell and Miller, 1983).

Channel Blockade: For single ion channels, we just saw that conductance and permeating ion concentration are related by a Michaelis-Menten type of relationship; i.e., we can identify a maximum conductance, $G_m(i)$, and a dissociation constant, $K_d(i)$. Now, if a second species of ions having different $G_m(i)$ and $K_d(i)$ values is added to the solution bathing the channel, the two ion types will compete for conduction through the channel. If the second ion can enter the channel but does not permeate [$G_m(i) = 0$], this ion becomes a blocker.

I shall briefly outline the blockade model proposed by Woodhull (1973) to account for the voltage dependent blockade of Na^+ channels by protons in squid axon. This approach has been very useful in the understanding of blockade in many different systems (Armstrong, 1973; Neher and Steinbach, 1978; Coronado and Miller, 1982; Miller, 1982; Vergara and Latorre, 1983). The model assumes that the blocking ion can

only interact with the open state of the channel and that when the blocking ion is bound to a site in the channel the permeant ion cannot go through. If the site to which the blocker binds is located within the electric field in the channel, the dissociation constant of the reaction is voltage dependent. Therefore, in the presence of the blocker, the channel can be either closed, open or blocked. For the case of a two state open-closed channel, we have:



where α and β are the reaction rates for the gating reaction and K_d is the voltage dependent dissociation constant of the blocking reaction.

The dissociation constant of the reaction is given by:

$$K_d(V) = K_d(0) e^{-z\delta FV/RT} \quad (21)$$

where $K_d(0)$ is the dissociation constant at zero voltage, z is the valence of the blocking ion, δ is the fractional electrical distance at which the blocking site is located, V is the membrane potential, and F , R and T have their usual meaning.

With respect to the kinetics of blockade, there are two possibilities. The first possibility is that the blocking reaction is much faster than the gating reaction. In this case when the channel opens, a fast equilibrium between the open and the blocked state will occur.

If the blockade reaction is faster than the time resolution of the recording system, one will observe an apparent decrease in the single

channel conductance that corresponds to a time averaged value determined by the blocking and unblocking rate constants. Increasing the concentration of blocker will reduce the conductance according to the expression (Coronado and Miller, 1979):

$$\frac{\langle G \rangle}{G_0} = \left(\frac{[B]}{K_d(V)} + 1 \right)^{-1} \quad (22)$$

where $\langle G \rangle$ is the channel conductance in the presence of blocker at concentration $[B]$, G_0 is the unblocked single channel conductance and $K_d(V)$ is the voltage dependent dissociation constant of the blocking reaction defined by equation (21).

Combining equations (20) and (21) results in:

$$\frac{\langle G \rangle}{G_0} = \left(1 + \frac{[B]}{K_d(0)} \exp(z\delta FV/RT) \right)^{-1} \quad (23)$$

This expression can be linearized giving:

$$\ln \left(\frac{G_0}{\langle G \rangle} - 1 \right) = \ln \frac{[B]}{K_d(0)} + \frac{z\delta FV}{RT} \quad (24)$$

Then, from a plot of $\ln (G_0/\langle G \rangle - 1)$ vs voltage the value of δ and $K_d(0)$ can be obtained (Coronado and Miller, 1979).

According to the model, a blocked channel cannot close (R-6). One then expects that the apparent duration of the open state in the presence of the blocker ($\bar{\tau}_o$) should increase according to (Neher and Steinbach, 1978):

$$\tau_o = \frac{1}{\beta} \left(1 + \frac{[B]}{K_d} \right)^{-1} \quad (25)$$

It is also possible that the dwell time in the blocked state is long enough to permit the direct observation of the blocking reaction as brief flickers of the open state conductance (Neher and Steinbach, 1978; Coronado and Miller, 1980).

The second possibility is that the kinetics of the blocking reaction is much slower than the gating reaction. If this is the case, the open/closed transitions due to the gating reaction will be interrupted by periods of inactivity, the blocked intervals (Ohmori et al., 1981; Vergara and Latorre, 1983). Again, if the blocking site is located within the electric field in the membrane, the dissociation constant of the reaction is described by equation ²⁶(20).

If blocking ions interrupt the access of permeant ions to the conduction pathway, they should behave as competitive inhibitors of conduction even though they may not physically reach the same sites as the conducting ions. Furthermore, blocker studies can give information on channel occupancy. For channels where only one ion is allowed within the channel at a given time, blocker and permeant ions can only compete for entrance to the channel (Miller, 1982; Vergara and Latorre, 1983). On the other hand, for channels that can be simultaneously occupied by more than one ion, it is possible that permeant ions can "knock off" blocker ions (increase the rate constant of blocker exit from their binding site) (Armstrong, 1975b).

In conclusion, then, although we are far from understanding the process of ion permeation in complete molecular terms, quite a lot has been learned from the study of channel properties. Selectivity studies

have given some insight on the type of groups and type of interactions occurring at the selectivity filter. The study of channel gating has shown that the opening of channels occurs through a complicated sequence of reactions involving several transitions. On the other hand, conductance and blockade studies have provided information on the architecture of channels.

CHAPTER 2

MATERIALS AND METHODS

Preparation of Transverse Tubule Membrane Vesicles

Transverse tubule (TT) membrane vesicles were prepared from adult rabbit fast skeletal muscle microsomes as described by Fernandez et al. (1980). The method consists of separating microsomal fractions of different densities on discontinuous sucrose gradients. Removal of contaminant Sarcoplasmic Reticulum (SR) was done through a calcium phosphate loading procedure in the presence of ATP. This procedure is summarized as follows:

Microsome suspensions (4 ml) containing 12-20 mg protein/ml in 0.3 M sucrose, 20 mM Tris maleate pH 7.0 were centrifuged in a discontinuous sucrose density gradient at 85,000 x g for 16 hours in an SW 27 rotor.

The gradients consisted of two layers of sucrose solutions (w/v), 20 ml of 35% and 14 ml of 25% sucrose in 20 mM Tris maleate pH 7.0. The surface membrane (SM) fraction that bands at the interface of the 25% and 35% sucrose layers, containing the partially purified TT, was collected from the top of the centrifuge tubes with a Pasteur pipette, diluted approximately 10 times with 20 mM Tris maleate pH 7.0 and collected by sedimentation at 150,000 x g for 30 minutes in a Ti 45 rotor. The pellets were homogenized in a small volume of 0.3 M sucrose, 20 mM Tris maleate pH 7.0 with a glass homogenizer. The heavy, intermediate and light SR fractions that formed the gradient pellet were discarded. The SM fraction is contaminated by vesicles of SR origin, as indicated by SDS electrophoresis retrograms and by a high level of Ca^{++} uptake activity (Fernandez et al., 1980). To remove the vesicles of sarcoplasmic

reticulum origin, the SM fraction was incubated in a solution containing 50 mM K^+ phosphate pH 7.4, 5 mM $MgCl_2$, 0.15 M KCl, 0.3 mM $CaCl_2$ and 2 mM ATP (loading solution). After an incubation period of 20 minutes at 22° C, the vesicles were collected by centrifugation at 150,000 x g, resuspended in a small volume (2-3 ml) of loading solution and layered on top of a two layer discontinuous density gradient consisting of 6 ml each 50% and 35% (w/v) sucrose in loading solution. After centrifugation at 150,000 x g for 75 minutes in an SW 40 Ti rotor, two fractions separated. The unloaded fraction remained on top of the 35% sucrose layer and was identified as purified TT vesicles by the following criteria, discussed in detail by Roseblatt et al. (1981);

- i) purified antibodies against this fraction do not cross react with SR or surface membrane;
- ii) this fraction has a characteristic protein pattern on SDS gels, very different from that of SR (which is the main component of the muscle microsomal fraction);
- iii) this fraction has a much higher cholesterol content than either crude microsomes, plasma membrane, or SR;
- iv) this fraction has a phospholipid content per mg protein twice as high as that of skeletal muscle, SR and plasma membrane;
- v) this fraction has a distinct phospholipid composition, with high contents of sphingomyelin and phosphatidylserine;

vi) this fraction contains a Mg^{++} -activated ATPase not found in SR.

Furthermore, Moczydlowski and Latorre (1983) used the differential ouabain/TTX binding ratio for TT and surface membrane (Jaimovich et al., 1976; Venosa and Hordwicz, 1980) as a criterium to follow purification of the two membrane systems. They found that the rabbit light microsomal fraction just described indeed has the low ratio of ouabain/STX binding sites expected for TT membranes. The TT fraction was collected from the top of the gradient and was diluted about ten-fold in 20 mM Tris/maleate, pH 7.0 in order to remove excess sucrose. It was centrifuged and resuspended in 0.3 M sucrose, 20 mM Tris/maleate pH 7.0 to a final protein concentration of 10-15 mg/ml. It was divided in small aliquots that were kept at $-70^{\circ}C$ and thawed as needed. The frozen preparation maintained channel activity for several months.

Bilayer Formation and Recording System

Planar bilayers were formed by the Mueller et al. (1963) brush technique. A plastic or glass rod was dipped into either 70%/30% mixtures of phosphatidylethanolamine (PE) and phosphatidylserine (PS), 100% PE or 100% PS in decane. (Unless specified, the 70%/30% mixture was used.) The lipid concentrations were 20-50 mM. Membranes were painted by "brushing" the rod over a hole (300-1000 μ m diameter) in a polystyrene partition separating two aqueous solutions. The aqueous solutions, unless otherwise specified, were 0.1 M KCl, 10 mM 4-morpholinepropanesulfonic acid (MOPS) adjusted to pH 7.0 with Tris base. Calcium concentrations from 3×10^{-8} M to 10^{-6} were obtained using

Ca⁺⁺-EGTA buffer solutions; concentrations from 10⁻⁶ M to 10⁻² M were obtained by addition of Ca⁺⁺ from concentrated stock solutions. The [Ca⁺⁺] of the stock solutions was determined by atomic absorption spectrophotometry (Perkin Elmer [Norwalk, CT] atomic absorption spectrophotometer model 5000).

Protein (final concentration 1-70 µg/ml) was added to one side of the chamber (cis side). After protein addition, the solution on the cis side was stirred with magnetic fleas until channels incorporated into the membrane (see below). A DC potential bias of ± 20-50 mV was applied across the membrane from an adjustable source connected to the cis side of the chamber. The current flowing through the membrane as the result of the applied potential difference was measured by an LF 157 operational amplifier (National Semiconductor, Santa Clara, CA) wired in a current-to-voltage converter configuration with a 10⁹ Ω feedback resistor. The amplifier was connected to the trans side of the bilayer and accordingly this side was virtual ground. Ag/AgCl electrodes were used in series with agar salt bridges for connection to the chamber pools. The resolution of the system was ~1 pA in amplitude and 1 ms in time for a membrane area of 7 x 10⁻⁴ cm². Current was monitored on a strip chart recorder (General Scanning RS2-5P, Boston, MA) and/or in an oscilloscope and was simultaneously stored on FM tape (Lockheed 4D 4714 recorder, Sarasota, FL). Current was taped at either 30 inches per second (10 KHz bandwidth) or 15/16 inches per second (300 Hz bandwidth). Appropriate filter levels for data analysis were chosen later by using a low-pass active filter (Krohn Hite 3202, Avon, MA). Unless otherwise stated, currents were filtered at 300-1500 Hz. Figure (4) shows a schematic diagram of the procedure of vesicle preparation and of the recording set up.

Channel Incorporation

After addition of protein, the bilayer conductance increased in discrete events as shown on Fig. (5). Each event represents the irreversible incorporation of a channel in the membrane inasmuch as extensive washing of the cis compartment with vesicle-free solution does not modify the membrane conductance value reached before washing. Some of the experiments presented here were done in bilayers containing only one or just a few channels (microscopic measurements) while others were done in membranes containing a large number of channels (macroscopic measurements). For single channel experiments either a low concentration of protein was used or, after the first incorporation event occurred, the cis chamber was perfused with vesicle free solution. The new solution had either the same composition or was different (for the selectivity experiments, see Results). Solutions were changed by using two volume-matched syringes in a push-pull configuration. The time which elapsed between the addition of protein and the first conductance jump was highly variable, ranging from 2 minutes to 1 hour or two. The presence of an osmotic gradient (cis side hyperosmotic) sped up the process but was not 100% reproducible. The incorporation process was not characterized any further. Typically, membranes lasted 1-2 hours, although sometimes 5 hour records were obtained. All measurements were done at room temperature (18-21°C). Specific experimental details will be described on the different chapters.

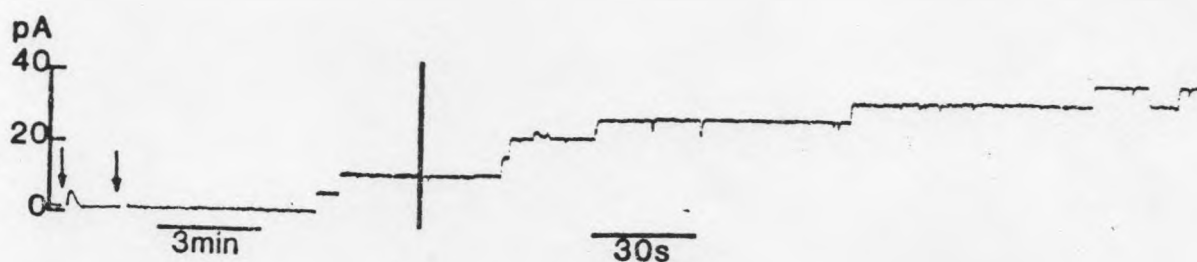


Fig. 5. Time course of channel incorporation. The current vs time record was obtained after the addition of TT vesicles to a bilayer formed in 100 mM KCl, 10 mM MOPS-Tris, pH 7.0, 5 M Ca^{2+} . (a) indicates Ca^{2+} addition to the cis chamber to a final concentration of 1 mM. (b) indicates the addition of membrane vesicles. The vertical mark indicates a change in the time scale. The applied voltage was 20 mV. Each current step corresponds to a conductance change of 230 pS. Record filtered at 100 Hz.

Data Analysis

Conductance values were determined mostly by hand by measuring the height of the current fluctuations obtained at a given voltage clamp potential directly on the chart recorder or after replaying of the tape recorder. Dwell times in the open and closed states were analyzed in a Mine 11/23 computer (Digital Equipment Corp., Marlboro, MA) or in a signal processor model TN-1710 (Tracor Northern, Madison, WI). The average conductance for macroscopic experiments was obtained by heavily filtering the current records (1 Hz).

Chemicals

Lipids (PE and PS) were purchased either from Avanti Polar Lipids (Birmingham, AL) or from Supelco (Bellefonte, PA). Decane and triethylnonylammonium were obtained from Eastman Organic Chemicals (Rochester, NY). All inorganic salts--namely, KCl, NaCl, LiCl, RbCl, CsCl, KCH_3COO , TlCH_3COO , CaCl_2 , BaCl_2 , MgCl_2 , SnCl_2 , CdCl_2 , KH_2PO_4 --were puratronic grade from Alfa/Ventron (Danvers, MA) or reagent grade from Fisher Scientific Co. (Boston, MA). EGTA, MOPS, Tris base, Tris maleate, ATP, apamin and quinine were obtained from Sigma Chemical Co. (St. Louis, MO). Sucrose ultra pure was purchased from Schwartz/Mann Inc. (Spring Valley, NY).

CHAPTER 3

Gating Characteristics of the Ca^{2+} -Activated K^+ Channels

Summary

This chapter shows that the macroscopic conductance induced by the interaction of TT membrane vesicles with artificial lipid bilayers results from the incorporation of Ca^{2+} -dependent K^+ channels into the bilayers. The macroscopic conductance is both voltage and Ca^{2+} dependent. This voltage and Ca^{2+} dependence is explained at the single channel level by the effect of these two parameters on the fraction of time that a channel spends in the open state. The channels are also activated by Cd^{2+} , but not by Mg^{2+} , Ba^{2+} or Sr^{2+} . Potassium, Cs^+ and Tl^+ ions seem to compete with Ca^{2+} for the activating site but forming an inactive complex that does not lead to channel opening.

Results

Voltage Dependence of the Macroscopic Conductance

Figure 6 shows a current voltage (I-V) curve for a membrane containing several channels. While at positive potentials the current increases linearly with voltage, at negative potentials a strong rectification is observed. In other words, the membrane conductance is constant for potentials higher than +20 mV and decreases for more negative potentials.

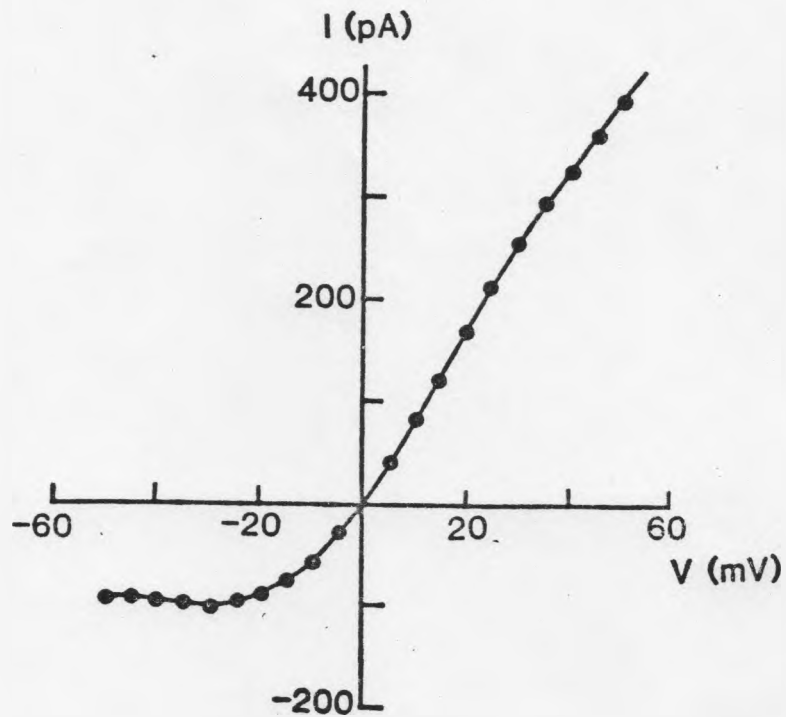


Fig. 6. Macroscopic (~35 channels) current-voltage curve. After an initial "burst" of incorporation events, current reached a steady state. At that moment, the membrane potential was varied between ± 60 mV. The resulting currents, filtered at 10 Hz, were measured. The aqueous solution was 100 mM KCl, 10 mM MOPS-Tris, pH 7, $100 \mu\text{M Ca}^{2+}$. The membrane contained 35 channels.

Ca²⁺ Dependence of the Macroscopic Conductance

For a many channel membrane the current measured at a fixed potential is a function of the concentration of Ca²⁺ present on the cis side of the bilayer. Fig. 7 shows a current vs time record obtained at +50 mV for a membrane containing five channels. (The fluctuations on the current level are due to a Ca²⁺-induced channel block that will be described on Chapter 6). At the time indicated by the arrow, EGTA was added to the cis compartment. Addition of EGTA decreases the concentration of ionic Ca²⁺ from 1 mM to 50 nM. After EGTA addition, the current decreased to the level shown by the bare bilayer before the addition of protein. This effect is completely reversible inasmuch as after readdition of Ca²⁺ the current recovers to its original level. The decrease in membrane current cannot be attributed to a direct effect of EGTA on the channels. We used Ca²⁺ buffers made with different Ca²⁺/EGTA ratios and the final value of the membrane conductance obtained was always related to the free [Ca²⁺] irrespective of the amount of EGTA on the buffer. The Ca²⁺ effect on membrane conductance is asymmetric inasmuch as changes in trans [Ca²⁺] do not affect the current. Moreover, the effect of Ca²⁺ on the membrane conductance is specific. Figure 8 shows that Mg²⁺ cannot replace Ca²⁺ on its channel activating role and also shows the reversibility of the Ca²⁺ activating effect. Thus, the current in the presence of 5 μM Ca²⁺ cis decreases to the bare bilayer level after reducing the [Ca²⁺] to 25 nM (Figs. 8A,B). Mg²⁺ ions do not cause any activation of the current even when added to a final concentration of 2 mM (Fig. 8C). Addition of Ca²⁺ to a final concentration of 1 mM causes the current to increase to a level higher than that shown on Fig. 8A (Fig. 8D).

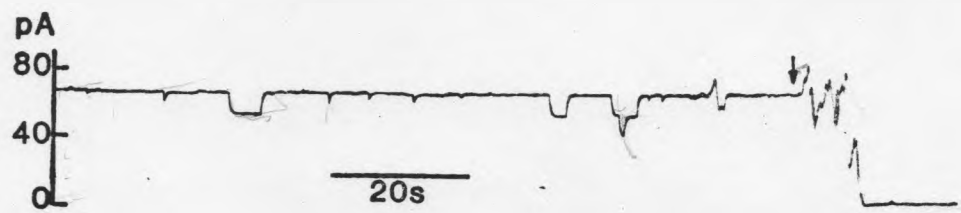


Fig. 7. Current trace as a function of time obtained at 50 mV for a membrane containing 5 channels. The aqueous solutions were 100 mM KCl, 10 mM MOPS-Tris, pH 7.0, 1 mM Ca^{2+} . At the time indicated by the arrow, EGTA was added (final concentration 4.2 mM) to the cis side only. The final free $[\text{Ca}^{2+}]$ was 50 nM.

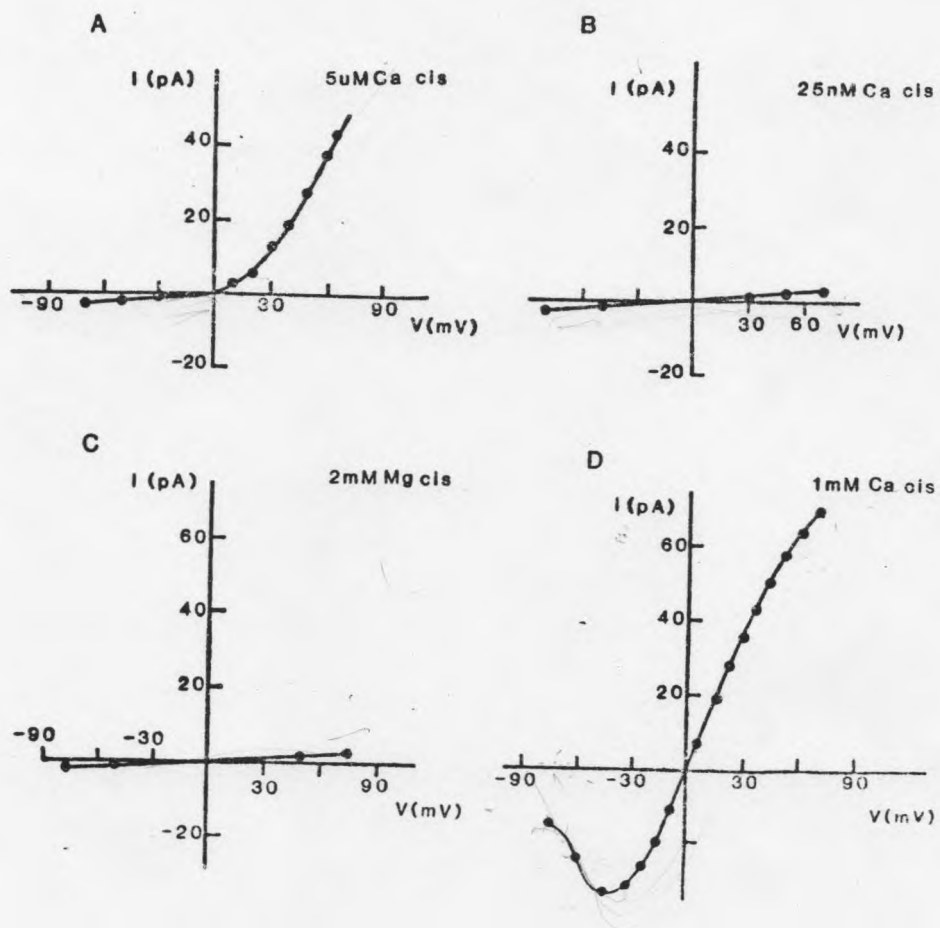


Fig. 8. Macroscopic current-voltage curves under various experimental conditions. The aqueous solution was 100 mM KCl, 10 mM MOPS, pH 7.0 and contained initially 5 μ M Ca^{2+} (A). EGTA was added to the cis compartment in order to reduce free $[\text{Ca}^{2+}]$ to 25 nM (B). Mg^{2+} ions were added to the cis and trans compartments up to a final concentration of 2 mM (C). Ca^{2+} ions were added to a final free $[\text{Ca}^{2+}]$ of 1 mM (D).

A replot of the data shown on Fig. 8 as conductance vs voltage (Fig. 9) shows that changes in the cis $[Ca^{2+}]$ shift the conductance-voltage curve along the voltage axis without changing its shape (c.f. curves 1 and 2). The reduction in the $[Ca^{2+}]$ from 1 mM to 25 nM makes the observed conductance decrease to a small value, independent of voltage (curve 3). Mg^{2+} does not change the magnitude or the shape of the residual voltage independent conductance (curve 4).

If we assume that the channels activated by Ca^{2+} behave as a two state open/closed system, then the voltage dependence of the macroscopic conductance is that described by eq. (8) in the introduction. A replot of the data as $\ln [G(V)/G_m - G(V)]$ vs voltage (Fig. 9 inset) shows that the points lie on a straight line and, therefore, the data are consistent with the Boltzmann relationship given by eq. (8). At 1 mM Ca^{2+} , n (the number of equivalent charges moving across the whole transmembrane field during the open/closed transition) is 2.2 and V_0 (the potential at which the number of open channels is equal to the number of closed channels) is -15 mV. At $5 \mu M Ca^{2+}$, n is 2.0 and V_0 is +67 mV. Therefore, it appears that Ca^{2+} modifies the equilibrium distribution between open and closed channels but not the number of gating charges.

Single-Channel Properties

From eq. (1) we see that the observed effects of Ca^{2+} and voltage on the macroscopic conductance could reflect an effect on the single channel conductance or in the channel gating properties. The next step after the macroscopic characterization of the Ca^{2+} activated current was then to characterize the effect of voltage and Ca^{2+} on the single channel behavior.

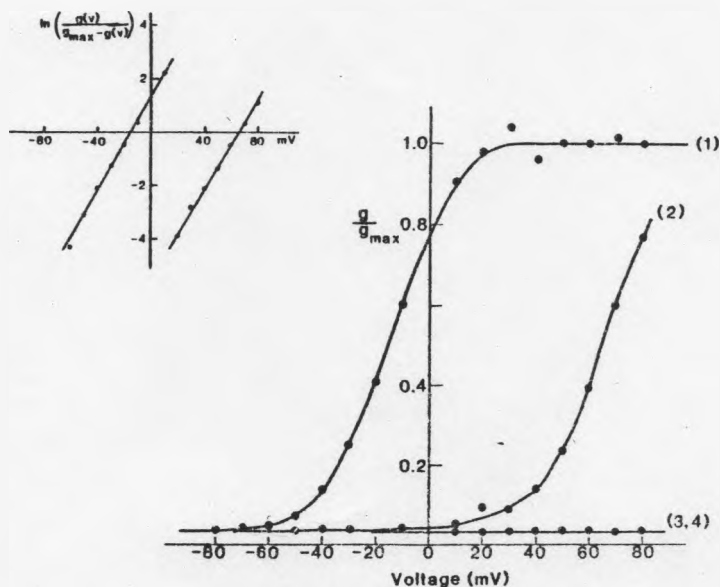


Fig. 9. Steady-state conductance characteristics for the experiment illustrated on Fig. 8. G_{max} was defined as the conductance at +60 mV and 1 mM Ca^{2+} and was 230 nS. Curve 1: normalized conductance in 1 mM Ca^{2+} . Curve 2: normalized conductance in 5 μ M Ca^{2+} . Curves 3 and 4: normalized conductances in the presence of 25 nM Ca^{2+} and 2 mM Mg^{2+} . **Inset:** a replot of the points in curves 1 and 2 as $\ln[g(V)/G_{max} - g(V)]$ vs V. The solid lines are the best fit to eq. (9).

Current fluctuations due to the presence of a single channel in the membrane are shown on Fig. 10. Two processes with different kinetics are evident. The channel can rapidly fluctuate between an open and a closed state (region labeled b) or can remain closed for several seconds (region labeled B). The conductance of the open state in 100 mM KCl, 10 mM MOPS-Tris, pH 7.0, is 230 pS. I will characterize first the fast channel kinetics that occurs between quiescent periods.

Single Channel I-V Curve

A plot of the height of the current jumps (e.g., Fig. 12) observed as a function of the applied voltage is shown on Fig. 11. Between +60 and -60 mV the I-V curve is linear. This result implies that the single channel conductance in this voltage range is voltage independent and, thus, the voltage dependence of the macroscopic conductance (fig. 6) must reside in a different parameter than the single channel conductance.

Fraction of Time The Channel Remains Open as a Function of Membrane Potential

Fig. 12 shows single channel current fluctuations obtained at a constant $[Ca^{2+}]$ for different membrane potentials. It is very clear that the time the channel spends in the open or closed state is a function of the applied voltage. As the voltage is made more positive, the channel dwells more time in the open configuration.

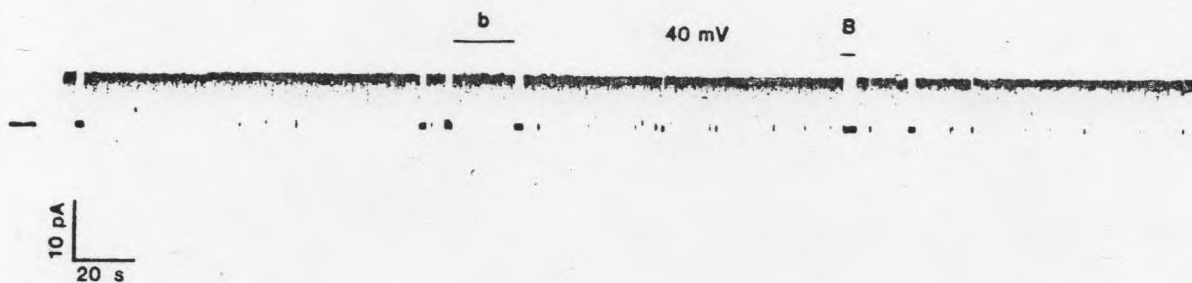


Fig. 10. Current fluctuations due to the presence of a single channel in a membrane. The aqueous solution was 100 mM KCl, 10 mM MOPS-Tris, pH 7.0, 1 mM Ca^{2+} . The membrane potential was 40 mV. Two different processes are evident in the figure. Fast fluctuations in the order of msec as well as long lasting periods of inactivity (seconds).

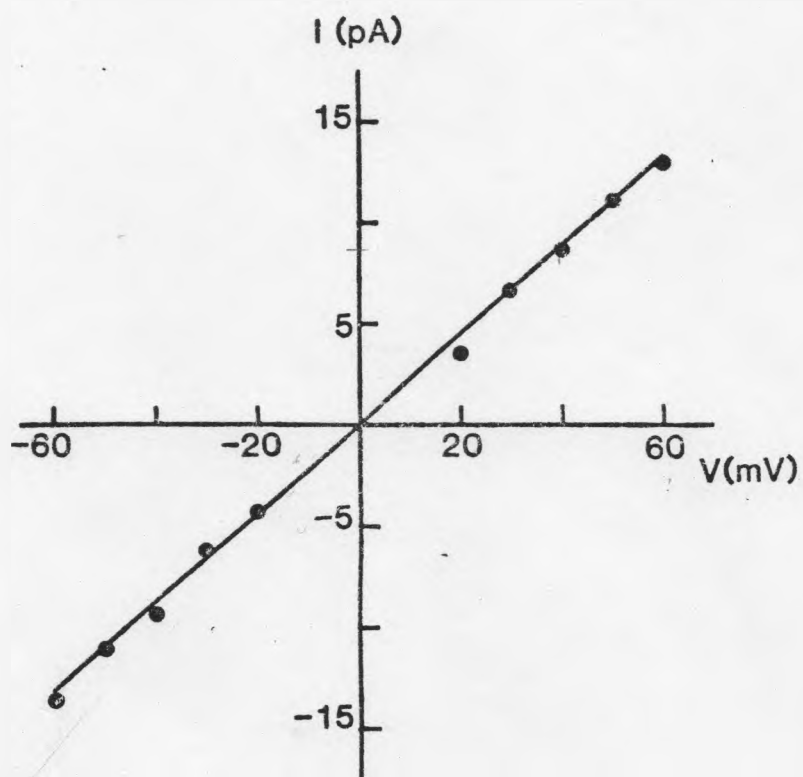


Fig. 11. Current passing through an open channel. The current-voltage curve was obtained by measuring the height of the current jumps for a single channel as the membrane potential was changed. The data was obtained in a membrane under symmetric 100 mM KCl, 10 mM MOPS-Tris, pH 7.0. $[Ca^{2+}]$ was $95 \mu M$. The channel behaves as an ohmic resistor with a slope conductance of 230 pS.

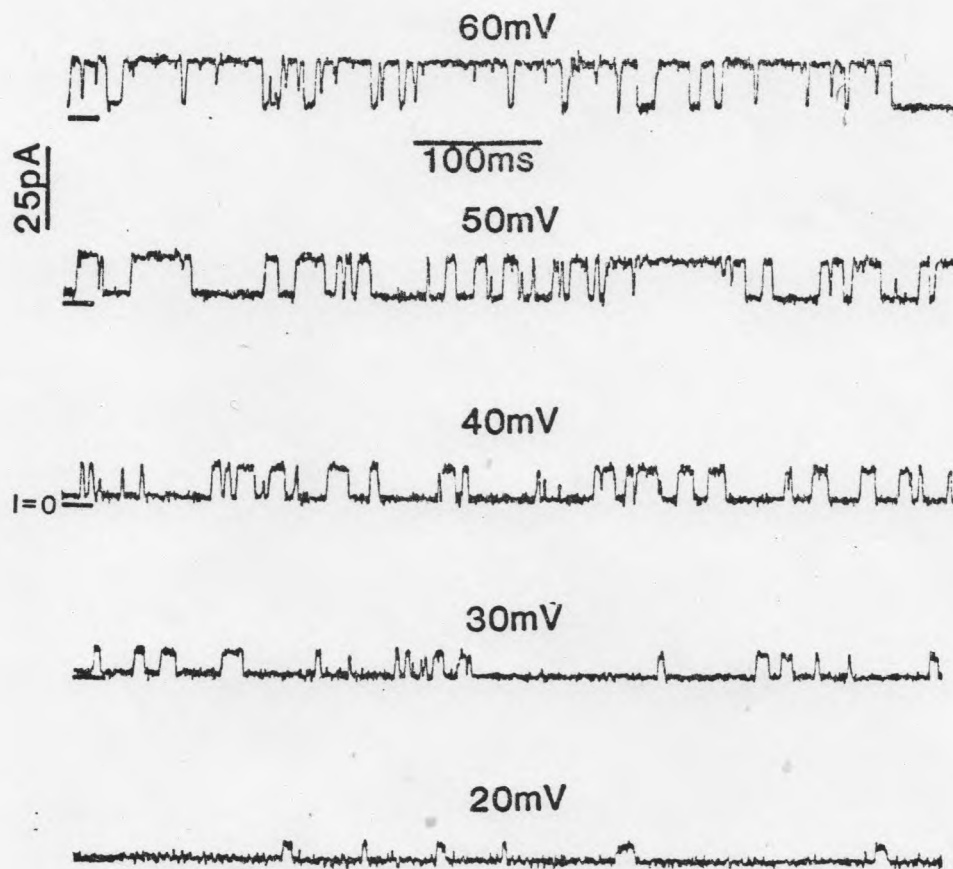


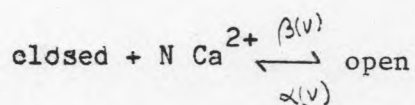
Fig. 12. Current fluctuations due to the presence of a single channel in the membrane at different potentials. $[Ca^{2+}] = 35\mu M$. The lines at the left indicate the zero current level. Note that the current fluctuations amplitudes are proportional to the membrane potential and the mean open time increases as potential increases.

Fraction of Time The Channel Remains Open as a Function of cis [Ca²⁺]

At a constant applied voltage, the fraction of time a single channel dwells in the open configuration is a function of the cis [Ca²⁺] as shown on Fig. 13. The higher the value of cis [Ca²⁺], the higher the fraction of time the channel remains open. However, the channel conductance is not modified by [Ca²⁺]. The results of measurements of the fraction of time that a channel stays open, $f(V)$, at a given voltage and [Ca²⁺] are shown on Fig. 14. The experimental points were fitted to eq. 10 in the introduction. It is possible, then, to use eq. (10) to compare quantitatively the voltage dependence of the single channel with the voltage dependence obtained in membranes with a large channel population. The similarity of the macroscopic channel conductance vs voltage curves (i.e., Fig. 9) and the $f(V)$ vs voltage curves indicate that the channels are independent of each other. Moreover, considering that the single channel I-V curve is linear, the macroscopic voltage dependence must reside on the opening and closing of the individual channels. On the other hand, the macroscopic dependence on cis [Ca²⁺] reflects the shift along the voltage axis of the open/closed equilibrium caused by Ca²⁺ ions.

Number of Ca²⁺ Ions Involved in the Gating Reaction

For a reaction scheme:



(R-7)

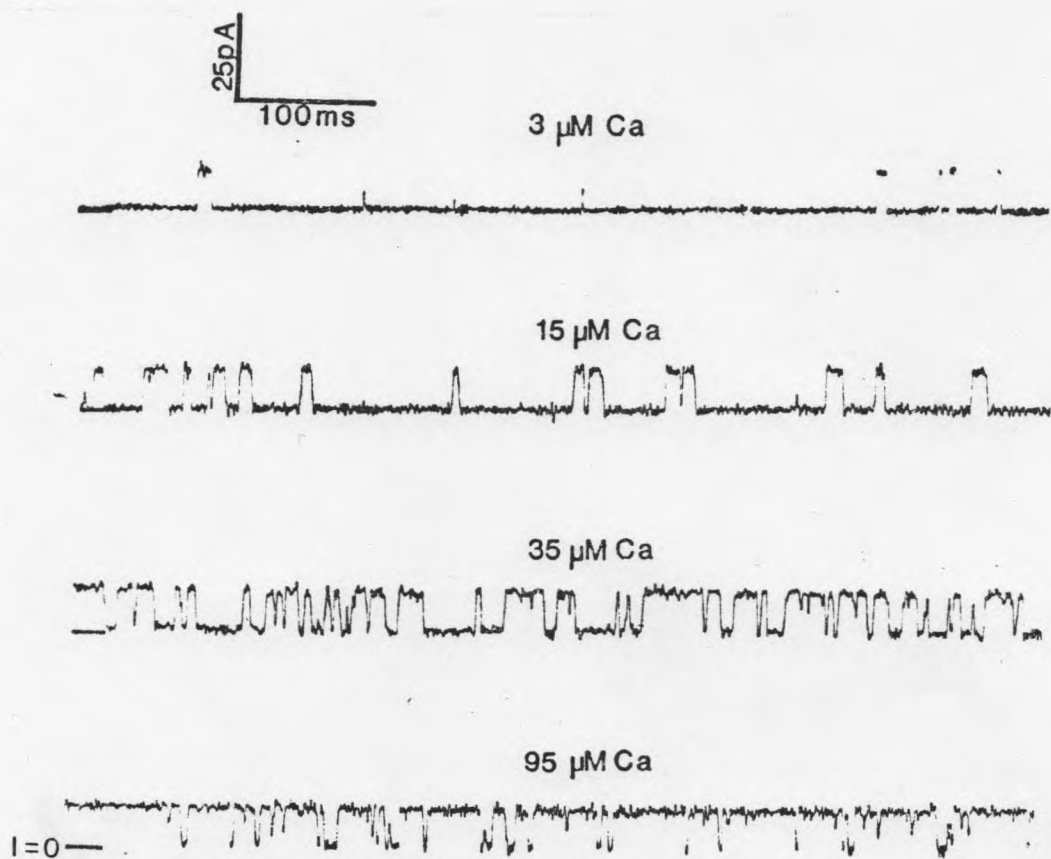


Fig. 13. Effect of $[\text{Ca}^{2+}]$ on channel activity. The current fluctuations were obtained for a single channel membrane when the cis $[\text{Ca}^{2+}]$ was varied by successive additions of Ca^{2+} from concentrated stock solutions. Trans $[\text{Ca}^{2+}]$ was $95 \mu\text{M}$ and the applied voltage was +50 mV. The lines at the left indicate the zero current level.

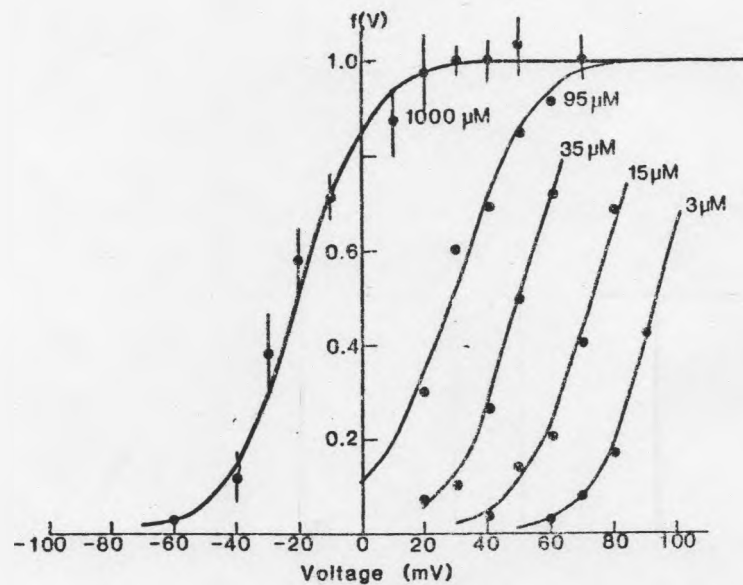


Fig. 14. Fraction of time a channel is in the open state [$f(V)$] as a function of voltage at different [Ca^{2+}]. The curves were drawn according to eq. (11). Curve 1: 3 μM Ca^{2+} , $n = 2.3$, $V_0 = 94$ mV. Curve 2: 15 μM Ca^{2+} , $n = 2.1$, $V_0 = 73$ mV. Curve 3: 35 μM Ca^{2+} , $n = 2.2$, $V_0 = 50$ mV. Curve 4: 95 μM Ca^{2+} , $n = 2.0$, $V_0 = 32$ mV. Curve 5: 1 mM Ca^{2+} , $n = 2.0$, $V_0 = 20$ mV. For curve 5 the $f(V)$ values are the mean \pm S.D. for three different channels. All other curves are for a single channels.

the fraction of open time $f(V)$ according to eq. (10) is

$$f(V) = \frac{\beta [Ca]^{2+}}{\beta [Ca]^{2+} + \alpha} \quad (26)$$

eq. (20) can be rearranged as

$$\frac{1 - f(V)}{f(V)} = \frac{1}{K_{eq} [Ca]^{2+}} \quad (26a)$$

where $K_{eq} = \frac{\beta}{\alpha}$

Accordingly, the slope of $\log - \log$ plots of the open/closed equilibrium vs $[Ca^{2+}]$ will give the number of Ca^{2+} ions, N , involved in the reaction. The data of Fig. 14 have been replotted this way (Fig. 15) and show a slope of 2, suggesting that at least two Ca^{2+} ions are necessary to activate a channel fully. The figure also includes data for the rat muscle Ca^{2+} activated K^+ channel showing that these two preparations differ with respect to their Ca^{2+} sensitivity but not with respect to the number of Ca^{2+} ions involved in the reaction.

Effect of Ca^{2+} and Voltage on the Mean Open and Mean Closed Times of the Channel

Fig. 16 shows a plot of the channel mean open (Fig. 16A) and mean closed (Fig. 16B) times as a function of membrane potential for different $[Ca^{2+}]$. The results show that both dwell times are voltage and $[Ca^{2+}]$ dependent. The $[Ca^{2+}]$ dependence of both, mean open and mean closed times, together with the fact that at least two Ca^{2+} ions are involved in

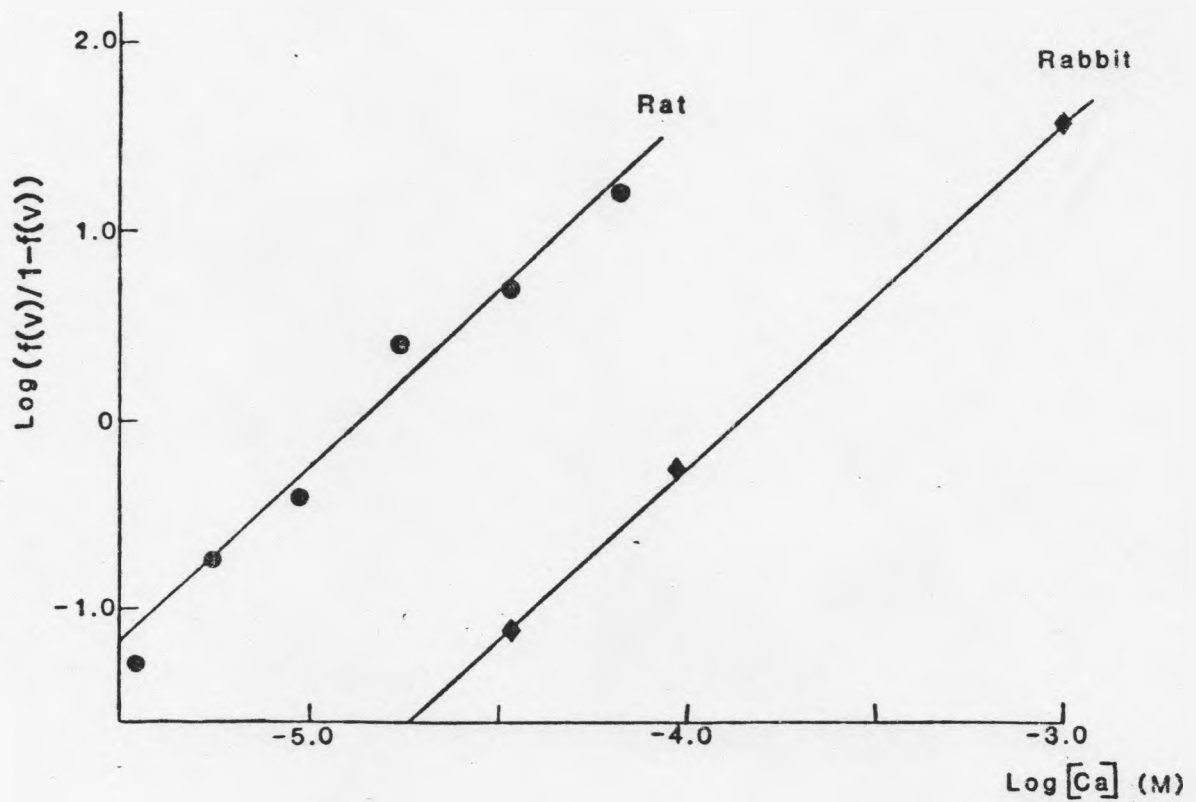


Fig. 15. Open-closed equilibrium as a function of $[Ca^{2+}]$ for the rabbit and rat Ca^{2+} -activated K^+ channels. The data for the rabbit channel were taken from Fig. 14 for a membrane potential of 20 mV. The figure also shows data for the rat Ca^{2+} -activated K^+ channel at the same potential. The two channels differ in sensitivity as shown by the displacement of the curves along the $[Ca^{2+}]$ axis. Both curves have a slope of 2.

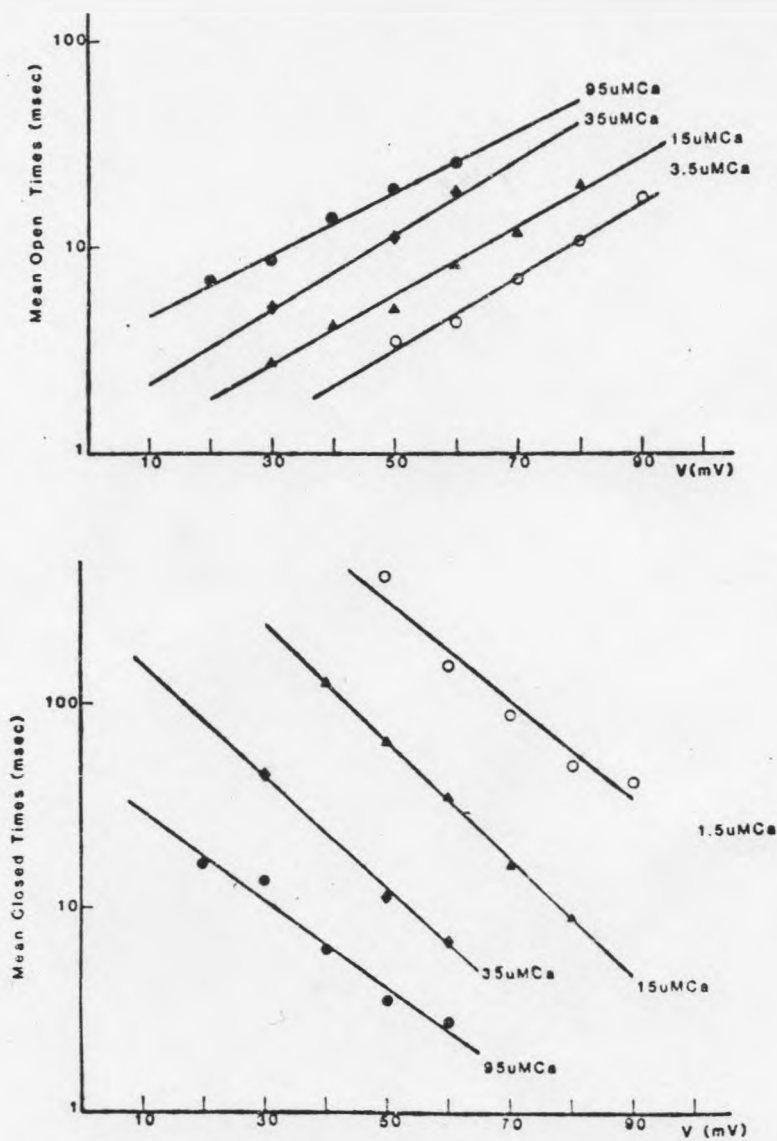


Fig. 16. Channel mean open (A) and mean closed times (B) as a function of membrane potential for different cis $[Ca^{2+}]$.

the gating reaction are consistent with a reaction sequence having a minimum of two open states.

Channel Activation by Other Divalent Cations

Fig. 17 shows current fluctuations in the presence of $10\ \mu\text{M}\ \text{Ca}^{2+}$ and after the addition of 10 and $30\ \mu\text{M}\ \text{Cd}^{2+}$. Clearly, as the $[\text{Cd}^{2+}]$ is increased, there is an increase in the fraction of time the channel stays open at a fixed potential.

For the experiment shown on Fig. 16, the fraction of open times, $f(V)$, were 0.52, 0.74 and 0.80 for $10\ \mu\text{M}\ \text{Ca}^{2+}$, $10\ \mu\text{M}\ \text{Ca}^{2+}$ plus $10\ \mu\text{M}\ \text{Cd}^{2+}$, and $10\ \mu\text{M}\ \text{Ca}^{2+}$ plus $30\ \mu\text{M}\ \text{Cd}^{2+}$, respectively. If Cd^{2+} ions would activate the channel as efficiently as Ca^{2+} ions do, the expected $f(V)$ values for the two different Cd^{2+} concentrations tested are 0.8 and 0.94 (estimated from the slope of two obtained for the log - log plots of the open/closed equilibrium vs $[\text{Ca}^{2+}]$ shown on Fig. 15). Therefore, Cd^{2+} is not as effective as Ca^{2+} to activate the channel. Even though Cd^{2+} ions can activate the channel, they produce an irreversible damage at concentrations above $300\ \mu\text{M}$. Current fluctuations cannot be recovered even after extensive perfusion of the Cd^{2+} containing compartment with a Cd^{2+} -free solution. Neither Sr^{2+} nor Ba^{2+} cause channel activation. Moreover, Ba^{2+} ions cause a slow blockade of the channel that will be discussed in Chapter 6.

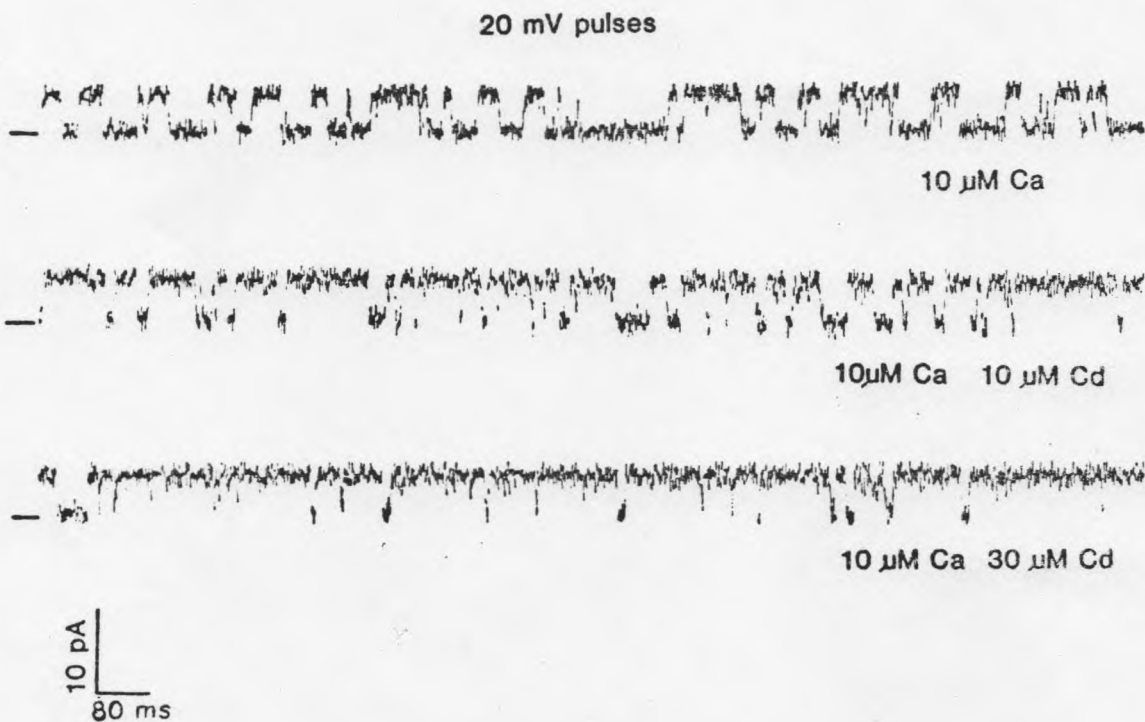


Fig. 17. Effect of Ca^{2+} on the mean open time of the channel. The first trace shows current fluctuations in the presence of symmetric 100 mM KCl, 10 mM MOPS-Tris, pH 7.0 and $10\ \mu\text{M}$ Ca^{2+} at +20 mV. Under these conditions the fraction of open time [f(V)] was 0.52. The second trace shows current fluctuations after Ca^{2+} ions were added to the ois side to a final concentration of $10\ \mu\text{M}$. The fraction of open time under these conditions increased to 0.74. The third trace shows current fluctuations when the [Ca^{2+}] on the ois side was increased to $30\ \mu\text{M}$. The fraction of open time under these conditions was 0.80. The lines at the left indicate the zero current level.

Effect of Monovalent Cations on Channel Gating

Fig. 18 shows current fluctuations in the presence of $100\ \mu\text{M}\ \text{Ca}^{2+}$ at two different K^+ concentrations. It is evident from the figure that as the $[\text{K}^+]$ is increased, the fraction of time the channel stays open decreases. I have considered this as an indication that K^+ ions can compete with Ca^{2+} ions for binding to the activating site(s) but forming a complex that does not lead to channel opening. In the presence of Tl^+ and Cs^+ ions, the rate of channel opening decreases dramatically as if these ions could bind to the Ca^{2+} activating site(s) but form an "inactive complex" (see also Selectivity section).

Discussion

I have found that the channels always incorporate in the membrane with the same orientation and in a stepwise manner. If fusion between the channel containing vesicles and the bilayer is the mechanism of incorporation, it would mean that on the average the vesicles contain at most one channel. Freeze etching electronmicrographs of the TT vesicles show that indeed the density of particles, presumed to be proteins, is very low (Mario Roseblatt, unpublished results).

From the $[\text{Ca}^{2+}]$ and voltage dependence of the channel, we can identify the cis facing part of the channel as the region facing the intracellular compartment in the cell. It is surprising that none of the characteristics that the channel presents in cell membranes (Pallota et al., 1981; Barret et al., 1982; Methfessel and Boehm, 1982; Wong et al., 1982; Maruyama et al., 1983; Adams et al., 1982; Marty, 1981; 1983) seem

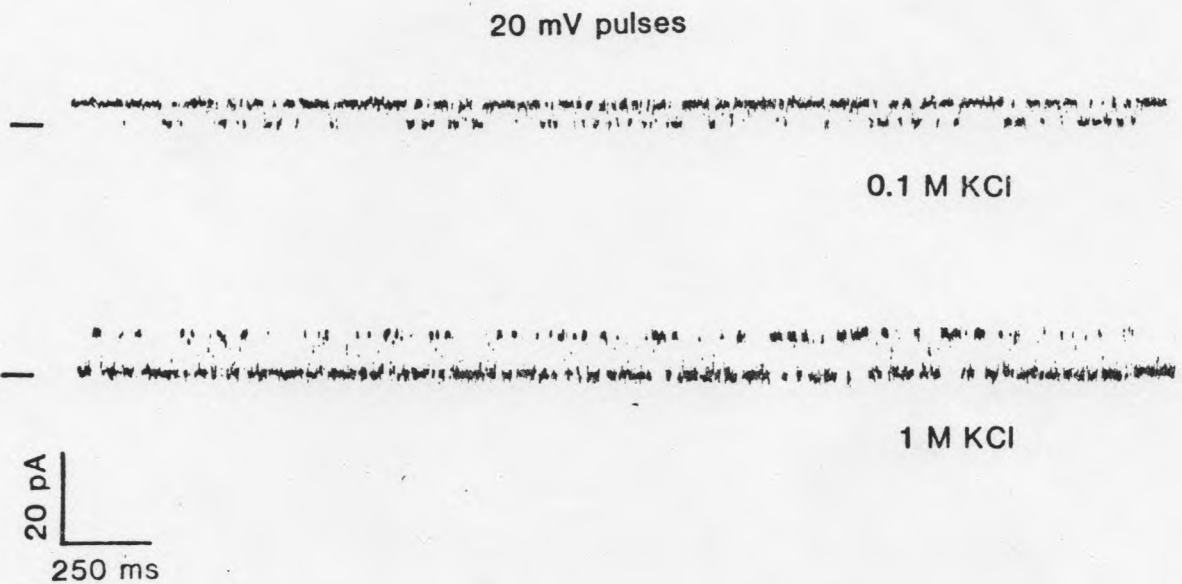


Fig. 18. Effect of K^+ on channel gating. Top record: Single current fluctuations were obtained in symmetric 100 mM KCl, 10 mM MOPS-Tris, pH 7.0, $100\mu\text{M Ca}^{2+}$ at +20 mV. The bottom record was obtained after a symmetrical increase in the $[K^+]$ to 1 M.

to be modified by the isolation procedure and/or transfer to the bilayer. Therefore, I believe that channel reconstitution is a powerful technique to use in the study of membrane ion channels.

Number of Ions Involved in the Gating Reaction

There is some controversy with respect to the number of Ca^{2+} ions involved in the gating reaction. Methfessel and Boheim (1982) and Barret et al. (1982) have studied a Ca^{2+} -activated K^+ channel from rat myotubes using patch clamp and they report the involvement of two and three ions, respectively. In agreement with Methfessel and Boheim's (1982) results, the bilayer data for the rat and rabbit Ca^{2+} -activated K^+ channel suggests the involvement of only two Ca^{2+} ions. On the other hand, Wong et al. (1982) find that three Ca^{2+} ions are involved in the opening of the Ca^{2+} -activated channel from pituitary cells. From macroscopic current measurements, Meech and Thomas (1980) also report the involvement of three Ca^{2+} ions to activate $I_{\text{K,Ca}}$ in *Aplysia* neurons. It is not clear whether this is a real difference between the different channels or is just due to the scatter of the data. Given that the channels from different preparations seem so similar in other respects, I think that their gating mechanisms will turn out to be alike. Most probably, the number of Ca^{2+} ions involved in the gating reaction will turn out to be the same for all the Ca^{2+} -activated K^+ channels presenting a high conductance and high selectivity.

Channel Regulation?

An interesting observation that was not presented in the results section is that the $[Ca^{2+}]$ dependence may vary quite a bit from channel to channel. Moreover, when the fluctuations of a single channel are observed for a period of minutes, it is not rare to observe dramatic shifts in the gating behavior, i.e., a channel that spends most of the time in the open state ($f(V) \sim 0.8$) may suddenly shift to a mode where it spends most of the time in the closed state ($f(V) \sim 0.2$) or viceversa. These changes cannot be attributed to channel damage inasmuch as most of the time they are reversible. Changes in gating behavior have also been reported for the glutamate-activated channel in muscle (Gration et al., 1981) and the Ca^{2+} -activated K^+ channel in rat myotubes (Methfessel and Boehm, 1982). Studies on isolated membrane patches on Helix neurons have shown that the probability of opening of the Ca^{2+} -activated K^+ channels present in these cells increases after perfusing the patch with the catalytic subunit of protein kinase (Irwin Levitan, personal communication). Also, De Peyer et al. (1982) have suggested that the macroscopic sensitivity of $I_{K,Ca}$ in Helix neurons is modulated by protein phosphorylation. Inasmuch as the membrane fraction we use most probably contains kinases, phosphatases and possibly other enzymatic activities, the observed differences between channels and the changes occurring in a single channel could reflect the same phenomenon observed in Helix neurons; i.e., modification of the channel sensitivity by phosphorylation or other similar reaction.

Comparison of Gating Reaction Mechanisms

The reaction schemes proposed by Methfessel and Boheim (1982) and Moczydlowski and Latorre (1983) predict that the mean open and mean closed times (\bar{t}_o and \bar{t}_c) should be linear functions of $[Ca^{2+}]$ and $1/[Ca^{2+}]$, respectively. The data of both groups, as well as the data for the rabbit Ca^{2+} -activated K^+ channel are in agreement with this prediction. Methfessel and Boheim (1982) assumed that the voltage dependence of the reaction resides on the open/closed conformational change. Moczydlowski and Latorre (1983), on the other hand, found that the rate constants determining the mean open/closed transition are voltage independent inasmuch as their values for the channel mean open and mean closed times at all voltages converge in the limits of zero and infinite $[Ca^{2+}]$, respectively. I have replotted the mean open and mean closed times that Methfessel and Boheim (1982) give as a function of membrane potential for different $[Ca^{2+}]$ (Fig. 8, Methfessel and Boheim, 1982) as mean open and mean closed times as a function of $[Ca^{2+}]$ and $1/[Ca^{2+}]$, respectively, for different membrane potentials. When the data are plotted this way, the same behavior found by Moczydlowski and Latorre is observed; i.e., the points show a clear tendency to converge at the zero and infinite $[Ca^{2+}]$ limits. Therefore, I think that Methfessel and Boheim's assumption about the voltage dependence of the reaction should be reconsidered. On the other hand, this is further evidence showing that the properties of the channel in the bilayer are not different than in the cell.

A Molecular Interpretation of Gating

Moczydlowski and Latorre (1983) have proposed two different hypotheses to explain the voltage dependence of the Ca^{2+} binding constants on their reaction scheme (R-5). First, the conventional interpretation implies that the Ca^{2+} binding sites are located in the membrane electric field. They found that the fractional electrical distances felt by Ca^{2+} at its binding sites are ~ 0.75 and ~ 0.95 for the first and second binding reactions of R-5; i.e., the sites "feel" most of the field. If this is the case, then the binding sites could be physically located either at the channel mouth (at some point facing the conduction pathway for K^+ ions) or in a separated "activation cleft" (a region separated from the conduction pathway). In either case, the sites must be close enough to the membrane phospholipids so as to be sensitive to the membrane surface potential. The evidence for this comes from experiments comparing the Ca^{2+} concentration dependence of the activation kinetics in PE vs PS membranes. The activation curves for PS membranes are shifted to the left along the voltage axis when compared to those found on PE membranes at the same bulk $[\text{Ca}^{2+}]$. (Experiments by Edward Moczydlowski.) We have interpreted this result as indicating that the $[\text{Ca}^{2+}]$ near the binding sites increased over the bulk $[\text{Ca}^{2+}]$ in the negatively charged PS membranes (Moczydlowski, Latorre and Vergara, manuscript in preparation).

The second hypothesis considers that the binding rates may be voltage independent. In this case, a dipole in the membrane coupled to the Ca^{2+} binding sites would cause the binding affinity to be modulated by the membrane potential.

Comparison with Other Ca²⁺-Activated K⁺ Channels

The divalent cation selectivity for the activation of macroscopic $I_{K,Ca}$ has been studied in Aplysia and Helix neurons by comparing the currents induced by electrophoretic injection of different divalent cations (Gorman and Hermann, 1979; Meech, 1980). They find that Ca^{2+} is the most effective cation but they also find activation by Cd^{2+} , Hg^{2+} , Sr^{2+} , Mn^{2+} and Fe^{2+} although to a lesser extent. Ba^{2+} , Co^{2+} , Cu^{2+} , Mg^{2+} , Ni^{2+} and Zn^{2+} were found ineffective; moreover, Ba^{2+} ions in Aplysia neurons were found to block $I_{K,Ca}$ and all the other currents carried by K^+ ions. The effectiveness of a divalent cation to activate the channel seems to be related, at least in part, to its ionic radius. Ions with radii between 0.76 and 1.13 Å can fit in the site and activate the channel (Gorman and Hermann, 1979).

In regard to the apparent competition between some monovalent cations and Ca^{2+} ions for the activating site, Marty (1983) has reported that Na^+ ions decrease the opening rate of the Ca^{2+} -activated K^+ channel found in chromaffin cells. He also proposes that Na^+ ions can displace Ca^{2+} ions from their activating sites forming thus an "inactive complex."

CHAPTER 4

Selectivity of the Ca^{2+} -Activated K^+ Channel

Summary

This chapter shows that the channel is Nernst-selective for K^+ over Cl^- , is permeable only to Tl^- and K^+ and is blocked by other monovalent cations (Li^+ , Na^+ , Rb^+ , Cs^+ , NH_4^+ , Tl^+).

Methods

For all the experiments in this chapter the salts concentrations were varied by either adding salt from concentrated stock solutions or by replacing the solution on the cis compartment. Inasmuch as Cl^- salts of Tl^+ are highly insoluble, 0.1 M acetate salts of Tl^+ and K^+ were used to measure Tl^+ selectivity. The $[\text{Ca}^{2+}]$ was 100 μM unless otherwise stated. Tl^+ experiments were done in neutral PE membranes.

Results

Measurements of K^+ Over Cl^- Selectivity by Reversal Potentials

Figure 19 shows an I-V curve for a Ca^{2+} -activated channel obtained in the presence of a KCl gradient across the membrane (0.3 M KCl cis/0.1 M KCl trans). Under these conditions, the zero current potential is -24 mV. This value is within experimental error from the expected value for a perfectly cation selective channel (-25 mV). I conclude, then, that

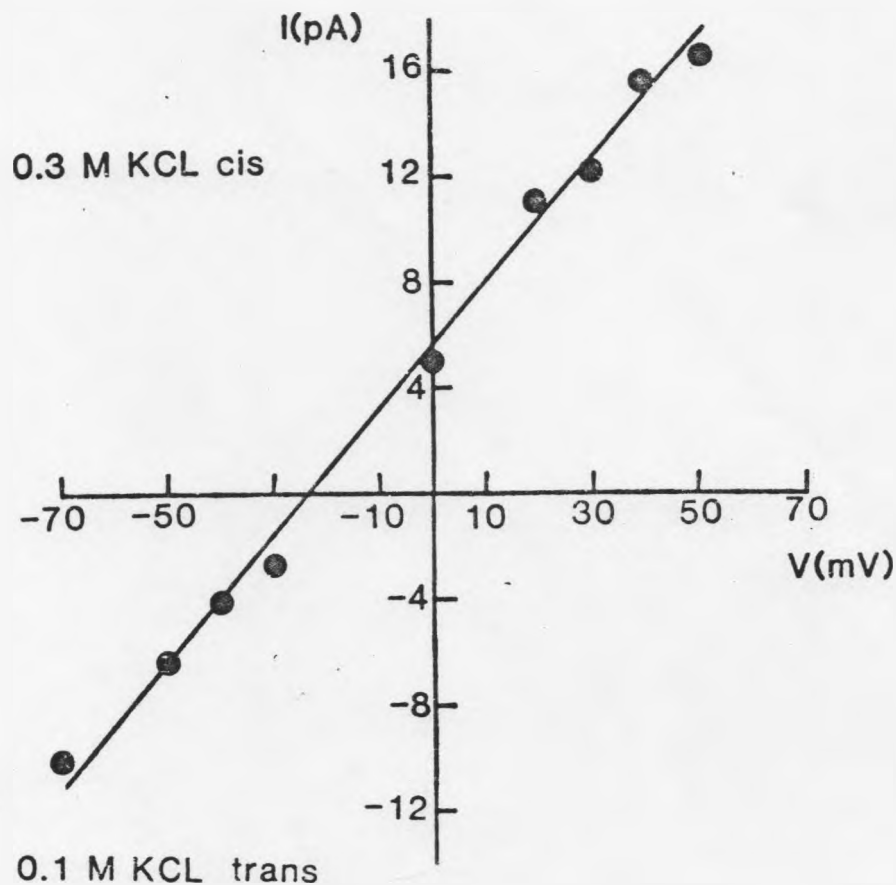


Fig. 19. K^+ over Cl^- selectivity determined by reversal potential of indicated channels. The current voltage curve was obtained when a KCl gradient was present across the membrane. The cis compartment [KCl] was 0.3 M and the trans compartment [KCl] was 0.1 M. $[Ca^{2+}]$ was $100 \mu M$. The positive current points were the average of 4 independent experiments and the negative current points were the average of two independent experiments. The zero current or reversal potential under these conditions was -24 mV.

the channel only allows K^+ ions to move through it completely excluding Cl^- ions.

Selectivity to Alkali Cations, NH_4^+ and Tl^+ as Measured by Reversal Potentials

Figure 20 shows the I-V curves obtained under bilionic conditions for Li^+ , Na^+ , Rb^+ and NH_4^+ ; i.e., KCl was always present on the trans side at 0.1 M and the cis side contained 0.1 M salts of the mentioned cations. A striking feature of all these curves is the bending of the current towards the potential axis as the potential is made more positive. Positive currents are defined as movement of cations from the cis towards the trans side of the bilayer (see General Methods). The figure shows a linear region in all the I-V curves for negative potentials when the net driving force is for K^+ ions to move towards the cis side. As the potential is made more positive, the net driving force is for the cations on the cis side (Li^+ , Na^+ , Rb^+ , NH_4^+) to move towards the trans side. In this potential region all the curves asymptotically approach the potential axis; therefore, we were unable to observe reversal currents. This fact suggests first that the permeability of these ions is very small and second that they block the channel. Further evidence for channel blockade comes from experiments where Na^+ or Li^+ ions were added to symmetric 0.1 M KCl solutions bathing the channel. The addition of these ions caused an apparent reduction of the single channel current consistent with a fast equilibrium between the open channel and a Na^+/Li^+ blocked state. In the presence of symmetric 0.1 M KCl, the addition of 0.1 M NaCl to the cis side caused a 40%

reduction of the single channel current at 40 mV (measured on a neutral PE membrane).

When the solution on the cis side chamber was replaced by 0.1 M CsCl, I could only measure accurately current fluctuations in a very small potential range (-10 to +20 mV). For more negative potentials, only rare very fast openings occurred whose amplitude could not be determined. Even after increasing cis $[Ca^{2+}]$ to 1 mM the rate of channel opening did not increase. For potentials more positive than 20 mV no current fluctuations were observed. Furthermore, when Cs^+ ions were added over the KCl solutions bathing the channel, the single channel conductance also decreased as mentioned for Li^+ and Na^+ . Thirty mM CsCl added to the cis side of the bilayer caused a 28% decrease of the single channel conductance at 40 mV (also measured in neutral PE membranes). These results indicate that Cs^+ ions can block the channel and moreover they seem to interact with the channel gating process.

The only ion for which I could measure reversal currents under bilionic conditions was Tl^+ . Unfortunately, in the presence of Tl^+ ions the channels only rarely open as if Tl^+ also interferes with the gating process. Fig. 21 shows the I-V curves obtained for two different channels in the presence of 0.1 M Tl^+ Ac cis/0.1 M K^+ Ac trans. The reversal potential is around -10 mV, consistent with a permeability ratio $P_{Tl^+}/P_{K^+} \sim 1.5$ (eq. 3). In these experiments the current decreases as the potential is made more positive, suggesting a voltage dependent block. To determine whether this phenomenon is real or just due to scatter of the measures, further work is needed. When Tl^+ ions are added to the symmetric K^+ solutions bathing the channel they also cause a decrease in single channel conductance. Addition of 50 mM Tl^+ symmetrically caused a 23% reduction of the current at 50 mV.

Discussion

Selectivity to Alkali Cations

Unfortunately, all the alkali cations behave as channel blockers so I could not define an ion selectivity sequence quantitatively. However, with the qualitative information I have, it is possible to obtain some of the gross architectural features of the selectivity filter of the channel. For these ions to block, they must have access up to a given point located in the conduction pathway from where they cannot go further. Therefore, the channel must have a region (at least 1.7 \AA in radius to accommodate Cs^+ ions) which at some point narrows down to a size that only allows K^+ (1.33 \AA) to go through.

Block of the delayed and inward rectifier channels of different preparations by Li^+ , Na^+ and Cs^+ ions has been previously reported (Bezanilla and Armstrong, 1972; French and Wells, 1977; Bergman, 1970; Gay and Stanfield, 1977; Hagiwara et al., 1976; Schwarz et al., 1981). Also, Cs^+ ions block the K^+ channel from sarcoplasmic reticulum and Na^+ ions block the Ca^{2+} -activated K^+ channel from chromaffin cells (Coronado and Miller, 1979; Marty, 1983).

For biionic conditions between Na^+ and K^+ , Methfessel and Boehm (1982) in the myotube Ca^{2+} -activated K^+ channel also find that the current asymptotically approaches the voltage axis as "the reversal potential" is approached. They estimate a minimum $P_{\text{K}^+}/P_{\text{Na}^+}$ of 15. For Cs^+ ions they estimate a $P_{\text{K}^+}/P_{\text{Cs}^+}$ between 4 and 10. Other

Ca^{2+} -activated K^+ channels show the same behavior, at least with respect to Na^+ ions (Pallotta et al., 1981; Maruyama et al., 1983).

Reuter and Stevens (1980) found that the delayed rectifier from snail neurons is less selective to K^+ than the nodal or squid K^+ channels and, moreover, the selectivity sequence measured from reversal potentials does not follow any of the sequences predicted from Eisenman's theory. In an attempt to describe these results, they assumed that a single energy barrier is the rate limiting step for permeation and developed a theory that relates reversal potentials to barrier heights and barrier heights to physical properties of the channel structure. They related some parameters describing barrier height to the difference in dipole moment at the surface of an ion when this is at the selectivity binding site as compared to water. Also, they related the rate of change in dipole moment of channel groups induced by different permeant ions as a function of ion radius. Finally, the "degree of rigidity" of channel sites to accommodate ions of different sizes as compared to free water was also considered. It seems possible, then, that the very high selectivity displayed by some Ca^{2+} -activated K^+ channels is related to a very "rigid" selectivity filter that can only accommodate K^+ ions excluding all other alkali cations.

From a comparison of the selectivity (and also blockade properties) displayed by different K^+ channels, Latorre and Miller (1983) have concluded that they all share some basic structural features while, at the same time, each presents peculiar characteristics like degree of rigidity of the selectivity filter that define each peculiar type of channel. The same conclusion was reached by Gorman et al. (1982) from

their measurements of selectivity of the Ca^{2+} -activated K^+ channel from Aplysia and the light dependent K^+ channel of the scallop. These investigators found the same selectivity sequence for both these channels as well as for delayed rectifiers from other preparations.

Selectivity to Fingerprint Ions

We tested Tl^+ and NH_4^+ ions with the hope of obtaining information on the chemical structure of the group(s) determining selectivity. The selectivity pattern displayed by ions like NH_4^+ , Tl^+ and Ag^+ on several model systems (solvents and carriers of known structures) have been used as fingerprints of the ligand orientation and/or chemical groups involved in determining selectivity (Krasne and Eisenman, 1973). Krasne and Eisenman (1973) compared the behavior of Tl^+ and NH_4^+ when complexed by the cation carriers nonactin and valinomycin. The structures of these two molecules are known. Thus, valinomycin has six octahedrally oriented carbonyl ligands, whereas nonactin has four tetrahedrally directed carbonyl and four tetrahedrally directed ether ligands. Experimentally it is found that for nonactin, both Tl^+ and NH_4^+ are preferred as compared with alkali cations of comparable size (e.g., Rb^+). For valinomycin, the reverse is true; i.e., alkali cations like Rb^+ are preferred over Tl^+ and NH_4^+ . These results can be understood by comparing the known structures of the carrier and the ions used as selectivity "fingerprints." NH_4^+ , having a tetrahedral, structure is expected to have a favorable interaction with four tetrahedrally oriented oxygens like nonactin. For Tl^+ , the distribution of electrons is increasingly distorted as the electric field is increased. This

characteristic of Tl^+ ions implies that it does not have a fixed charged distribution, but it depends on the magnitude of the electric field. Tl^+ is in consequence called a polarizable ion. Accordingly, Tl^+ will display increased or decreased affinities for certain groups depending on the particular charge distribution of the ligand group and, therefore, it is expected to provide a diagnostic tool for distinguishing particular ligands (e.g., ether vs carbonyl). Moreover, K^+ and Tl^+ ions have a similar crystal radius (1.33 and 1.40 Å, respectively; Pauling, 1960), so a priori one might expect a good fit of Tl^+ ions onto sites normally occupied by K^+ ions.

Although I cannot quantitate the permeability ratio between K^+ and NH_4^+ , the sequence for the "fingerprinting" ions Tl^+ and NH_4^+ with respect to K^+ is $P_{Tl^+} > P_{K^+} > P_{NH_4^+}$. This is the same sequence found for the squid and frog nerve delayed rectifiers as well as for the starfish egg and muscle inward rectifiers (Hille, 1972; Hagiwara et al., 1972; Hagiwara and Takahashi, 1974; Standen and Stanfield, 1980). I propose that the selectivity filter of the Ca^{2+} -activated channel studied here is composed of six-fold coordinate oxygens which are not simply ester carbonyls but rather ether-like oxygens. Inasmuch as the channel presents the same type of preference for NH_4^+ as valinomycin, I conclude that the site is octahedrally oriented. On the other hand, the channel prefers Tl^+ over K^+ and, therefore, as in nonactin, the channel's ligands appear to be ether-like oxygens.

CHAPTER 5

Conductance of the Ca²⁺-Activated K⁺ Channel

Summary

This chapter shows that in neutral PE membranes the channel conductance vs K⁺ activity curve shows a more complicated behavior than the expected for a single ion channel with a fixed energy profile (Lauger, 1973; Lauger et al., 1980). The deviation from the expected rectangular hyperbola is evident in the low activity region. Possible explanations of this behavior are mentioned. For negatively charged PS membranes the conductance-activity data are consistent with the idea that the [K⁺] at the entry of the conducting pore is determined at least in part by the surface potential. The channel entrance seems to be at some distance away from the surface of the membrane.

Methods

All the results presented in this chapter were obtained in pure PE or pure PS membranes as indicated on the figures. Because channel incorporation in low salt (1-50 mM) occurs with low frequency, especially in neutral PE membranes, a concentration gradient of KCl was created across the membrane to speed up channel incorporation (cis side more concentrated). Once a channel incorporated into the membrane, the gradient was eliminated by replacing the cis side solution with a solution to match the [K⁺] on the trans compartment. The [K⁺] was increased symmetrically by addition of concentrated K⁺ stock solutions. The membranes were started at high salt for [K⁺] > 1 M. The [K⁺] of the

1-6 mM stock solutions was checked by atomic absorption spectrophotometry. All solutions for these experiments were buffered with MOPS-KOH rather than with MOPS-Tris. Salt activity was calculated from Robinson and Stokes (1955). All conductance data were calculated from the slope of I-V curves obtained between +40 mV except for the 1 mM values that were obtained at higher potentials. I present here pooled data for the rat and rabbit channels. The experiments on the rat channel were done by Edward Moczydlowski. $[Ca^{2+}]$ was between 1 and 10 μ M.

Conductance-Activity Relationship in Neutral and Negatively Charged Membranes

Figure 22 shows single channel conductance as a function of K^+ ion activity for membranes made of PE (solid symbols) and PS (open symbols). The figure includes data for the rat and rabbit channel. For both PE and PS membranes conductance is a saturating function of K^+ activity but the shape of the curve is quite different for neutral or negatively charged membranes.

Conductance in PE Membranes

For PE membranes, in the low ion activity range the data deviate from a rectangular hyperbola expected for a single ion channel with fixed energy barriers (Lauger, 1973). The best fit to a rectangular hyperbola for the data points in the high ion activity regions is indicated by the broken line that was drawn considering a K_0 of 80 mM and G_{max} of 520 pS. The inset of the figure shows a Scatchard plot of the same data where the

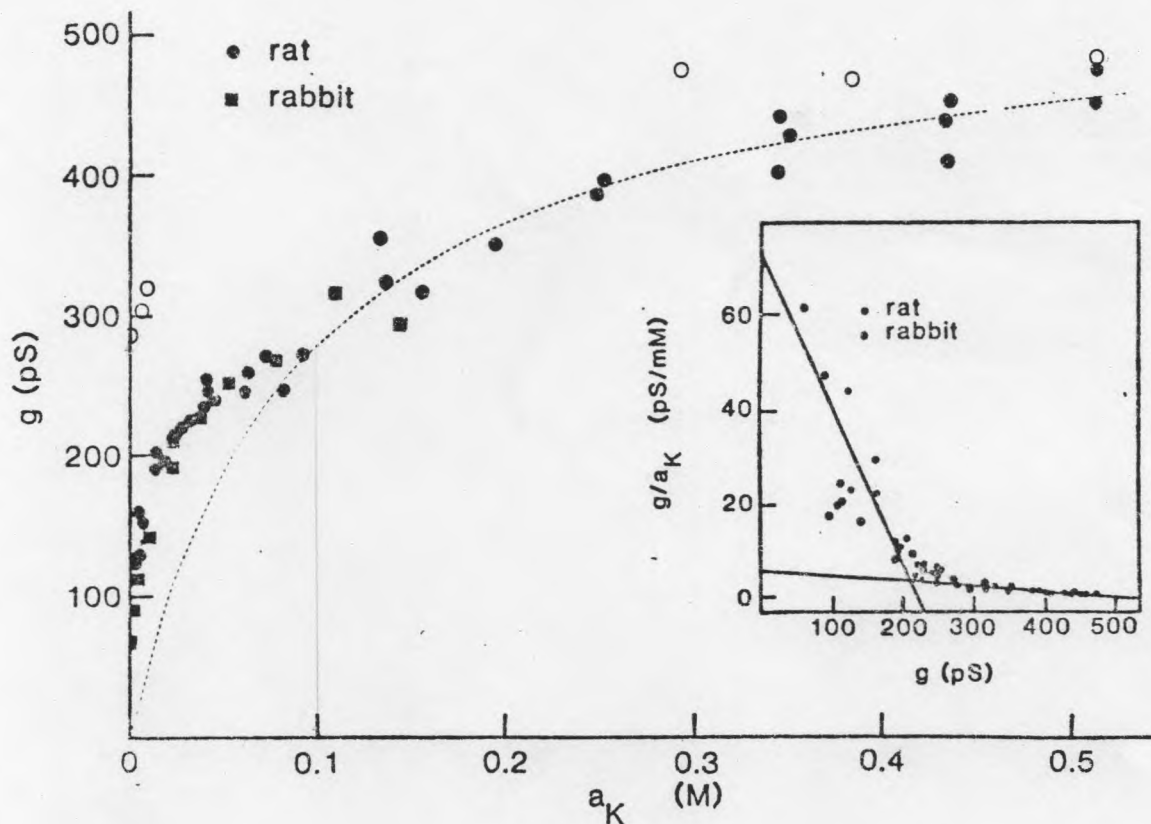


Fig. 22. Channel conductance as a function of K^+ activity. The g values were determined from the slope of current-voltage curves obtained between ± 40 mV in the presence of symmetric KCl-MOPS buffers of different salt concentrations adjusted to pH 7.0 with KOH. Closed symbols represent conductance values obtained in PE membranes, open symbols are for values obtained in PS membranes. In the salt range between 1 and 50 mM KCl for PE membranes, channel incorporation was obtained when a KCl concentration gradient was created across the two compartments (higher salt concentration on the cis compartment). After channel incorporation the cis side was perfused with a buffer containing a $[K^+]$ matching that of the trans compartment. $[Ca^{2+}]$ was 1-10 μ M symmetric. The dotted line for PE membranes was drawn according to eq. (13) with a $G_{max} = 520$ pS and $K_d = 80$ mM. Inset: Eadie-Hofstee plot of the conductance-activity data shown for PE membranes.

limiting behavior in the low and high ion activity range is shown by the two straight lines. One can interpret these lines as if they revealed the existence of low and high affinity sites (see below). The maximal conductance and apparent dissociation constants for the low and high affinity sites are 220 pS-3 mM and 530 pS-90 mM, respectively. The figure also shows that conductance does not decrease in the high activity range as would be expected for multi-occupied channels (Hille and Schwarz, 1978). (I have measured channel conductances in 70% PE-30% PS membranes up to 3 M KCl and no sign of decrease in conductance is observed.)

Based on this last evidence, I propose that the channel behaves as a single ion channel; i.e., in the concentration range tested (1 mM to 3 M) it does not contain more than one ion at a time.

Several mechanisms could explain the observed behavior in the low ion activity range: a) Coulombic interactions between K^+ and its binding site could trigger "slow" (slow with respect to the ion transit time) changes in the conformation of the site (Lauger et al., 1980). If this were the case, the low and high affinity sites apparent in the inset of the figure would reflect the behavior of two different site conformations; b) Fixed negative charges existing in the protein (or lipids) surrounding the ion binding site; c) A site external to the conduction pathway could regulate conduction.

Conductance in PS Membranes

The conductance values (open symbols) at $[K^+]$ from 6 to 30 mM are much higher than those measured in PE membranes at the same $[K^+]$. For

$[K^+] > 300$ mM, the conductances are very similar to the maximal conductance measured in neutral membranes. (These last values were obtained in Tris-containing membranes; see results in Chapter 6.) Two conclusions can be drawn from these results: a) The channel "feels" the increased $[K^+]$ at the surface of the membrane generated by the presence of fixed negative charges on the PS inasmuch as the conductance values measured in the low salt region are substantially higher than those on neutral membranes; b) The channel entrance does not seem to be located at the plane of the membrane but at some distance away from it. Estimating the charge density from the area/molecule as 0.0167 charges/ \AA^2 , at 10 mM K^+ on the bulk solution, the surface potential is -197 mV (eq. 16) and, therefore, the $[K^+]$ at the surface of the membrane should be 25 M (eq. 20). If the channel entrance were at the plane of the membrane, one would expect to observe the maximal conductance even at this low salt value. Instead, conductance raises from ~280 pS at 6 mM K^+ (the lowest $[K^+]$ tested) to ~500 pS in 0.9 M K^+ .

Discussion

With the available information, it is difficult to decide on a mechanism that would explain the observed deviations in channel conductance from the expected behavior for a single ion channel with fixed barriers. We have some information that rules out the possibility of fixed negative charges. On the one hand, from surface potential measurements on monolayers, we found that under the conditions tested PE is 2-3% charged (experiments by Ramon Latorre). If we think that this amount of charge is distributed all over the membrane, it does not seem

to be enough to explain the observed deviations. On the other hand, if fixed negative charges existed, a limiting conductance value in the low activity region is expected (Appel et al., 1979). Even at the lowest $[K^+]$ tested (1 mM) we found no evidence of a limiting conductance.

Inasmuch as we do not have an empirical description of conductance as a function of ion activity in neutral membranes, an estimation of the distance from the plane of the membrane where the channel entrance is located was not possible (see Bell and Miller, 1983).

Comparison With Other Channels

The effect of surface charge on ion conduction has been specifically tested in bilayers for the gramicidin channel, the SR K^+ channel and the rat and rabbit Ca^{2+} -activated K^+ channel (Appel et al., 1979; Bell and Miller, 1983 and results presented herein). In the three cases, a large fraction of the surface potential due to fixed charges in the lipid is felt by the conduction pathway. On the other hand, for the Na^+ and K^+ channels in Mixycola axons, for the Na^+ and K^+ channels in squid, and a Cl^- channel from Torpedo electroplax studied in lipid bilayers, it has been found that conduction is not affected by changes in the surface potential (Egenisich, 1975; Hille et al., 1975; Fohlmeister and Adelman, 1982; White and Miller, 1981). Therefore, in these examples, the entrance to the channel seems sufficiently away from the plane of the membrane that ion accumulation due to the presence of fixed charges does not affect conduction.

CHAPTER 6

Block of the Ca²⁺-Activated K⁺ Channel

Summary

This chapter presents the characteristics of the block induced by TEA, C₉, Ca²⁺ and Ba²⁺ ions. The results show widely different kinetics for TEA and C₉ ions as compared to Ca²⁺ and Ba²⁺. Other channel blockers are Tris, decamethonium, and quinine.

Methods

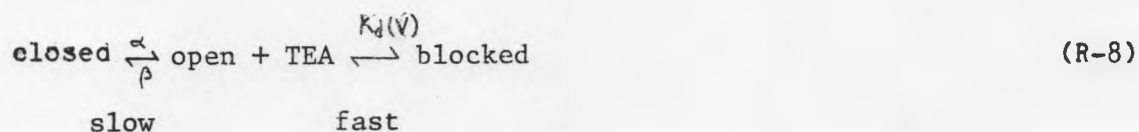
Unless otherwise specified, all the blocking experiments were done in symmetric 0.1 M KCl solutions. Quinine was dissolved in ethanol. All other blockers were aqueous solutions. C₉ experiments were done in neutral PE membranes.

The current records obtained while studying the Ca²⁺- and Ba²⁺-induced slow channel blockage were filtered at 20 Hz or less. The reason for doing this is that the filtering can separate the fast kinetic process from the slow closings shown on Fig. 10. Under all the conditions used for these experiments, the contribution of closings from the fast gating to the slow kinetic process was less than 1%. To characterize the Ba²⁺ effect, we used a [Ca²⁺] of 0.1 mM and a [K⁺] of 0.1 M for most of the experiments, the reasons being that under these conditions the channel is open almost all the time at the voltages the Ba²⁺ action was studied, and that contamination of the Ba²⁺-induced slow kinetics by the Ca²⁺-induced slow kinetics was minimal.

Results

Tetraethylammonium Block

Figure 23 shows macroscopic I-V curves obtained in a membrane containing approximately 100 channels. Addition of 5 mM TEA to the cis compartment caused a 20% reduction of the current (Fig. 23B). When 5 mM TEA was added to the trans side of the bilayer, a much greater reduction of the current was observed (Fig. 23C). This effect of TEA is reversible inasmuch as after perfusion of the trans compartment with TEA-free solution, the current recovers almost completely up to the level present before trans TEA addition (Fig. 23D). Fig. 24 shows that addition of TEA to either side of a membrane containing single channels causes a decrease in the single channel conductance. However, the concentrations needed to cause a 50% reduction of the channel conductance are very different for cis (Fig. 24A) or trans (Fig. 24B) TEA additions. The block caused by cis or trans TEA is well described by a single site titration curve. Moreover, the decrease in single channel conductance observed implies that the blocking reaction between TEA and the channel is much faster than the gating kinetics. The following reaction scheme can explain the experimental findings.



where α and β are the rate constants describing the gating reaction

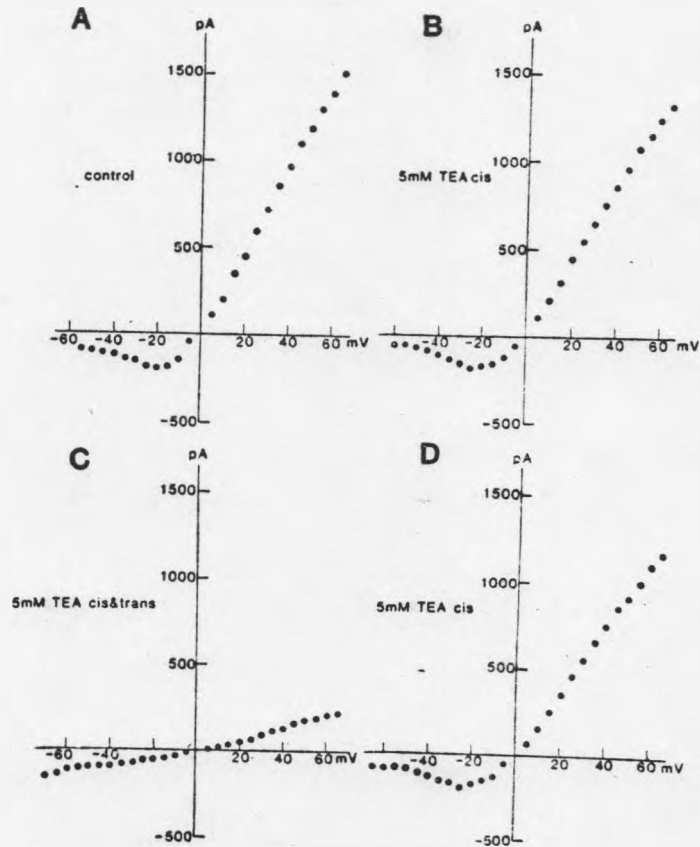


Fig. 23. TEA effect on macroscopic current-voltage curves. (A) The control current voltage curve was obtained under symmetric 0.1 M KCl, 10 mM MOPS-Tris, pH 7.0, 1 mM Ca^{2+} . (B) TEA ions were added to the cis side to a final concentration of 5 mM. The current decreased by ~20%. (C) TEA ions were added to the trans side to a final concentration of 5 mM. The current was reduced by ~81% as compared to (B). (D) The trans compartment was perfused with TEA-free buffer.

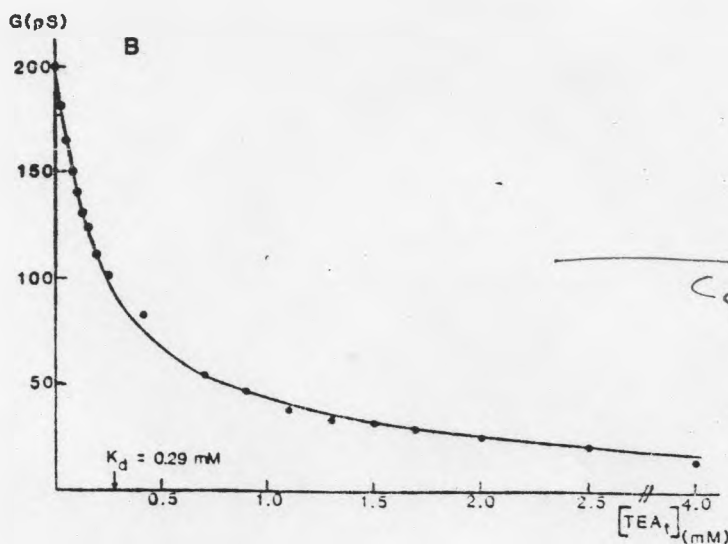
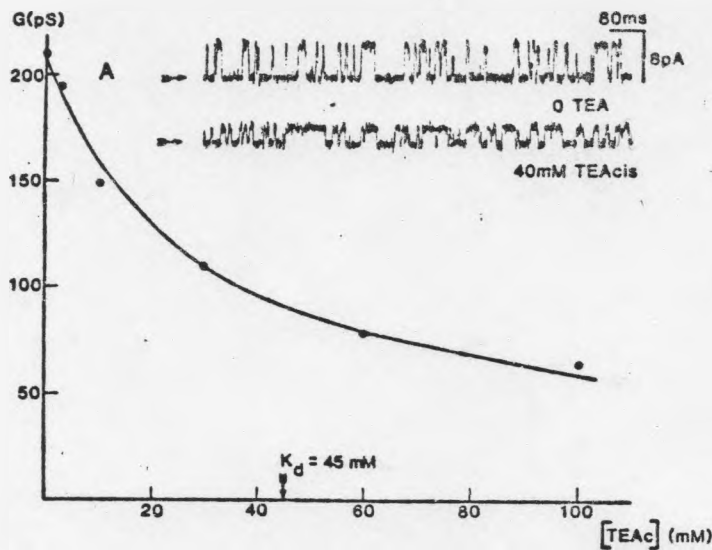


Fig. 24. TEA effect on single channel conductance. Channel conductance was measured in the presence of cis TEA at the indicated concentrations in symmetric 0.1 M KCl, 10 mM MOPS-Tris pH 7.0, $100 \mu\text{M Ca}^{2+}$. (A) The applied voltage was +40 mV. The points are the average of at least 15 different determinations in seven different channels. The solid line was drawn according to eq. (22) with a $K_d(0) = 45$ mM. Inset: current records obtained in the absence and in the presence of 40 mM TEA cis. Note the difference in the fraction of open time in the two records. (B) channel conductance measured in the presence of trans added TEA ions. Other conditions as in (A). Solid line drawn according to eq. (22) with $K_d = 0.29$ mM.

(therefore, they are Ca^{2+} and voltage dependent) and $K_D(V)$ is the dissociation constant of the blocking reaction that in general can be voltage dependent.

Voltage Dependence of the Blocking Reaction

a) Trans TEA Block: Fig. 25A shows that in the presence of trans TEA, the single channel conductance measured at any given [TEA] is independent of membrane potential. I have interpreted this result as indicating that the site to which trans added TEA ions bind is located outside the region where the membrane potential falls.

b) Cis TEA Block: Fig. 25B shows that in the presence of cis TEA, the single channel conductance is a function of membrane potential. The block is enhanced for positive and is relieved for negative membrane potentials. Fitting the data to the linearized expression describing channel conductance in the presence of a blocker for a reaction scheme like R-8 (eq. 24, Introduction), I obtained the zero volt dissociation constant and the fraction of the total voltage drop across the membrane felt by cis TEA ions at their binding site. These parameters are $K_D(0) = 45 \pm 7$ mM (mean \pm S.D. for seven different experiments) and $f = 0.34 \pm 0.07$. On the other hand, $K_D(0)$ for trans TEA block is 0.29 ± 0.04 mM.

Apparent Increase in Mean Open Time

For a reaction scheme like R-8 one expects an apparent increase in the mean time the channel is in the open configuration, the reason being that a blocked channel cannot close. The inset of Fig. 25A shows that

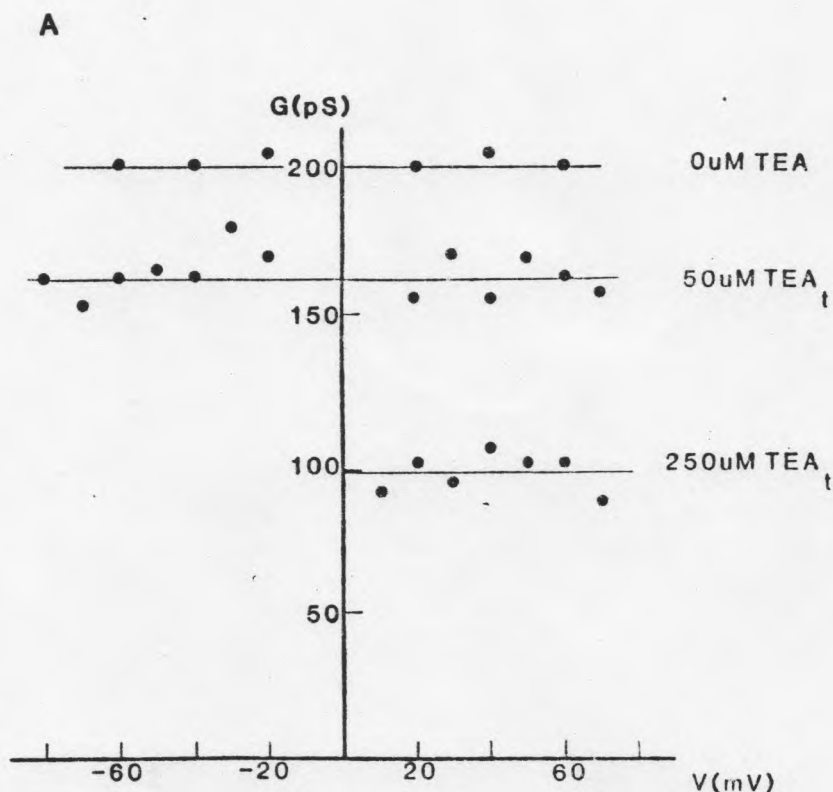
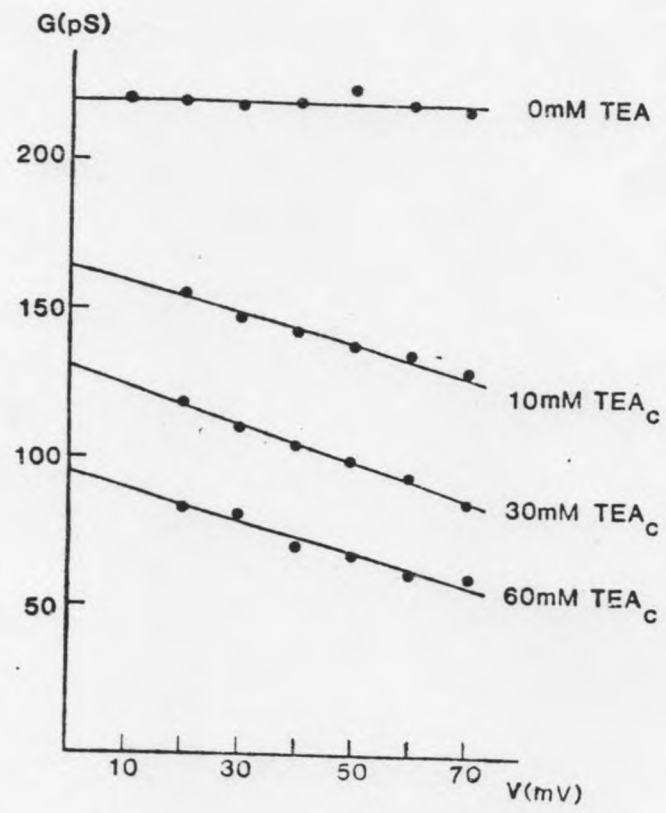


Fig. 25. Voltage dependence of trans and cis TEA block. (A) Channel conductance measured as a function of membrane potential in the presence of the indicated trans TEA concentrations. In the voltage range measured, the channel conductance at any given trans TEA concentration is independent of voltage. (B) Channel conductance measured as a function of membrane potential in the presence of the indicated cis TEA concentrations. While in the absence of TEA the channel conductance is independent of voltage in the range shown, in the presence of cis TEA, the channel conductance becomes increasingly smaller as the membrane potential is made more positive. The solid curves were drawn according to eq. (24) with $K_D(0) = 45$ mM and $\delta = 0.35$.

B



this prediction is fulfilled for cis TEA block. According to eq. (25), the apparent increase in the mean open time provides an independent way of calculating the dissociation constant of the reaction. When the K_d for cis TEA block were calculated from this method, the values obtained were within 2- to 3-fold those calculated from the conductance data. Inasmuch as the mean open times for a channel often fluctuate (see Discussion, Chapter 3), I feel that the obtained values are in agreement with the predictions of the scheme proposed. The very striking differences between cis and trans TEA block with respect to affinity and voltage dependence indicate that the two sites have different characteristics. On the other hand, the fact that TEA blocks from either side implies that at the cis and trans channel entrances, there is an opening at least 8 Å in diameter that can accommodate TEA.

Triethylnonylammonium (C_9) Ions Block

For a blocker ion of high affinity, the dwell time in the blocked state will be long enough so as to be able to resolve the blocked state as brief interruptions (flickers) of the open state conductance (Neher and Steinbach, 1978; Coronado and Miller, 1980). C_9 ions were found to present this characteristic.

Fig. 26 summarizes the properties of channel blockade by C_9 ions. Two main points are illustrated on the figure. a) As for the case of TEA, the affinity of the cis and trans C_9 binding sites are widely different but in this case the site with higher affinity is the cis binding site. This is evident comparing the control records with those obtained at $200 \mu\text{M } C_9$ added to the trans side and those obtained at $3 \mu\text{M}$

Missina
102

C_9 added to the cis side; b) The cis blockade reaction is voltage dependent: When C_9 ions are added to the cis compartment, at positive membrane potentials the flickering rate can become so high (see trace at +50 mV for $10 \mu\text{M}$ cis C_9) that no discrete openings or closings can be observed. On the other hand, at negative membrane potentials (see trace at -40 mV for 3 and $9 \mu\text{M}$ cis C_9), the open and closed states can still be resolved. Thus, for cis added C_9 negative potentials relieve the blockade caused by this ion. The average values of the channel conductance in the presence of $10 \mu\text{M}$ cis C_9 ions was measured between +60 mV. Fitting these data to eq. 24, I obtained a zero volt dissociation constant for the cis C_9 blocking reaction equal to $3.5 \mu\text{M}$ and I found that the C_9 binding site is located at 35% of the total voltage drop across the membrane from the cis side. Inasmuch as the cis TEA binding site is also located at the same electrical distance ($34\% \pm 0.07$), I consider this finding as an indication that both C_9 and TEA ions bind to the same site in the channel.

When C_9 ions are added to the trans compartment, a slight decrease in single channel conductance was observed. (The control channel conductance was 200 pS while in presence of $300 \mu\text{M}$ trans C_9 the conductance at -40 mV was 185 pS). Reaction scheme 8 predicts that for a fast blocking reaction (fast with respect to the gating kinetics) the mean open time in the presence of a blocker should increase (eq. 25). Although the increased mean open times apparent for the 100 and $200 \mu\text{M}$ C_9 current traces was not quantitated, they seem in excess of what one would expect given that trans C_9 block is of low affinity. As I mentioned above (see Discussion on Chapter 3), the channel gating may spontaneously change. The observed behavior could then be due to a change in gating.

Channel Block by Tris

Fig. 27 shows the channel conductance measured in symmetric KCl at the indicated Tris concentrations. At +40 mV, the block caused by Tris is well described by a single site titration curve with a K_d of 12 mM. The block caused by Tris appears to be competitive with K^+ ions. For example, in the presence of 100 mM K^+ , 50 mM Tris causes a 21% decrease in channel conductance, whereas that at 26 mM K^+ , the conductance decrease is 71% (values taken at +40 mV). Although I did not characterize the block caused by Tris in detail, I present these results because they explain the previous report (Latorre and Miller, 1983) that channel conductance is well described by eq. (13), whereas I report here that this is not the case (see Chapter 5). Previously, I measured single channel conductance in the presence of 10 mM Tris. Inasmuch as Tris block is competitive with K^+ ions, at low salt concentrations, the channel conductance was underestimated. At higher salt concentrations the block becomes negligible and, therefore, the maximal channel conductance previously observed coincides with the values obtained when no Tris is used in the solutions.

Ca²⁺ Block

Figures 28A and 28B show the effect of cis $[Ca^{2+}]$ and membrane potential on the slow channel kinetics. At low (30 μ M) Ca^{2+} concentration, the channel fluctuates rapidly between two conductance states, and this type of channel activity may remain unmodified for

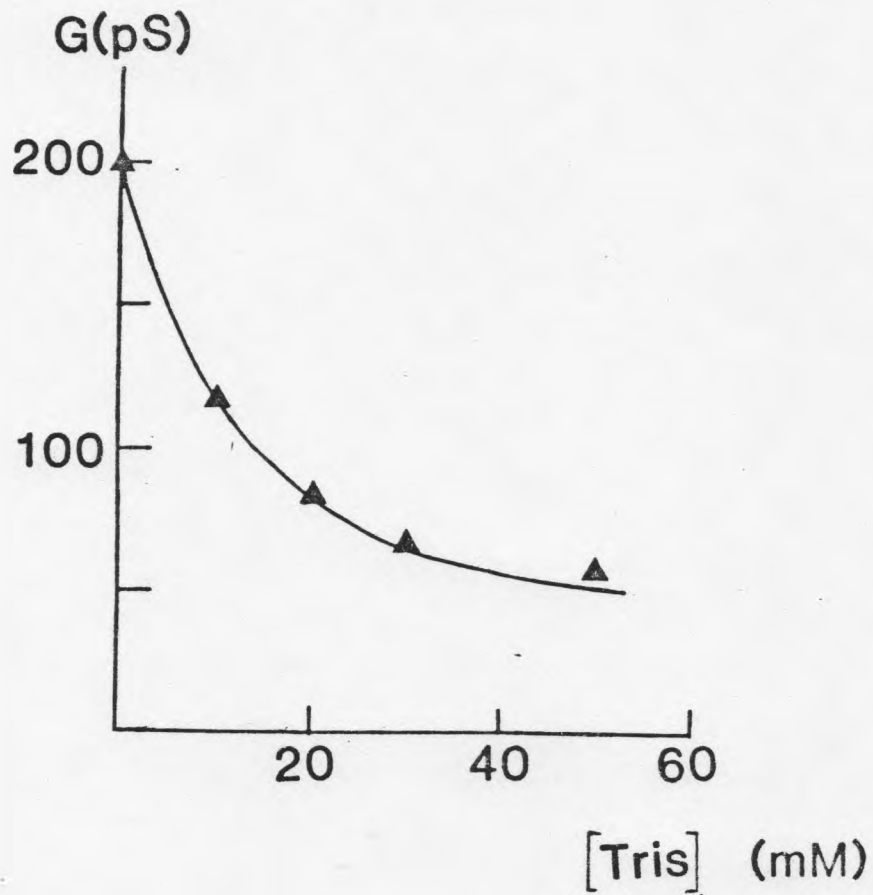


Fig. 27. Tris effect on single channel conductance. Channel conductance was measured in a PE membrane in the presence of symmetric KCl at the indicated symmetric concentrations of Tris. The applied potential was 40 mV. $[Ca^{2+}]$ was $10 \mu M$. The solid line was drawn according to eq. (22) with a K_d of 12 mM.

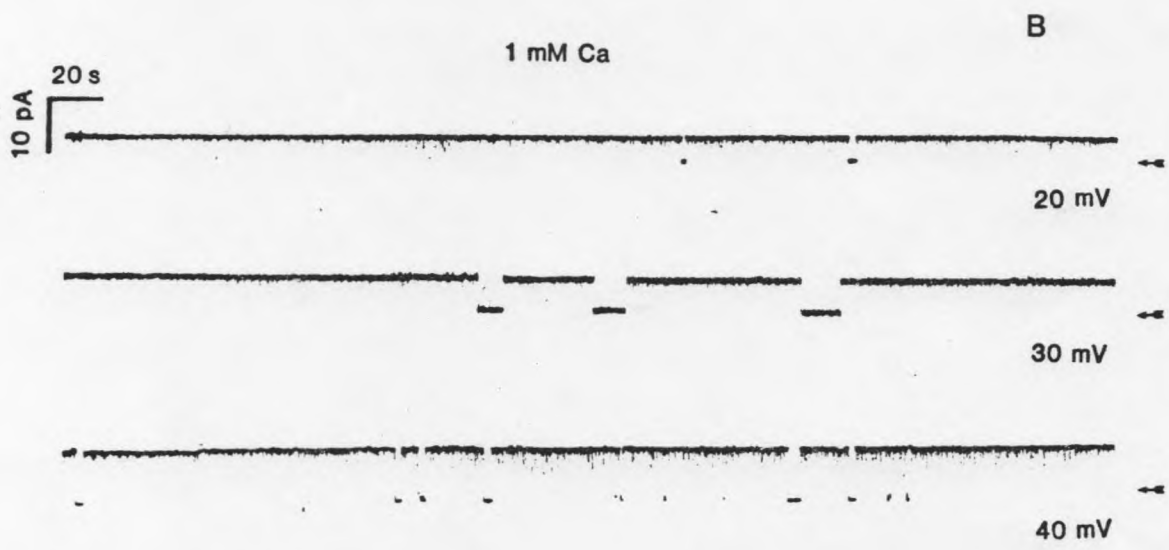
several minutes. However, if the Ca^{2+} concentration in the cis side is increased to about $100\ \mu\text{M}$, the appearance of a second type of channel kinetic behavior becomes apparent. For example, the records of Fig. 28A exhibit periods of several seconds in which the channel remains in a non-conductive state. Increasing the $[\text{Ca}^{2+}]$ (Fig. 28A) or voltage (Fig. 28B) has the effect of increasing the number of these "slow closings." In other words, bursts of activity (e.g., the region labeled b in the second record of Fig. 28A) are interrupted by long periods of quiescence.

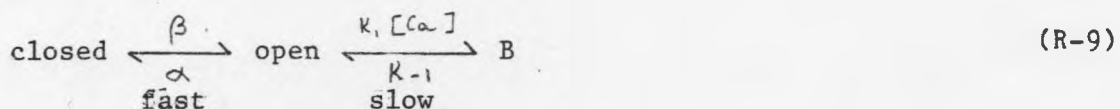
When the $[\text{Ca}^{2+}]$ is increased from 0.1 mM to 10 mM we found a decrease of 35% in the channel conductance (from 220 to 143 pS). This effect was also found when the channel is incorporated in the zwitterionic phosphatidylethanolamine membranes and we believe it can be due to a fast channel blockade caused by Ca^{2+} ions.

As seen on Figs. 12 and 13, increasing the Ca^{2+} concentration or increasing the voltage has the effect of increasing the time the channel dwells in the open configuration inside a burst. It can be concluded, then, that the slow process apparent in the records of Figs. 28A and B has a voltage and Ca^{2+} dependence opposite to that of the fast openings and closings.

A Sequential Kinetic Model Can Account for the Slow Process

A kinetic model for the Ca^{2+} -activated channel which comprises, in a simplified manner, both the fast kinetic process (i.e., the activity during a burst) and the slow kinetic process is outlined below.





where the rate constants α and β are both Ca^{2+} concentration and voltage dependent. In order to account for the slow process seen at high Ca^{2+} concentration and high voltages, we have added a non-conductive state, B. The Ca^{2+} effect we study here is so slow that one cannot discard a priori a model of the type, $B \rightleftharpoons C \rightleftharpoons O$. The reason for not considering this type of model is discussed with respect to the Ba^{2+} -induced blocked state.

I propose here two hypotheses for the origin of state B: (a) Ca^{2+} binds to a "low affinity receptor," different from those that lead to activation, and this binding induces channel closure; and (b) Ca^{2+} enters into the channel and blocks it.

Regardless of the detailed molecular mechanism whereby the transition from open to B occurs, the rate constants k_1 and k_{-1} to describe the process can be inferred from measurable parameters obtained from records such as those shown in Fig. 28. These parameters are the mean time that the channel dwells in the B state, $\bar{\tau}_B$, and the mean burst time, $\bar{\tau}_b$. According to reaction scheme R-9, $\bar{\tau}_B$ is given by the inverse of the rate constant for leaving state B:

$$\bar{\tau}_B = \frac{1}{k_{-1}} \quad (27)$$

On the other hand, the mean burst time, $\bar{\tau}_b$, is given by:

$$\bar{\tau}_b = \frac{1}{[Ca] k_1} \left(\frac{\alpha}{\beta} + 1 \right) \quad (28)$$

Termination of a burst is leaving the set of states closed and open of scheme R-9; i.e., only the open channel can undergo a transition from open to B. The reaction rate for this process is $k_1 [\text{Ba}^{2+}] P(o/o \text{ or } c)$, where $P(o/o \text{ or } c)$ is the conditional probability that the channel is open given it is in one of two states, open or closed. Assuming that the gating kinetics is much faster than the blocking reaction, $P(o/o \text{ or } c)$ is given approximately by $\beta/(\alpha + \beta)$ and eq. (28) is immediately obtained. The mean burst time given by eq. (28) differs from the case where the blocking reaction is faster than the gating in that termination of a burst in the latter implies leaving the set of states open and blocked (Neher and Steinbach, 1978).

Since under all the experimental conditions in which we characterized the slow kinetic process we have $\beta \gg \alpha$ (see Table 1), $\bar{\tau}_b$ can be expressed as:

$$\bar{\tau}_b \approx \frac{1}{k_1 [\text{Ca}^{2+}]} \quad (29)$$

For the slow process, the reaction scheme (R-9) predicts that: (a) the measurable quantities, $\bar{\tau}_B$ (time in state B) and $\bar{\tau}_b$ (burst time), have exponential distributions; (b) $\bar{\tau}_b$ decreases with increasing Ca^{2+} concentration; and (c) $\bar{\tau}_B$ is independent of Ca^{2+} concentration.

Voltage and Ca^{2+} Dependence of the Slow Reaction

In order to calculate $\bar{\tau}_b$ and $\bar{\tau}_B$, the treatment of the data requires that a burst of activity not be confused with intervals between two "fast closings" (i.e., a transition from closed $\xrightarrow{\beta}$ open and from open $\xrightarrow{\alpha}$ closed) or with a series of transitions consisting of B $\xrightarrow{k-1}$ open

$\xrightarrow{\alpha}$ closed and viceversa (see scheme R-1). In order to exclude contamination of the fast process in the analysis of the slow reaction, a minimum cut-off time resulting in a single exponential distribution for the B state dwell times must be found. ~~We~~ ^I found that by filtering the data at 20 Hz or less (see Fig. 29 and Table 1), the dwell times in state B and the burst dwell times are effectively distributed as a single exponential at all the voltages and Ca^{2+} concentrations under which the slow process was studied (e.g., Figs. 29B and C). $\bar{\tau}_B$ and $\bar{\tau}_b$ can, therefore, be calculated either from curve fitting of the dwell time distribution or from the average dwell time (Ehrenstein et al., 1974; Moczydlowski and Latorre, 1983b). The kinetic constants of the slow reaction, R-9, can then be obtained from eqs. (27) and (28).

Fig. 30 shows that the main predictions of reaction scheme R-9 are confirmed experimentally: first, Fig. 30A shows that $1/\bar{\tau}_b$ is directly proportional to $[\text{Ca}^{2+}]$ and, second, Fig. 30B shows that $1/\bar{\tau}_B$ is independent of $[\text{Ca}^{2+}]$. Fig. 30C shows that both $\bar{\tau}_B$ and $\bar{\tau}_b$ are voltage dependent; however, most of the voltage dependence resides in $\bar{\tau}_b$. Inasmuch as $\bar{\tau}_B$ is independent of $[\text{Ca}^{2+}]$, k_{-1} , the voltage dependence of backward rate constant, was determined as a linear regression of all the experimental values in a log plot (Fig. 30C; see eq. 27).

$$k_{-1} = 0.24 \exp(-0.012 V) \quad (30)$$

where k_{-1} is given in s^{-1} and V in mV. k_{-1} , therefore, changes an e-fold for an 83 mV change in voltage. On the other hand, we found that k_1 (the slope of the straight line shown in Fig. 30A; see eq. 29) depends exponentially on voltage, according to:

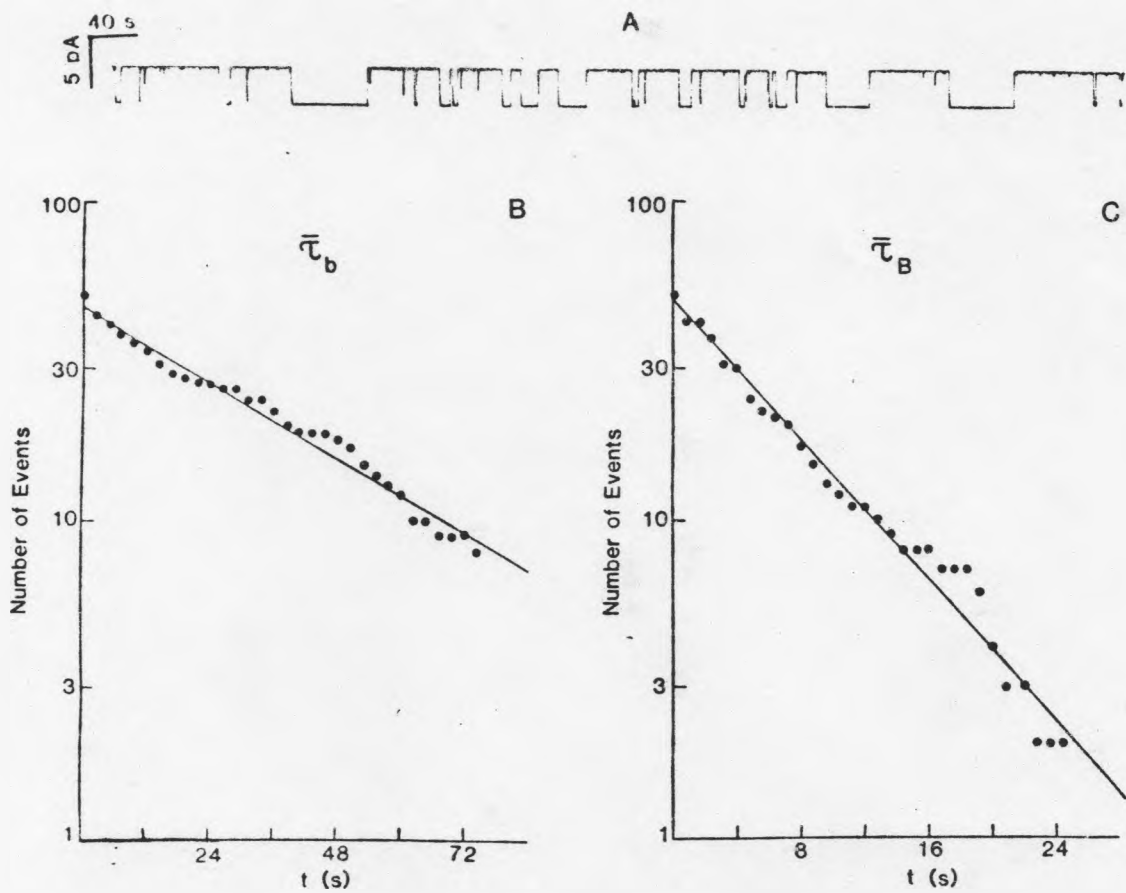


Fig. 29. Burst and "slow" closed dwell time distributions. A: current vs. time record obtained at +40 mV in symmetrical 10 mM Ca^{2+} , 100 mM K^+ and filtered at 5 Hz. B: distribution of burst dwell times ($\bar{\tau}_b$). C: slow closed dwell times distributions ($\bar{\tau}_B$). Data taken from a single channel record, part of which is shown in A. Total record time was 2700 seconds. The solid lines are the least square fit to the points.

Table 1

MEAN DWELL TIMES FOR THE DIFFERENT Ca^{2+} -ACTIVATED CHANNEL KINETIC PROCESSES

	Mean Open Time ^a (s)	Mean Closed (Blocked) Time ^b (s)
Fast process		
100 μM Ca^{2+}	0.1	0.003
^c Ca^{2+} -induced slow process		
1 μM Ba^{2+} , 100 μM Ca^{2+}	13	5.9
^d Ba^{2+} -induced slow process		
100 μM Ca^{2+}	200	5.3

^{a,b}All values are for a membrane potential of +40 mv.

^{c,d}Values after filtering at 20 Hz. At this frequency, the fast flickering present between long closings is absent, and the channel appears to be in either a conductive or blocked state.

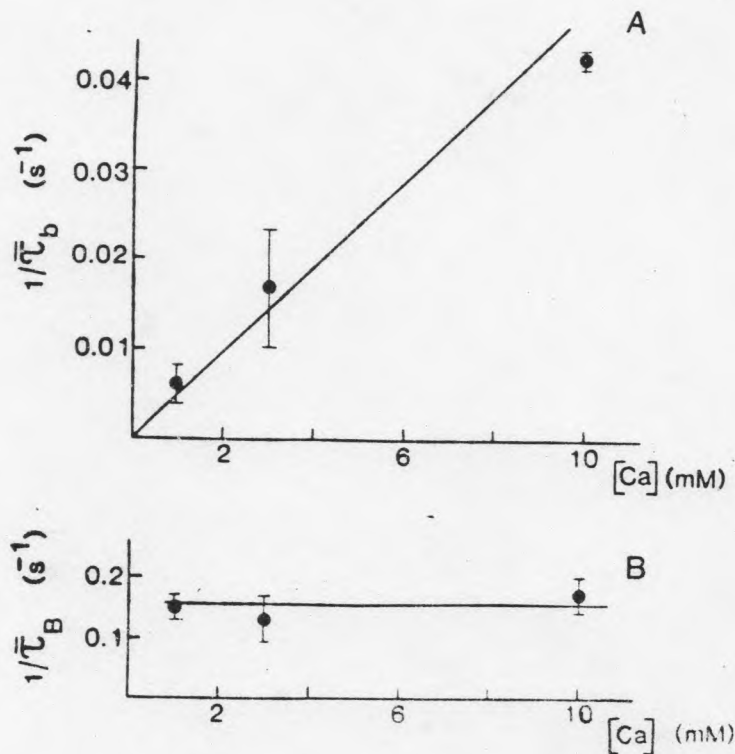
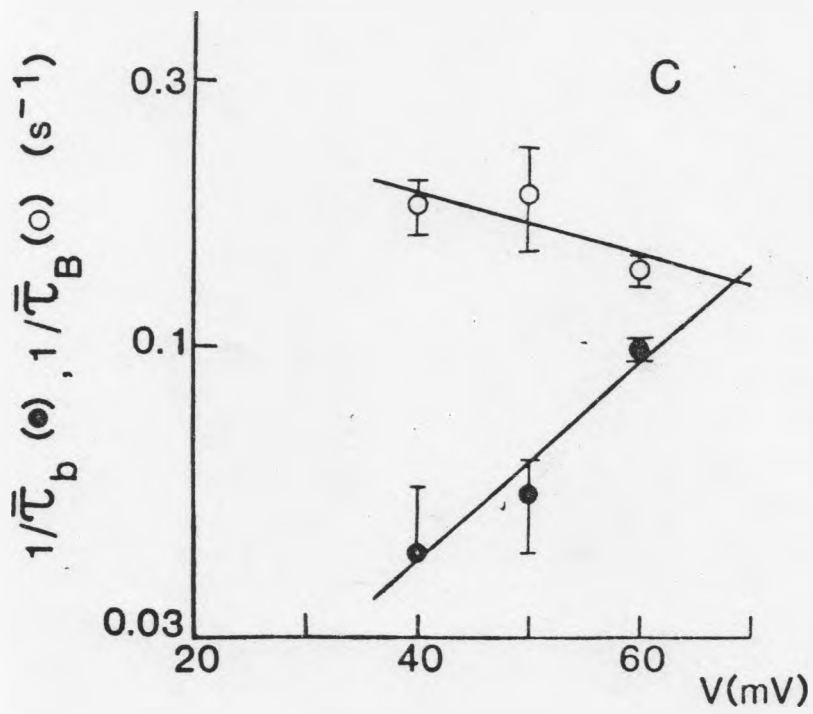


Fig. 30. Ca^{2+} concentration and voltage dependence of the slow kinetics induced by Ca^{2+} . A: reciprocal mean burst time ($1/\bar{\tau}_b$) vs. $[Ca^{2+}]$. B: reciprocal mean slow closed dwell time vs. $[Ca^{2+}]$. Channel kinetics was analyzed as in Fig. 29 at +40 mV in symmetrical 100 mM K^+ . Each point represents the mean \pm S.D. for 3 different channels and corresponds to the analysis of 40 to 110 transitions. C: voltage dependence of Ca^{2+} -induced slow kinetics. In this particular experiment, $1/\bar{\tau}_b$ changed e -fold/24 mV while $1/\bar{\tau}_B$ changes e -fold/77 mV. The points are the mean \pm S.D. for 3 different channels at +40 mV and +50 mV and for 2 different channels at +60 mV. $[Ca^{2+}] = 10$ mM, 100 mM KCl. The solid line is the least square fit to the points. The analysis was done considering 50 to 115 transitions for each point.



$$k_1 = 0.85 \exp(0.040 V) \quad (31)$$

where k_1 is given in $s^{-1} M^{-1}$ and changes an e-fold for a change in V of 25 mV. From eqs. (30) and (31) for the backward and forward rate constants, ~~we~~^I found that the apparent equilibrium dissociation constant for the binding reaction of the slow process, $K_D^{Ca}(V) = k_{-1}/k_1$, is:

$$K_D^{Ca}(V) = 0.29 \exp(-0.052 V) \quad (32)$$

where $K_D^{Ca}(V)$ is given in M and changes an e-fold for a change in voltage of 19 mV (see Table 2).

According to the blocking scheme of Woodhull, the voltage dependent dissociation constant for the binding of a blocker to the channel is given by eq. (21). After equating eqs. (32) and (21), ~~we~~^I found that Ca^{2+} at the blocking site senses approximately 65 ± 13 percent of the total membrane electric field, taking into account all the experiments done (see Table 2).

K⁺ Modifies the Slow Kinetic Process

At this point, ~~we~~^I would like to reconsider the type of molecular mechanism that could account for the effects of Ca^{2+} on the slow process. For example, if the long periods in which the channel remains silent are due to Ca^{2+} entering the lumen, binding to the site and blocking the channel, one expects to find competition for that site between the divalent cation and potassium. Fig. 31 shows that as K^+

Table 2

KINETIC AND EQUILIBRIUM CHARACTERISTICS OF THE Ca^{2+} - AND Ba^{2+} -INDUCED "SLOW" PROCESSES

	$k_{-i}(0)$	e-fold/mV	$k_i(0)$	e-fold/mV	K_D	δ
	(s^{-1})		($\text{s}^{-1} \text{M}^{-1}$)		(M)	
Ca^{2+}	0.24 ± 0.05	83 ± 13	0.85 ± 0.01	25 ± 1	0.29 ± 0.05	0.65 ± 0.13
$\text{Ba}_{\text{cis}}^{2+}$	0.30 ± 0.06	80 ± 8	$(8.3 \pm 0.7) \times 10^3$	19 ± 6	$(3.6 \pm 0.7) \times 10^{-5}$	0.80 ± 0.22
$\text{Ba}_{\text{trans}}^{2+}$	0.35		1.9×10^2		1.8×10^{-3}	0.35

k_{-i} and k_i correspond to the backward and forward reactions, respectively. Values are mean \pm S.D. of at least 4 experiments.

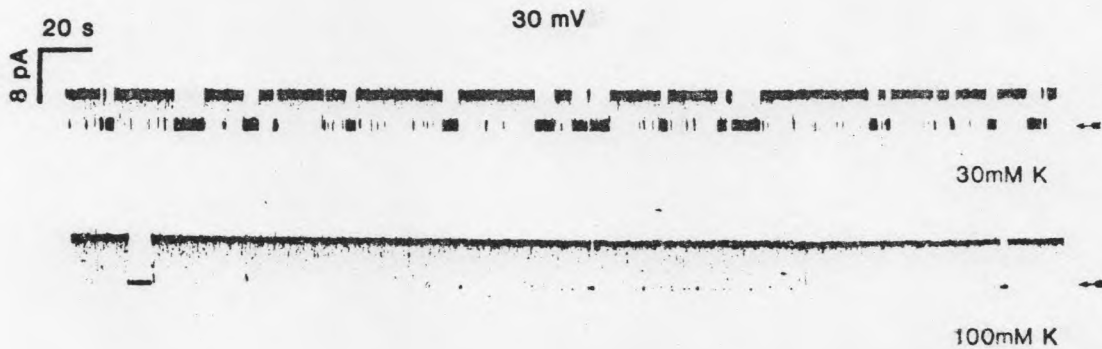


Fig. 31. Frequency of slow closing events as a function of $[K^+]$. The upper record was obtained in symmetric 30 mM K^+ , 0.1 mM Ca^{2+} at +30 mV. The lower record corresponds to a different channel at the same $[Ca^{2+}]$ and membrane voltage but in symmetrical 100 mM K^+ . Note that the frequency of blocking events is dramatically increased at the lower $[K^+]$. The arrows indicate zero current level. The records were low-pass filtered at 300 Hz.

concentration is decreased the frequency of the slow closure events increases dramatically with respect to the standard 0.1 M KCl used for most of the experiments. In terms of a blocking scheme, the records of Fig. 31 can be interpreted as competition between K^+ and Ca^{2+} for the same site.

The simplest blocking situation arises for channels that cannot contain more than one ion at a given time (Coronado and Miller, 1979; Miller, 1982). Based on the finding that single channel conductance does not decrease with ion activity, as expected for multi occupancy, I think that the Ca^{2+} -activated K^+ channel is a single ion channel.

Therefore, all the competition between Ca^{2+} and K^+ must reside in the forward rate constant, k_1 . In other words, for a single ion channel, knock-off of Ba^{2+} from the site by K^+ is not allowed (Armstrong, 1975b). In agreement with the above prediction, at +40 mV applied potential, I found an 18-fold increase for k_1 and less than a 2-fold decrease for k_{-1} for a decrease in $[K^+]$ from 100 to 30 mM.

In summary, the kinetic behavior of the slow process for the Ca^{2+} -activated K^+ channel is consistent with a Ca^{2+} blockade of the type described for the blockade of the sarcoplasmic reticulum K^+ channel by Cs^+ (Coronado and Miller, 1979) or the block of the acetylcholine-receptor channels by local anesthetics (Neher and Steinbach, 1978). However, if a Ca^{2+} block is the actual process by means of which the slow process is originated, then one is forced to conclude that, different from the cases mentioned above, the blocking reaction proceeds at a very slow pace.

Ba²⁺ Block

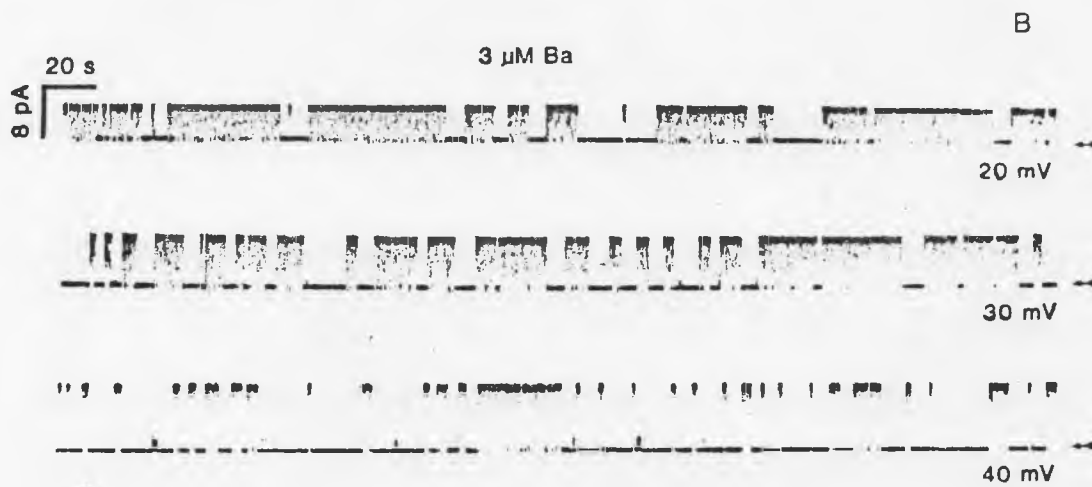
Cis Ba²⁺ Strongly Affects the Slow Kinetics

I found that Ba²⁺ does not activate the channel but promotes dramatic changes in the slow process. In other words, Ba²⁺ is a convenient ("faster") analog of Ca²⁺ for studying this process.

Fig. 32A shows the channel activity in the presence of three different Ba²⁺ concentrations at +40 mV applied voltage. Addition of Ba²⁺ to the cis side causes a reduction in the mean burst time (c.f. Fig. 32 A). Fig. 32A also shows that the frequency of appearance of the quiescent periods is dependent on Ba²⁺ concentration. However, contrasted with the situation with Ca²⁺, Ba²⁺ does not change the fraction of time the channel remains open within a burst. I have also investigated the possible role of Ba²⁺ in channel activation at low Ca²⁺ concentrations (1 to 10 μ M). Under these conditions, I found that Ba²⁺ does not increase the probability for a channel to be open in the Ba²⁺ concentration range of 1 to 80 μ M and up to +50 mV. Fig. 32B shows that the slow process induced by Ba²⁺ is also voltage dependent. Also, different from Ca²⁺, the probability of finding a quiescent period is relatively high even at low voltages (e.g., the 20 mV record of Fig. 32B).

Trans Ba²⁺ Also Affects the Slow Kinetics

Fig. 33 shows that when Ba²⁺ is added to the trans side the slow kinetic process is also altered. However, much larger concentrations of the divalent cation are necessary to obtain the same effects observed



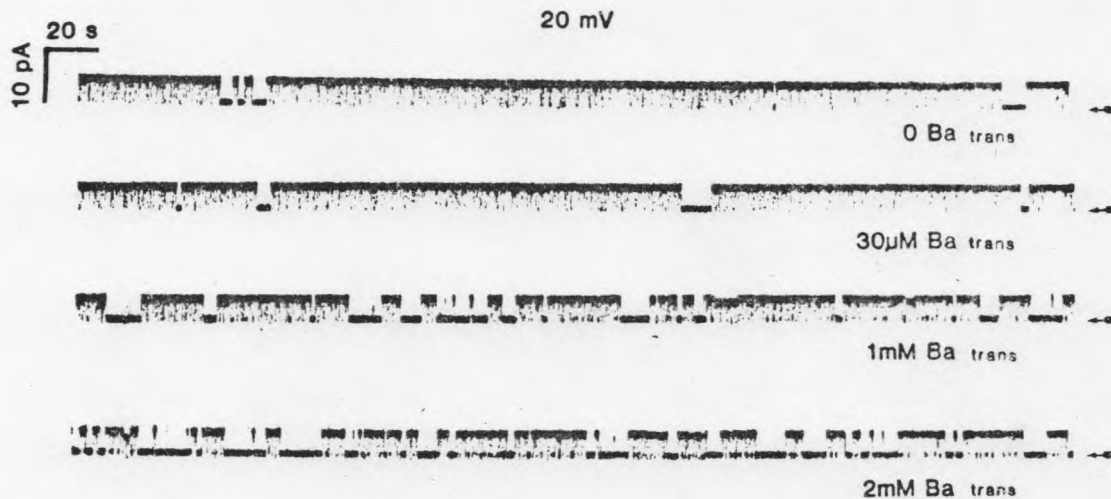
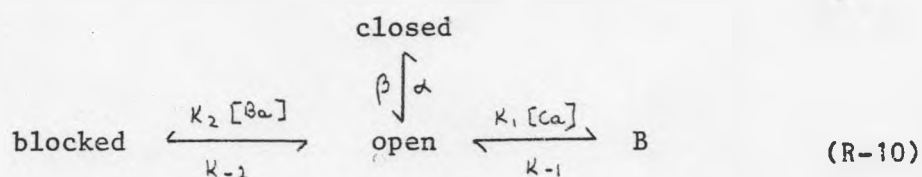


Fig. 33. Variation of the channel slow kinetics in the presence of trans Ba²⁺. The mean burst time and the mean time for the slow closing at 30 µM trans Ba²⁺ is not different from that obtained in the absence of Ba²⁺. As trans Ba²⁺ is further increased, the slow channel kinetics is modified. The records were obtained at +20 mV applied voltage in symmetrical 0.1 mM Ca²⁺, 100 mM K⁺. The arrows indicate the zero current level. Records were low-pass filtered at 300 Hz.

when Ba^{2+} is added to the cis side. Note that the cis and trans Ba^{2+} effects were measured in both cases at positive potentials. Positive potentials would favor entrance of cis Ba^{2+} , whereas they would not favor entrance of Ba^{2+} from the trans side. Therefore, Figs. 32 and 33 are not directly comparable (see below). Negative potentials were not tested since the mean closed time became too long. In other words, eq. (35) cannot be applied and the analysis of the data becomes difficult.

A Model For Ba^{2+} Action

As a starting point, we took the previous finding that both the inward and delayed rectifier channels are blocked by Ba^{2+} (Armstrong and Taylor, 1980; Eaton and Brodwick, 1980; Standen and Stanfield, 1978; Hagiwara et al., 1978). By analogy, then, we postulated that the Ca^{2+} -activated K^+ channel is also blocked by this divalent cation. The simplest kinetic model for ion blockade is the single site model of Woodhull (1973). Accordingly, we assumed that Ba^{2+} can only interact with an open channel following the reaction sequence:



where the Ba^{2+} blocking reaction is described by $k_2[Ba]$ --the pseudo first order rate constant of entry of the blocker, and k_{-2} --the first order rate constant for the backward reaction.

The relationship between the steps of reaction scheme R-10 and the current traces obtained in the presence of Ba^{2+} and Ca^{2+} of Fig. 32 is

the following: the long non-conductive periods correspond to a channel blocked with Ba^{2+} or to the slow reaction induced by Ca^{2+} . Comparison of the records in Fig. 32 with the second record from the top of Fig. 28A indicates that most of the long silent periods correspond to the Ba^{2+} blockade reaction. On the other hand, the bursts of activity between non-conductive periods represent the closed/open reaction.

For the Ba^{2+} experiments, we work under experimental conditions where the Ba^{2+} -induced slow reaction was predominant. Therefore, the expressions for the mean blocked time, $\bar{\tau}_s$, and for the mean burst time, $\bar{\tau}_{b, Ba}$, are approximately given by:

$$\bar{\tau}_s \approx \frac{1}{k_{-2}} \quad (33)$$

and

$$\bar{\tau}_{b, Ba} \approx \frac{1}{k_2 [Ba]} \left(1 + \frac{\alpha}{\beta} \right) \quad (34)$$

at $[Ca^{2+}] = 100 \mu M$ (the $[Ca^{2+}]$ used in all Ba^{2+} experiments) $\beta \gg \alpha$ and thus eq. (34) reduces to:

$$\bar{\tau}_{b, Ba} \approx \frac{1}{k_2 [Ba]} \quad (35)$$

Exact expressions for the unconditional mean time for the long silent periods, $\bar{\tau}_s$, and for the unconditional mean burst time, $\bar{\tau}_{b, Ba}$, on the basis of scheme R-10, can be obtained using the procedure described

by Colquhoun and Hawkes (1977). Through these expressions, since k_1 and k_{-1} are known from the previous experiments, one can calculate the exact contribution of Ba^{2+} to the overall slow kinetic process by measuring $\bar{\tau}_s$ and $\bar{\tau}_{b,Ba}$. Table 1, shows measurements of the parameters describing the slow process in the absence and in the presence of Ba^{2+} . Under these experimental conditions, k_{-2} and k_2 are overestimated by 4% and 9%, respectively, if the slow kinetic process induced by Ca^{2+} is not considered. At higher Ba^{2+} concentrations, the overestimation of the rate constants describing the Ba^{2+} blockade is even smaller. This quantitatively supports the contention made above that most of the silent periods seen in the presence of Ba^{2+} in Fig. 32 are the manifestation of the Ba^{2+} reaction. Furthermore, dwell times for the blocked and burst states are exponentially distributed. This further corroborates that, under the experimental conditions used, the Ca^{2+} reaction hardly influences the Ba^{2+} block.

For a reaction scheme of the type $\text{Blocked} \xrightleftharpoons{\alpha} \text{closed} \xrightleftharpoons{\beta} \text{open}$, eq. (34) becomes $\bar{\tau}_{b,Ba} = (1/k_2[Ba^{2+}]) (1 + \beta/\alpha)$ and, therefore, $\bar{\tau}_{b,Ba}$ should decrease as α becomes small (low probability of opening). I found that as the probability of opening (P_o) decreases $\bar{\tau}_{b,Ba}$ increases as expected from eq. (34). For example, at a $P_o = 0.15$, I found that $\bar{\tau}_{b,Ba}$ increased by about 6-fold. The measured α and β at this P_o are 42 and 6 ms, respectively, which implies, according to eq. (34) that $\bar{\tau}_{b,Ba}$ must be 8-fold larger than the value found at a $P_o \sim 1$. This prediction is in good agreement with the experimental result. Therefore, I believe that a model in which the blocked state arises from a closed state is unlikely. Given the similarities between the Ca^{2+} - and Ba^{2+} -induced slow kinetics, I think this model is also unlikely for the Ca^{2+} -induced slow process.

According to reaction scheme R-10 and eq. (35), $1/\bar{\tau}_{b,Ba}$ should be a linear function of the Ba^{2+} concentration with the slope k_2 (in s^{-1}

M^{-1}). Fig. 34A shows that this prediction of the model holds, inasmuch as $1/\bar{\zeta}_{b,Ba}$ increases linearly with $[Ba^{2+}]$ from 1 to $10 \mu M$. Also in agreement with the proposed model, it is found that $1/\bar{\zeta}_s$ is independent of $[Ba^{2+}]$ when the $[Ca^{2+}]$ is held constant (Fig. 34B).

Figs 35A and B show the voltage dependence of $1/\bar{\zeta}_{b,Ba}$ and $1/\bar{\zeta}_s$, respectively. These experiments indicate that the voltage dependence resides mainly on the blocking rate constant, k_2 , and very little on the unblocking rate constant, k_{-2} . (On the average, k_2 changes an e -fold/19 mV; k_{-2} changes an e -fold/80 mV). This finding is similar to what was found for the slow Ca^{2+} reaction. k_2 was obtained from experiments like the one shown on Fig. 32A and eq. (35) and was found to depend exponentially on voltage. k_{-2} , on the other hand, can be obtained from Fig. 35B, and eq. (33). The best fit to the experimental points give the following relationships.

$$k_2 = 8.3 \times 10^3 \exp(0.052 V) (s^{-1} M^{-1}) \quad (36)$$

$$k_{-2} = 0.3 \exp(-0.013 V) (s^{-1}) \quad (37)$$

$$K_D^{Ba}(V) = 3.6 \times 10^{-5} \exp(-0.065 V) (M) \quad (38)$$

From eqs. (21) and (38) we obtain $\delta = 0.80 \pm 0.22$ (see Table 2). This value is within experimental error similar to that found for the Ca^{2+} slow reaction ($\delta = 0.65 \pm 0.13$). The similarities in electric distances and in the slow kinetics induced by Ba^{2+} and Ca^{2+} suggest that they are acting at the same site, but that the affinity of the site for Ca^{2+} is much smaller than that for Ba^{2+} (c.f. eqs. 28 and 34; Table 2).

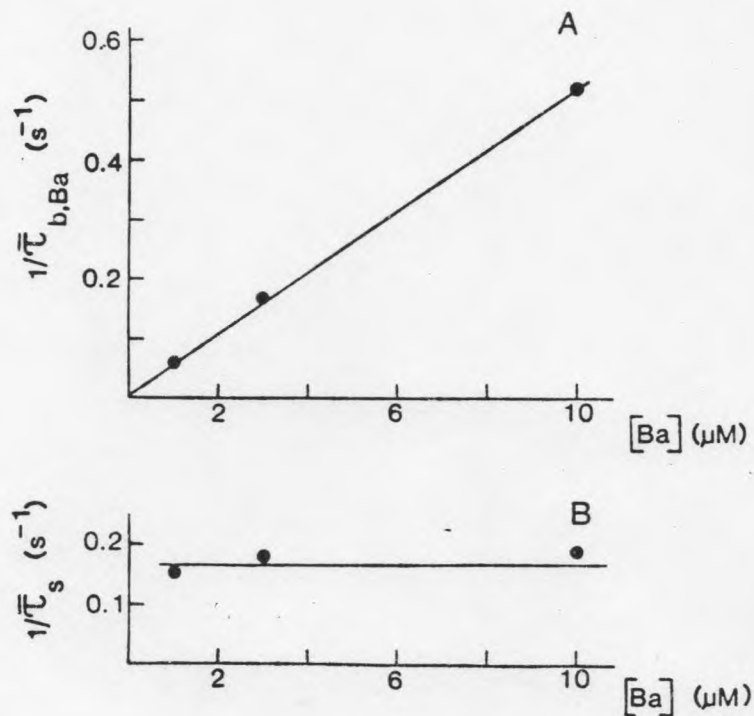


Fig. 34. Unconditional mean burst time ($\bar{\tau}_{b,Ba}$) and the mean slow-closing time ($\bar{\tau}_s$) as a function of the cis Ba²⁺ concentration. Single channel fluctuations were recorded at +30 mV in symmetrical 0.1 mM Ca²⁺ and 100 mM K⁺. The data was analyzed as described in Fig. 3 for Ca²⁺ but the records were low-pass filtered at 20 Hz. $\bar{\tau}_{b,Ba}$ (A) and $\bar{\tau}_s$ (B) were calculated as the time constant of a least square fit of the dwell time distribution. The same values for $\bar{\tau}_{b,Ba}$ and $\bar{\tau}_s$ are obtained if they are calculated as the simple average dwell time. Each point represents the analysis of 50 to 150 transitions.

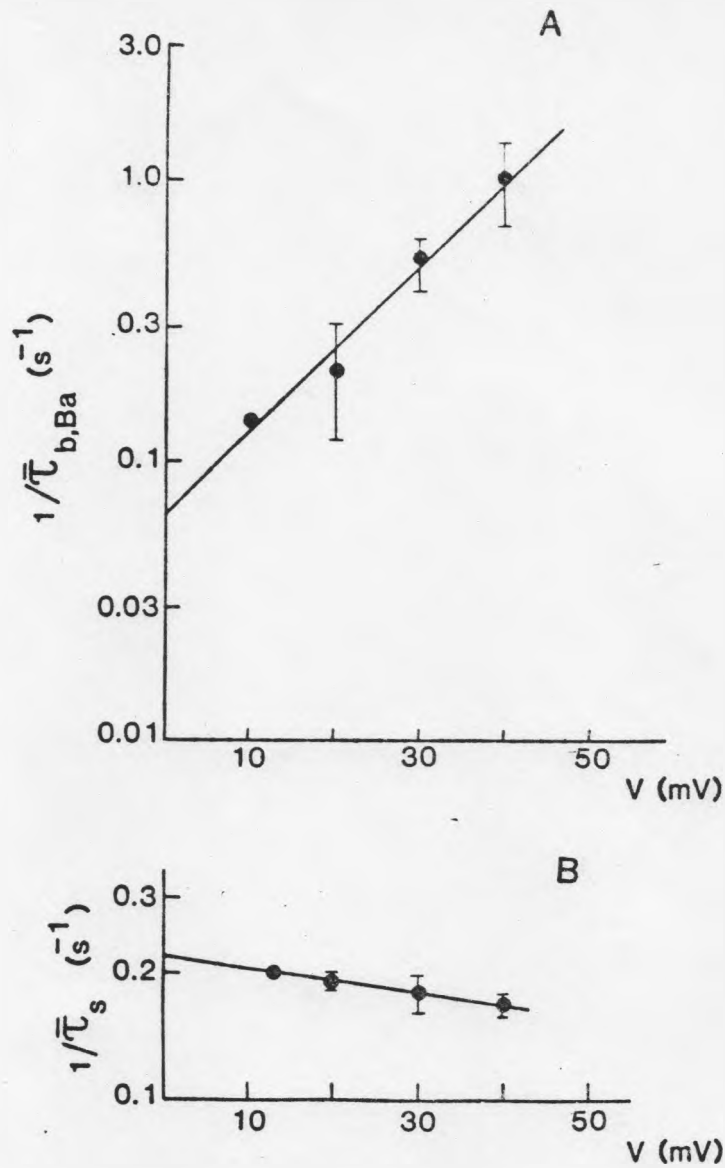


Fig. 35. A: Voltage dependence of the unconditional mean burst time ($\bar{\tau}_{b,Ba}$). B: Voltage dependence of the mean slow closing ($\bar{\tau}_s$) times. The experiments were done in symmetrical 0.1 mM Ca^{2+} , 100 mM K^+ in the presence of $10 \mu\text{M}$ *cis* Ba^{2+} . The points are the mean \pm S.D. for 5 membranes at +20 and +40 mV, and 2 membranes at +30 mV and one at 10 mV and 13 mV (A and B, respectively). Records as those shown in Fig. 6B but filtered at 20 Hz were used for the data analysis.

Trans Ba²⁺ Blockade

The characteristics of the trans Ba²⁺ effects shown in Fig. 33 were analyzed in the same way as done for the cis Ba²⁺ blockade. I found that $1/\bar{\zeta}_{b,Ba}$ increases linearly as the trans [Ba²⁺] is increased and that $1/\bar{\zeta}_s$ remains unchanged in the range of 0 to 2 mM.

If the site is reachable by Ba²⁺ from the cis and the trans side, then Ba²⁺ can leave the channel either by returning to the site of origin or by going towards the opposite site. The meaning of k_{-2} becomes, then, ambiguous inasmuch as in this case $\bar{\zeta}_s = 1/(k_{-2,cis} + k_{-2,trans})$. On the other hand, $k_{2,trans}$ and $k_{2,cis}$ are uniquely determined since they were obtained by setting [Ba²⁺]_{cis} or [Ba²⁺]_{trans} equal to zero. The values of $k_{2,trans}$ and $k_{2,cis}$ indicate that it takes 2.2 kcal/mole more energy for a trans Ba²⁺ than a cis Ba²⁺ ion to reach the site. If the Ba²⁺ site is the same regardless of the direction of ion flux, then it is unlikely for a trans Ba²⁺ to leave the channel towards the trans site because the trans energy barrier is larger. A trans Ba²⁺ leaves the channel through the cis side. A mechanism as the one proposed here predicts that as voltage is increased k_{-2} should become smaller. We found that on the average $k_{-2,trans}$ is voltage independent; in one experiment, however, k_{-2} decreased as voltage was increased, as expected when Ba²⁺ is leaving the channel through the cis side. It is also suggestive that both $k_{-2,cis}$ and $k_{-2,trans}$ have the same value at zero voltage. The difference between the cis and trans barrier heights lead us to believe that the voltage dependence shown by $k_{-2,cis}$ is due to the particular shape of the cis energy barrier. This

is so because a 2.2 kcal/mole difference in the energy peaks implies that at the voltages shown in Fig. 35B the block time reflects mainly a Ba^{2+} ion jumping from the site to the cis side. Furthermore, if the weak voltage dependence reflects cis and trans jumps, one should expect large departures from linearity when plotting $\log k_{-2}$ vs V. Fig. 35B shows clearly that this is not the case.

I further found that $1/\bar{z}_{b,Ba}$ changes an e-fold for a 36 mV change in voltage, and $1/\bar{z}_s$ is, within experimental error, voltage independent. The trans Ba^{2+} blockade is characterized by the following rate constants:

$$k_{2,\text{trans}} = 1.9 \times 10^2 \exp(-0.028 V) \text{ (s}^{-1} \text{ M}^{-1}\text{)} \quad (39)$$

$$k_{-2,\text{trans}} = 0.35 \text{ (s}^{-1}\text{)} \quad (40)$$

and, therefore, the trans apparent dissociation constant, $K_{D\text{trans}}^{Ba}$ is given by:

$$K_{D\text{trans}}^{Ba} = 1.8 \times 10^{-3} \exp(0.028 V) \text{ (M)} \quad (41)$$

The Ba^{2+} binding site according to eqs. (21) and (41) is at a fractional electrical distance, δ , of 0.35 from the trans side. If the cis and trans sites for Ba^{2+} blockade are the same, then the δ measured from the cis side plus the δ measured from the trans side must add up to one. I found that $\delta_{\text{cis}} + \delta_{\text{trans}} = 1.15$. I feel that, given the experimental uncertainties involved in the measurements of the Ba^{2+} blockade, the

value given above indicates that the Ba^{2+} site is the same whether coming from the cis or the trans sites (Table 2).

Competition of Ba^{2+} and K^+ Ions for the Blocking Site

Fig. 36 shows current records obtained at different symmetric K^+ concentrations. It is clear from these records that the effect of Ba^{2+} is relieved when the K^+ concentration is increased. Thus, at 300 mM K^+ , the number of slow closings is much smaller than at 100 mM K^+ . The fraction of blocked time (P_{bl}) in the presence of K^+ is given by the relationship (Segel, 1974):

$$\frac{1}{P_{bl}} = 1 + K_{Ba} \left(1 + \frac{[K^+]}{K_K} \right) \frac{1}{[Ba^{2+}]} \quad (42)$$

where K_{Ba} is the Ba^{2+} concentration at which $P_{bl} = 1/2$ and K_K is the dissociation constant for K^+ . Eq. (42) is, of course, derived assuming that the overall contribution of Ca^{2+} to the slow process is negligible.

Fig. 37 shows that the experimental results are well described by eq. (42) with:

$$K_{Ba} = 3 \times 10^{-6} \text{ M}$$

$$K_K = 6 \times 10^{-2} \text{ M}$$

K_{Ba} is, then, in good agreement with the value obtained from kinetic measurements (eq. 41). At +40 mV, the voltage at which the

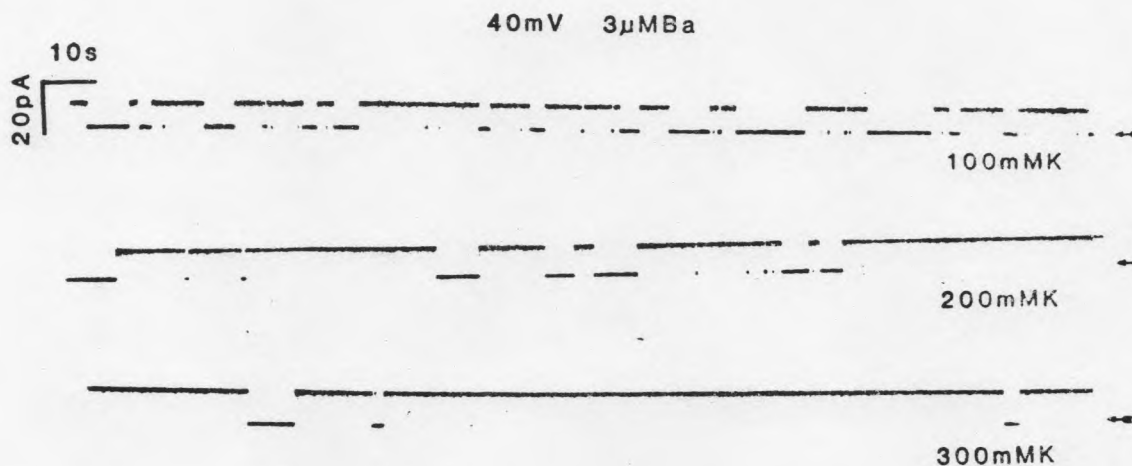


Fig. 36. Competition of cis Ba^{2+} and K^+ ions for the blocking site. The current records were obtained at +40 mV in the presence of 3 M cis Ba^{2+} with symmetrical 0.1 mM Ca^{2+} and symmetrical K^+ at the concentrations indicated. Note that as the $[K^+]$ is increased, the frequency of closings decreases. The arrows indicate the zero current level. Records were low-pass filtered at 300 Hz.

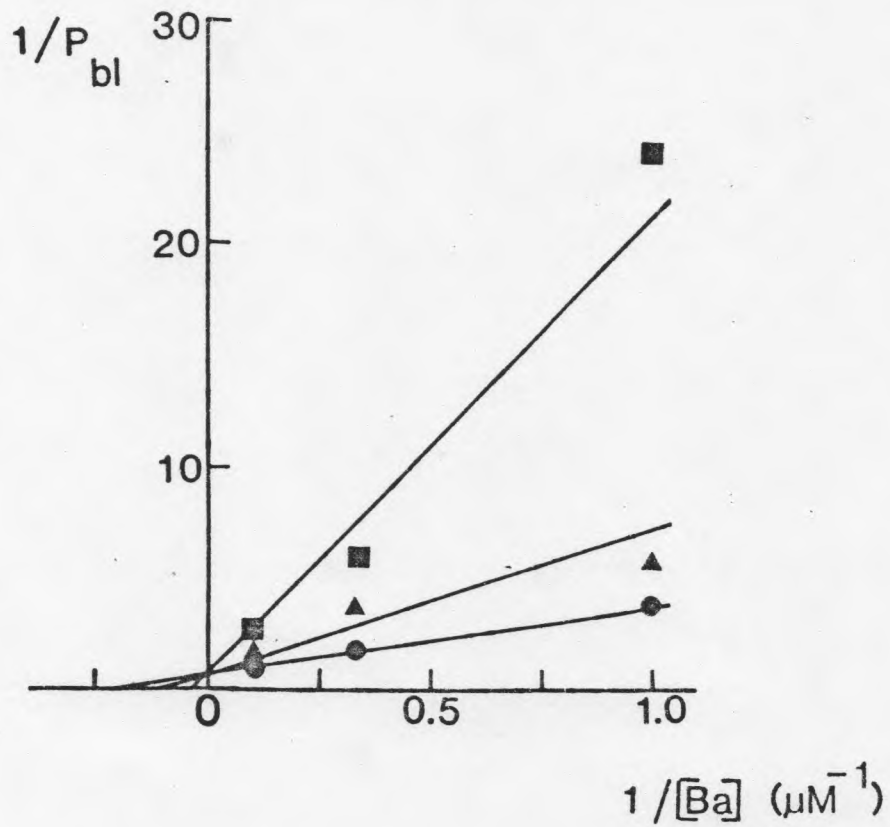


Fig. 37. The reciprocal of the fraction of blocked time (P_{bl}) as a function of the reciprocal of the cis $[Ba^{2+}]$ at different symmetrical $[K^+]$. K^+ behaves as a competitive inhibitor of the Ba^{2+} effect. (●) 100 mM K^+ ; (▲) 200 mM K^+ ; (■) 300 mM K^+ . Applied voltage: +40 mV.

competition experiments were done, eq. (41) predicts that $K_D^{Ba}(V) = 2 \times 10^{-6}$ M. On the other hand, the value for K_K obtained above compares well with that obtained by measuring the channel conductance vs. K^+ concentration ~ 0.1 M.

Fig. 38 shows $1/\bar{\tau}_{b,Ba}$ and $1/\bar{\tau}_s$ obtained from records as those shown in Fig. 36 as a function of K^+ concentration. The result is striking inasmuch as, in the range of K^+ concentrations tested, $k_2[Ba]$ changes 8-fold, whereas k_{-2} remains essentially constant. This is further evidence that Ba^{2+} ions cannot be "knocked off" the channel by K^+ . If K^+ were able to push Ba^{2+} out of the channel, then a change in k_{-2} as K^+ concentration is increased is expected.

Further evidence against a "knock-off" mechanism comes from experiments where only the trans K^+ concentration was increased. Fig. 39 shows current records obtained for different trans $[K^+]$. In these experiments, we found that the blocking rate constant is decreased while the unblocking rate constant is practically unaffected when the K^+ concentration is raised. With $3 \mu M$ cis Ba^{2+} and +40 mV applied voltage, $k_2[Ba^{2+}]$ is $0.265 s^{-1}$ in symmetrical $0.1 M K^+$ and $0.058 s^{-1}$ in $0.1 M K^+$ cis; $0.3 M K^+$ trans.

Other Channel Blockers

Quinine, apamin and decamethonium were also tested as blockers of the rabbit Ca^{2+} activated K^+ channel. Quinine has been reported to block the Ca^{2+} -induced K^+ efflux in red blood cells and the Ca^{2+} -activated K^+ currents in Aplysia neurons (Lew and Ferreira, 1978; Hermann and Gorman, 1981). Apamine has been reported to block the

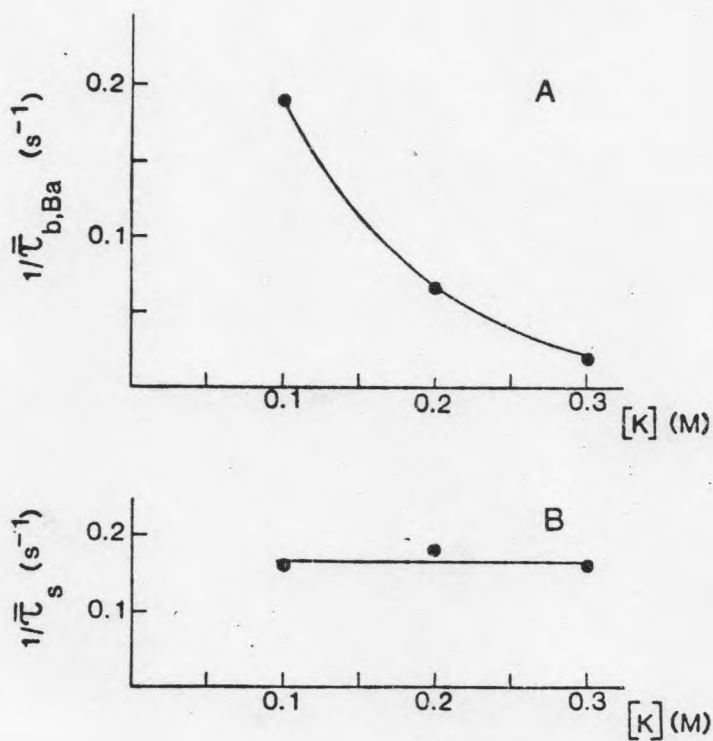


Fig. 38. Effect of $[K^+]$ on the Ba^{2+} -induced slow kinetics. The figure shows that as $[K^+]$ is increased from 100 to 300 mM, $1/\bar{\tau}_{b,Ba}$ (A) decreases while $1/\bar{\tau}_s$ (B) remains constant. The solid line in A has no theoretical meaning. The experiment was done at a $[Ba^{2+}]$ of $3\mu M$ and at an applied voltage of +40 mV.

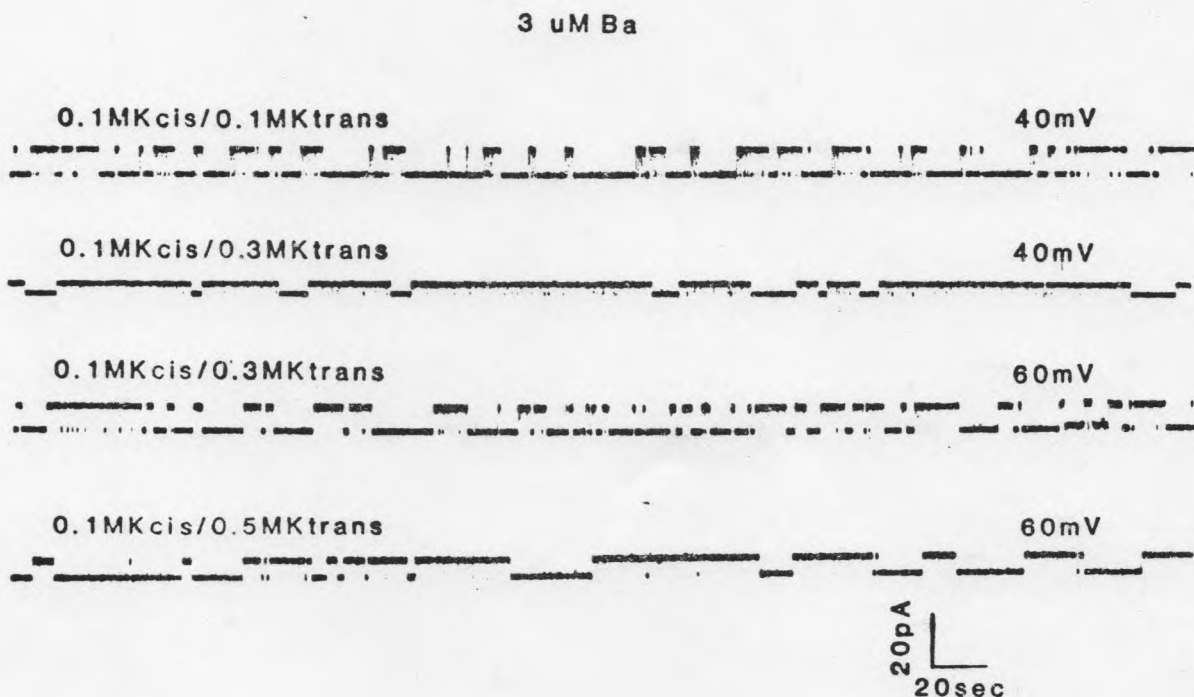


Fig. 39. Effect of trans $[K^+]$ on the Ba^{2+} -induced slow kinetics. The channel records were obtained at the indicated potentials in the presence of 0.1 M K^+ cis, 3 M Ba^{2+} cis and 0.1 mM Ca^{2+} symmetric. Trans $[K^+]$ was varied as indicated. Note that as trans $[K^+]$ is increased, the frequency of closings decreases.

Ca^{2+} -activated K^+ currents in neuroblastoma cells with very high affinity (complete current block was obtained with 100 nM external apamin) (Huges et al., 1982). Decamethonium has been reported to block the K^+ SR channel with relatively high affinity ($K_a(0) = 120 \text{ M}$) (Coronado and Miller, 1980).

Micromolar (50-100 μM) concentrations of cis added quinine were found to induce channel flickering; the block was not characterized.

Decamethonium added to the trans chamber up to concentrations of 2 mM had no effect on the single channel conductance. On the other hand, when added to the cis compartment in μM concentrations (10-20 μM) it caused a decrease in single channel conductance and an increase in channel flickering similar to that observed for cis C_9 block. Decamethonium block was not characterized in detail. Apamin was found ineffective as a blocker of the rabbit Ca^{2+} -activated K^+ channel.

Discussion

Block of K^+ Channels by TEA and TEA-Like Ions

TEA and its analogs have been found to block the delayed rectifier from squid, frog myelinated nerve, Aplysia neurones, the inward rectifier of muscle, the SR K^+ channel, and the Ca^{2+} -activated K^+ channel of Aplysia neurones but with peculiar characteristics in each case (Armstrong, 1971; Armstrong and Hille, 1972; Stanfield, 1970; Coronado and Miller, 1982; Hermann and Gorman, 1981). In squid, Armstrong (1969, 1971) showed that TEA and a number of ions having the general formula $(\text{C}_2\text{H}_5)_3\text{N}^+-\text{R}$ blocked the K^+ currents in a similar way.

These quaternary ammonium (QA) ions blocked only when applied to the inside of the nerve fiber once the voltage dependent channel gate was opened. He found that the blocking potency increased with the length (therefore, hydrophobicity) of the R group. On the other hand, octyl trimethylammonium was not found to cause K^+ current block, suggesting that the methyl derivatives are inactive. Based on these observations, Armstrong (1971) proposed that the binding site contained a hydrophobic region. He also proposed that the specificity for the K^+ conductance was due to the three ethyl groups surrounding the nitrogen atom. Inasmuch as TEA has a very similar radius as a K^+ ion with one hydration shell ($\sim 4.5 \text{ \AA}$), he suggested that the channel presents a wide antechamber that can accommodate either hydrated K^+ ions or TEA and its derivatives. At some point, this wide mouth narrows down into a "tunnel" region through which K^+ ions can advance by replacing some or all of its hydration waters with favorable interactions with sites along the tunnel. TEA, being unable to detach its ethyl groups, cannot move into the narrow tunnel. French et al. (1981) and Swenson (1981) studied the block by QA ion derivatives when the polarity and size of the head groups and/or tail groups was varied. Their results indicate that the inner mouth of the pore can be as wide as $11 \times 12 \text{ \AA}$ inasmuch as ions having head groups with these dimensions could block the channel. They also found that the ability of head group constituents to form hydrophobic bonds was correlated with blocking potency indicating that the hydrophobic interactions are allowed in the wide antechamber.

In myelinated axons, on the other hand, QA ions block when applied either internally or externally. The characteristics of the block induced by internally applied blockers are remarkably similar to those

observed in squid; therefore, Armstrong and Hille (1972) proposed that the same type of site is present in both channels. Nevertheless, the characteristics of the block by externally applied QA ions are different. No signs of voltage or time dependence are found for externally added QA ions; moreover, the blocking potency of the ions decreases with their degree of hydrophobicity. These differences between the block by internal and external QA ions have been considered as indications that the two binding sites are different (Armstrong and Hille, 1972).

Hermann and Gorman (1981) found that the delayed rectifier and the Ca^{2+} -activated K^+ channel from Aplysia neurones are blocked by either internally or externally applied TEA. Some TEA derivatives were also found to block the Ca^{2+} -activated K^+ currents when applied on the outside but with less potency than TEA.

The properties of the cis TEA and C_9 block presented for the rabbit Ca^{2+} -activated K^+ channel are very similar to the properties of the block by these ions on squid and frog nerve internal receptors (i.e., voltage-dependent block with C_9 representing a higher affinity than TEA). Therefore, the sites to which these blocker ions bind on the three different channels must present a high degree of homology. Moreover, the block by trans TEA and C_9 presents similar characteristics to those found for block by externally applied TEA and derivatives on the frog nerve (i.e., voltage independent block with TEA presenting higher affinity than C_9), suggesting that these sites are also similar. In conclusion, then, some structures like the described TEA and C_9 binding sites seem to be very well conserved on different types of K^+ channels.

Cis TEA Block of the Ca^{2+} -Activated K^+ Channel is Well Described by a Closed/Open/Block Reaction Scheme

The reaction scheme (R-8) demands that: a) In the presence of TEA, the time-averaged channel conductance should decrease according to a single site titration curve (eq. 22); b) The mean open time in the presence of the blocker should increase with blocker concentration according to eq. (25); c) If the reaction between TEA and its binding site takes place within the electric field in the channel, then the time averaged conductance should become voltage dependent according to eq. (21); d) The blocker should behave as a competitive inhibitor of conduction.

I found that for cis TEA ions, the first three predictions of the reaction scheme are fulfilled. The fourth prediction was not quantitated but qualitatively appears to hold. Therefore, I suggest that block by cis TEA ions is well described by R-8. On the other hand, for trans TEA block only the first prediction of the reaction scheme has been confirmed. (Note that trans TEA block is voltage independent). One of the characteristics of external TEA ion block on the frog node is that they reduce K^+ currents without changing its time course. A possibility to explain this result is to assume that a certain fraction of the channels is blocked at all times, whether open or closed (Armstrong, 1971). The alternative is that the binding and unbinding of TEA to the open channels is almost instantaneous and, therefore, once the channels open, a steady state of blockade is reached immediately. According to the first explanation, externally added TEA ions can block

a closed channel. From the available information for trans TEA block, I cannot discard the possibility that TEA interacts with the closed channel.

Characteristics of Ba²⁺ Block

In the results section, I have shown that addition of Ba²⁺ to the cis side can dramatically modify the slow kinetics of the Ca²⁺-activated K⁺ channel. The characteristics of Ba²⁺ action strongly suggest that Ba²⁺ interferes with K⁺ conduction by blocking the channel. They further suggest that cis Ba²⁺ blocks the channel by binding to a site located into the channel at about 80% of the way through the membrane field. Ba²⁺ also blocks the channel from the trans side. In this case, the blocking site senses about 30% of the applied field. I believe that the "cis" and "trans" sites for Ba²⁺ are the same. However, the rate of blocking is 44-fold larger for cis than for trans blockade. This implies that it is much harder for the Ba²⁺ ions in the trans site to get into the site than it is for cis Ba²⁺ ions.

The observations that support the blocking model of reaction scheme R-10 as the most economical for the Ba²⁺ effects are: (a) In the presence of micromolar amounts of Ba²⁺, the mean burst time is inversely related to Ba²⁺ concentration, and (b) The mean closed time is independent of Ba²⁺ concentration. On the other hand, the evidences that Ba²⁺ enters the pore when it blocks are: (a) The blocking equilibrium and kinetics are competitive with K⁺, and (b) Increasing the trans K⁺ concentration mainly modifies the rate of blocking. These observations would be difficult to reconcile with models in which Ba²⁺ binds to a site outside the K⁺ diffusion pathway.

Ba²⁺ blockade in Different K⁺ Channels

Ba²⁺ blockade has not been studied in Ca²⁺-activated channels of intact or patch-clamped cells. In Aplysia neurons, however, Ba²⁺ injected into the cells depresses both the Ca²⁺-dependent K⁺ conductance and the K⁺ currents through the delayed rectifier (Hermann and Gorman, 1979; Gorman and Hermann, 1979).

Ba²⁺ block of the delayed rectifier in squid axons has been studied by Armstrong and Taylor (1980) and by Eaton and Brodwick (1980). Both groups found that Ba²⁺ is a potent blocker of this channel when applied internally. In this case, the dissociation constant for the Ba²⁺ blocking reaction varies exponentially with voltage as predicted by eq. (21) such that Ba²⁺ occupies a site that is more than halfway through the membrane field. Armstrong and Taylor (1980) also found that Ba²⁺ can block the delayed rectifier if applied externally (but see Eaton and Brodwick, 1980). More recently, the external block of the delayed rectifier induced by Ba²⁺ was characterized by Armstrong et al. (1982) who concluded that Ba²⁺ applied externally can move two-thirds of the way into the channel and enter when the activation gates are closed. This is contrary to the case when Ba²⁺ is added to the internal perfusate since, in that case, Ba²⁺ can block only when the gates are open. From Armstrong et al.'s (1982) work emerges a picture for Ba²⁺ block in which Ba²⁺ ions appear to have at least two stable positions in the membrane, the occupancy of these being dictated by the membrane voltage. In other words, the delayed rectifier of squid has more than one binding site for Ba²⁺. K⁺ appears to compete for the binding

site(s) with Ba^{2+} , but raising the external K^+ concentration does not modify the voltage dependence of the block (Eaton and Brodwick, 1980; Armstrong et al., 1982). Further, Eaton and Brodwick have presented evidence for a knock off of Ba^{2+} by K^+ ions entering the channel at very negative potentials.

Externally added Ba^{2+} also blocks the inward rectifier of muscle (Standen and Stanfield, 1978). As found in the delayed rectifier of squid, the blockade is voltage dependent. The electrical distance, δ , for Ba^{2+} block of the muscle inward rectifier is 0.7. The Standen and Stanfield results are consistent with a model in which Ba^{2+} binds to a receptor in a 1:1 fashion with a $K_D^{Ba}(V) = 0.65$ mM at -5 mV. Here, as in the cases described above, K^+ ions compete for binding to the Ba^{2+} site. The binding affinities for the Ba^{2+} site are also in the mM range for externally induced Ba^{2+} block in the delayed rectifier. As stated above, Ba^{2+} also blocks the delayed rectifier when applied internally. The binding affinities for the internal site have been reported to be in the mM range by Armstrong and Taylor (1980) and Armstrong et al. (1982). However, using EDTA buffer to control the internal Ba^{2+} concentration, Eaton and Brodwick found that the delayed rectifier is blocked by Ba^{2+} in the nM range. We found that Ba^{2+} blocks the Ca^{2+} -activated channel when added in μ M amounts to the cis side and in mM amounts when added to the trans side.

Although Ba^{2+} blockade of the Ca^{2+} -activated K^+ channel shows several similarities with the Ba^{2+} blockade of both the delayed and inward rectifier, there are several important differences. First, although Ba^{2+} blockade is apparent from both the cis and trans sides of the channel, the data for the Ca^{2+} -activated K^+ channel can be explained

in terms of a single binding site for Ba^{2+} (c.f., Armstrong et al., 1982; but see Eaton and Brodwick, 1980). Second, there is no evidence in this channel of current dependent phenomena or "knock on" or "knock off" behavior in the Ba^{2+} block. Thus, I found that increasing the trans concentration of K^+ modifies only the Ba^{2+} entry rate, whereas in the delayed rectifier of squid, Eaton and Brodwick (1980) found that, at negative voltages, increasing the external K^+ concentration greatly increases the unblocking rate constant. I think that some of the differences between the Ba^{2+} block described here and that of the delayed rectifier are in agreement with differences in the structure of the two channels. The delayed rectifier is a multi-ion pore (Hille and Schwartz, 1978) whereas I propose that this Ca^{2+} -activated K^+ channel behaves as a single-ion pore. The evidence suggesting that the Ca^{2+} -activated K^+ channel is a single-ion pore is: (a) only the Ba^{2+} entry rate is modified by increasing either K^+ concentration at both sides of the membrane or at the trans side only; (b) the conductance of the channel saturates as K^+ concentration is increased (in the range of 1 to 3 M K^+).

Evidence for Ca^{2+} Blockade

The similarities between the slow kinetic phenomenon induced by Ca^{2+} and Ba^{2+} make it tempting to suggest that state B in reaction scheme R-9 is actually a Ca^{2+} blocked state. If this is the case, then Ca^{2+} at relatively high (>0.1 mM) concentrations or large voltages is not only able to activate the channel but can reach the site where Ba^{2+} binds and blocks the channel. I believe that both Ca^{2+} and Ba^{2+} bind to

the same site because the voltage dependence of the apparent equilibrium dissociation constant for the Ba^{2+} and Ca^{2+} reactions is about the same; i.e., the divalent ions travel the same electrical distance before reaching the binding site.

In patch-clamp experiments where single Ca^{2+} -activated K^+ channels can be resolved, quiescent periods like those we describe here have been observed (Wong and Lecar, 1982; Barret et al., 1982; Methfessel and Boheim, 1982). Although this process was not studied in detail, Methfessel and Boheim found that in Ca^{2+} -activated K^+ channels from cultured rat myoballs the bursts become shorter and the silent periods longer as the voltage is made more positive. Thus, the voltage dependence of the slow process in myoball Ca^{2+} -activated channels is qualitatively the same as that for the Ca^{2+} -activated channel of rabbit muscle.

Is there any evidence that this process occurs in cells? From macroscopic current measurements, Ecker and Lux (1977) described a Ca^{2+} -dependent depression of the Ca^{2+} -activated K^+ current in neurons from Helix. They measured currents under voltage-clamp conditions for a set of two depolarizing pulses and found an early activation of the K^+ current due to Ca^{2+} entry during the first pulse, but they found a depression of the current during the second pulse. They attributed this depression to the binding of Ca^{2+} ions to a site different from the activating site when Ca^{2+} ions accumulate near the membrane. It is difficult to estimate the local concentration of Ca^{2+} near the channel from this type of experiment, but it is possible that the Ca^{2+} block proposed by Ecker and Lux (1977) to explain their results is of the same type described here.

Mechanism of Ba²⁺ Block

The type of blocking described here is different from that caused by Cs⁺ ions or TEA and its derivatives on this Ca²⁺-activated K⁺ channel or in other types of K⁺ channels (e.g., Armstrong, 1975; Coronado and Miller, 1979). For those ions, the blocking rate is much faster than the channel closing rate, while the reverse situation is true for the Ba²⁺ blockade.

The basis for the strong blocking effect of Ba²⁺ on K⁺ channels has been attributed to the selectivity properties of K⁺ channels and the similarity in crystal ionic radius of these two ions (Standen and Stanfield, 1978; Armstrong and Taylor, 1980; Eaton and Brodwick, 1980). Blocker and permeability studies have indicated that K⁺ channels have a wide mouth of approximately 8 Å facing the intracellular side which at some point narrows down to approximately 3 Å. It is in this narrow region that selectivity takes place (Hille, 1975). For the Ca²⁺-activated K⁺ channel it is possible that Ba²⁺ ions can enter the wide mouth (as revealed by TEA experiments) but cannot go through the selectivity filter. Actually, the selectivity filter may be the binding site detected by the Ba²⁺ experiments! I believe that binding to the selectivity filter is possible since the crystal radii of K⁺ and Ba²⁺ are very similar (2.66 and 2.70 Å, respectively) and that it can be very tight because of the divalent nature of Ba²⁺.

CHAPTER 7

General Discussion

I want to emphasize again that the properties of the high conductance Ca^{2+} -activated K^+ channels that have been studied in cells and in bilayers have turned out to be the same. Inasmuch as the study of the Ca^{2+} -activated K^+ channel in bilayers can be done at a relatively fast pace as compared with its study in cells, many of the characteristics described here have not been reported for the channels studied in cells yet. It is tempting to predict that all the characteristics described should be also found in intact cells.

Other Types of Channels Present in the TT Vesicles

I found that other types of channels having different single channel conductances, voltage dependences and kinetic properties also incorporate into the bilayers. None of them was characterized. Under the experimental conditions used, the frequency of incorporation of "other channels" was low. Approximately 95% of the time the Ca^{2+} -activated K^+ channel was the only type of channel observed. Inasmuch as the muscle membrane contains Na^+ , K^+ Cl^- and Ca^{2+} channels (Stephani and Chiarandini, 1983), we expected to see different types of conductances in the bilayer. By looking for conditions that would allow selective incorporation of different types of channels, their properties could be characterized in detail.

Role of the Ca²⁺-Activated K⁺ Channel in Skeletal Muscle Cells

In neurones, there is good evidence indicating that Ca²⁺-activated K⁺ channels are involved in the control of repetitive activity displayed by pacemaker cells (Meech and Standen, 1975; Gorman and Hermann, 1982; Gorman et al., 1982). On the other hand, myotubes and adult denervated muscle show spontaneous discharges of membrane potential and their electrical activity is very similar. Barret et al. (1981) found that in cultured myotubes the rate of membrane depolarization is controlled, at least in part, by a Ca²⁺-activated K⁺ conductance. Given the similarities between the denervated adult cells and myotubes, they suggested that in the absence of innervation, the Ca²⁺-activated K⁺ conductance can regulate the pacemaker activity as proposed for neurones. Whether the Ca²⁺-activated K⁺ currents have a role during the normal action potential in adult innervated muscle cells is still an open question.

High Conductance And High Selectivity Are Not Exclusive

High conductance means that a large number of ions moves through the channel per unit time (10^8 for the Ca²⁺-activated K⁺ channel). Therefore, the rate of ion entry, the translocation rate, and the exit rate from the channel must be high. If at the same time the channel is highly selective, it is difficult to imagine it as a simple pore with a big diameter allowing free diffusion of ions. Latorre and Miller (1983) have proposed a particular "channel architecture" that can allow high rates of ion movement and at the same time high selectivity. In order

to allow for high rates of ion translocation, they propose that the region through which restricted diffusion takes place is only a short constriction or tunnel region connected to the external solutions through two wide mouths. To allow for a high rate of ion entry, the effective "ion capture area" of the channel must be large. This cannot be obtained by simply increasing the diameter of the tunnel because then selectivity is not allowed. Therefore, they propose that indeed a tunnel of "high" diameter exists but within the tunnel a constriction occurs. Furthermore, the applied voltage is assumed to drop only at the tunnel region.

"Thus, an ion in the mouth of the channel will diffuse randomly until it is captured by the short tunnel. Once inside the tunnel, the ion may now be swept through the channel by the applied electric field; it does not need to collide randomly with the narrower selectivity filter" (Latorre and Miller, 1983).

Channel Activation and Surface Charge

As mentioned on Chapter 3, the activation curves measured for channels inserted into PS membranes are shifted to the left along the voltage axis when compared to the activation curves measured for channels inserted into PE membranes at the same bulk $[Ca^{2+}]$. This effect is shown on Fig. (40). Assuming that the difference in the two curves is not due to a specific lipid effect but is a reflex of the surface potential (ψ_s) felt by the activating sites can be estimated. If the only difference between the activation curves in the two

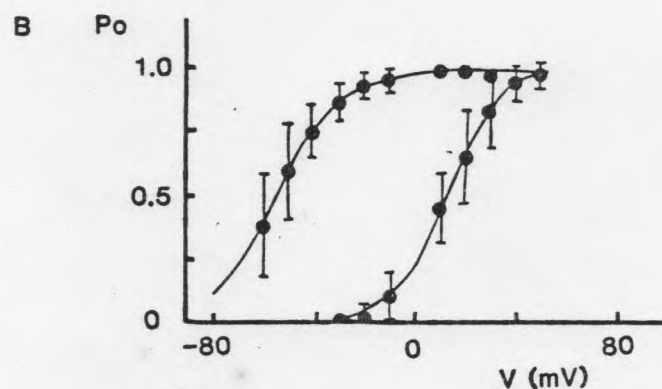
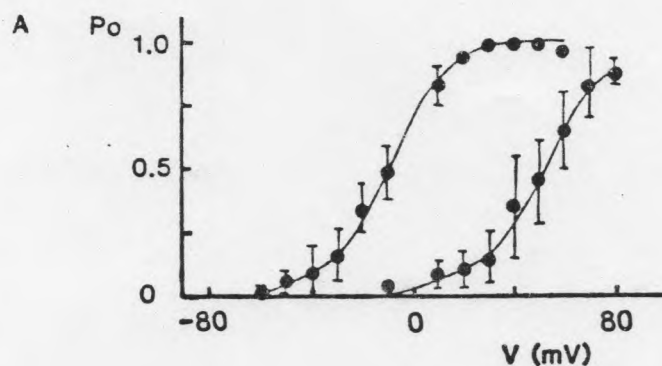


Fig. 40. Open state probability vs membrane potential at two different $[Ca^{2+}]$. (A) Data obtained in PE membranes. The curve at the left was obtained at $100 \mu M$ cis Ca^{2+} . The plots are the average for six different membranes with a total of 40 channels. The solid line was drawn according to eq. (11) with $n = 2$, $V_0 = 10$ mV. The curve at the right was obtained at $3 M$ cis Ca^{2+} , $n = 1.8$, $V_0 = 51$ mV (six membranes and 28 channels). (B) Data obtained in PS membranes. The curve at the left was obtained at $100 M$ cis Ca^{2+} . The points are the average of seven different membranes (eleven channels), $n = 2$, $V_0 = -54$ mV. The curve at the right was obtained at $3 M$ cis Ca^{2+} . The points are the average for six different membranes with a total of seven channels, $n = 2.6$, $V_0 = 13$ mV.

different membranes is due to the effect of surface charge, then a plot of the potential at which the channel is open 50% of the time (V_o) as a function of $[Ca^{2+}]$ for PE and PS membranes should give two parallel lines. At any given bulk $[Ca^{2+}]$ V_o should be shifted by a constant amount in PS vs PE membranes reflecting the increased $[Ca^{2+}]$ at the activating sites in the negatively charged membranes.

This was found to be the case (experiments by Edward Moczyłowski). The $[Ca^{2+}]$ at the activating site in PS membranes will be related to the bulk $[Ca^{2+}]$ by a Boltzman distribution; i.e.,

$$[Ca^{2+}]_{site} = [Ca^{2+}]_{bulk} \exp(-2F\psi_s/RT) \quad (43)$$

Assuming that the $[Ca^{2+}]$ at the activating sites in PE membranes reflects the bulk $[Ca^{2+}]$ (at pH 7.0 PE membranes bear a negligible amount of charge), from the V_o vs $[Ca^{2+}]$ plot one can obtain the $[Ca^{2+}]$ necessary to activate the channel by the same amount in the two different membranes. With this information, and eq. (16), one can obtain a value for the surface potential. For the rat Ca^{2+} -activated K^+ channel, this value was found to be -35 mV. Inasmuch as the surface potential at the plane of the membrane is \sim -130 mV in 0.1 M KCl, the site feels \sim 27% of the total potential. According to eq. (17) (see Introduction), this indicates that the Ca^{2+} activating site is located about 9 \AA away from the surface of the bilayer. As discussed on Chapter 3, the activating sites could be physically located facing the conduction pathway or in a separate cleft. Considering that the channel has two wide mouths (as indicated by the TEA experiments), and the channel architecture proposed by Latorre and Miller (1983) to explain

high conductance and high selectivity, I think it is more likely that the activating sites be in a separate cleft not facing the conduction pathway. Otherwise, approximately 80% of the field would have to fall in the wide mouth region, if indeed the voltage dependence of the Ca^{2+} binding reaction reflects binding to sites located in the field (see Discussion of Chapter 3).

Comparison With Other K^+ Channels

Although Ca^{2+} -activated K^+ channels of high single channel conductance have been described for many different preparations (Adams et al., 1982; Krueger et al., 1982; Marty, 1981; Pallota et al., 1981; Wong et al., 1982; Walsh and Singer, 1983; Maruyama et al., 1983; Latorre et al., 1982; Moczydlowski and Latorre, 1983; Methfessel and Boheim, 1982), a detailed analysis of the gating characteristics has only been done for a few of them (Methfessel and Boheim, 1982; Moczydlowski and Latorre, 1983). The channels studied in bilayers and in myotubes seem to present the same properties with respect to gating (Moczydlowski and Latorre, 1983; Methfessel and Boheim, 1982). The single channel recordings from other preparations look so similar that it is very possible that the gating machinery be the same in all of them.

At difference than classical voltage dependent and agonist dependent channels, the gating of Ca^{2+} -activated K^+ channels can be described by a voltage dependent binding of agonist (Ca^{2+} ions). Although not completely characterized in any channel, voltage dependent, agonist dependent and Ca^{2+} activated K^+ channels seem to share opening

reaction mechanisms that include several kinetically distinguishable steps.

High conductance Ca^{2+} activated K^+ channels from different preparations share a high degree of selectivity to alkali cations (Pallota et al., 1981; Maruyama et al., 1983; Methfessel and Boheim, 1982; results presented herein) as compared to other K^+ channels like the squid and frog nerve delayed rectifiers or the egg and muscle inward rectifiers (Hille, 1973; Binstock and Lecar, 1969; Standen and Stanfield, 1980; Hagiwara and Takahashi, 1974). Nevertheless, the selectivity sequence to the fingerprint ions Tl^+ and NH_4^+ is the same in all the K^+ channels studied. This suggests that the general structure of the selectivity filter is the same for all of them but the "degree of rigidity" of the filter changes for different channels.

At difference from the delayed and inward rectifier channels, the Ca^{2+} -activated K^+ channel behaves as a single ion channel (Hille and Schwartz, 1978) and presents a much higher single channel conductance. On the other hand, the channel pharmacology revealed by the TEA, C_9 and Ba^{2+} blockade points out that different K^+ channels share some common structures. Therefore, although K^+ channels from different cell membranes or organelles are responsible for different functions, they share some basic features.

An Estimate of the Energy Barrier for Ca^{2+} and Ba^{2+}

Clearly, the values of the rate constants for the rate of entry and unblocking indicate that in order to reach or to leave the site, Ba^{2+} ions must overcome a large energy barrier. This barrier appears to be

even larger for Ca^{2+} ions. The molecular origin of this barrier is not clear, but we know that the charging energy for a divalent cation in a narrow ($\sim 5 \text{ \AA}$ in diameter) pore is extremely high ($>20 \text{ kcal/mole}$; Parsegian, 1969; Levitt, 1978). Inasmuch as the energy required to transfer a Ba^{2+} (or Ca^{2+}) ion from solution into the pore is expected to be large on both theoretical and experimental grounds. Armstrong et al. (1982) have proposed the existence of negative charges inside the channel to explain the long residence time of Ba^{2+} inside the channel. The exact amount of energy that a Ba^{2+} ion must jump in order to get into the channel can be obtained from temperature studies (e.g., Eaton and Brodwick, 1980); however, one can obtain an-order-of-magnitude approximation to it by comparing the second order entry rate constants for K^+ , Ca^{2+} and Ba^{2+} . Denoting the entry rate constants for the ions k_K and $k_{X^{2+}}$, respectively, the ratio $k_K/k_{X^{2+}}$ is given by

$$\frac{k_K}{k_{X^{2+}}} = \exp \left[\frac{(\Delta G_{X^{2+}}^\ddagger - \Delta G_K^\ddagger)}{RT} \right] \quad (44)$$

where X^{2+} is Ba^{2+} or Ca^{2+} and $G_{X^{2+}}^\ddagger$ and G_K^\ddagger are the free energy of activation (barrier heights) for the rate of entry of the divalent cation and K^+ , respectively. Assuming that G_K^\ddagger is small, then eq. (44) allows us to obtain G_X^\ddagger . This is a good approximation of the activation energy if aqueous conductance and channel conductance are essentially the same (Frankenhauser and Moore, 1963). As discussed by Latorre and Miller (1983), the rate of entry can be obtained from the ratio between the maximum channel conductance, G_{max} , and K_D , the apparent dissociation constant. For the Ca^{2+} -activated K^+ channel, we have that $G_{\text{max}} = 500 \text{ pS}$ and $K_D = 140 \text{ mM}$; G_{max}/K_D , therefore, is 3.6 nS/M (Miller and Latorre,

1983). This corresponds to a rate of entry at 25 mV of $5.2 \times 10^8 \text{ M}^{-1} \text{ s}^{-1}$. From eq. (44) and taking the values for the entry rate of Ca^{2+} and Ba^{2+} at 25 mV from eqs. (31) and (36), respectively, we obtain $G_{\text{Ca}^{2+}} = 11.6 \text{ kcal/mole}$ and $G_{\text{Ba}^{2+}} = 6.6 \text{ kcal/mole}$.

Because of the different charges of K^+ and X^{2+} , the rate constants for these ions are differentially affected by voltage. This is so because, in the Eyring-type formulation, the applied voltage will increase the rate constant for divalent cations much more so than the rate constant for monovalent cations. We believe that 25 mV is a voltage low enough so that this effect does not introduce an error of more than 20% in our calculations of barrier heights and wells. Barrier heights would be underestimated and wells overestimated.

Fig. 13 shows what I think is a good approximation to the barrier shapes and magnitudes for Ba^{2+} and Ca^{2+} . In spite of the primitiveness of the calculations employed to obtain them, they explain the basic features of the Ba^{2+} and Ca^{2+} reactions of scheme R-10. The magnitude of the energy wells was estimated from the values of the dissociation constants for Ba^{2+} and Ca^{2+} . The energy well for Ba^{2+} is -7.1 kcal/mole and for Ca^{2+} it is -1.5 kcal/mole at 25 mV applied voltage.

In both the Ca^{2+} and Ba^{2+} experiments, we found that essentially all the potential dependence of the reaction was on the blocking rate constant. The lack of voltage dependence of the unblocking reaction can be due to the association of the blocker ion with the chemical groups contained in the site. This association can lead to a neutralization of the charges of the blocker ion and in this way, once the ion reaches the site, it is "shielded" from the electric field. One may compare this reaction with the association of Ag^+ with nigericin forming a neutral

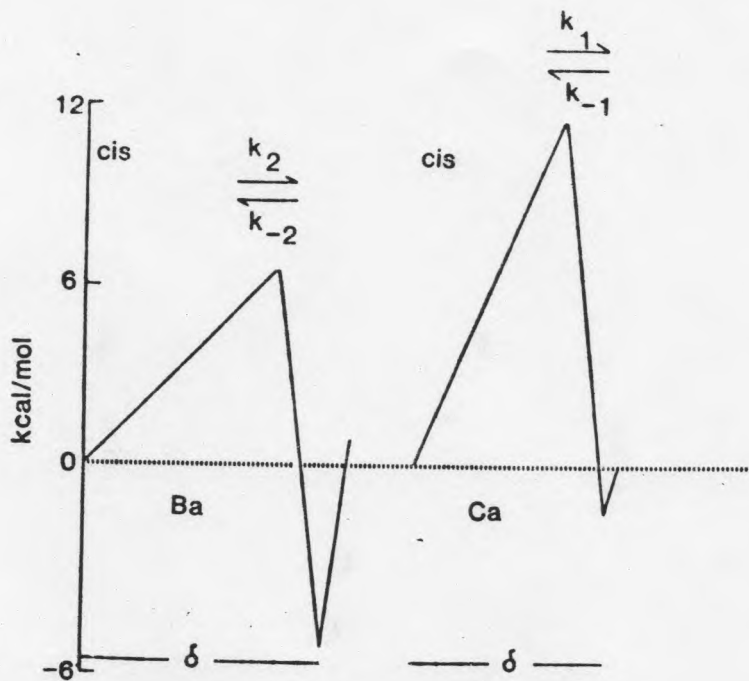


Fig. 41. Approximate energy profile for the interaction of Ba^{2+} and Ca^{2+} with the Ca^{2+} -activated K^+ channel. The energy in the trans side is taken as the reference state and is defined as zero. The energy in the cis side is modified by the applied voltage. k_2 and k_1 are the rate constants of the Ba^{2+} and Ca^{2+} movement from the cis to the blocking site, respectively. k_{-2} and k_{-1} are the rate constants of Ba^{2+} and Ca^{2+} movement from the blocking site to the cis side, respectively. The profile has been constructed to be consistent with the data presented in this paper; i.e. the apparent equilibrium constants, the electrical distances, the relationship between rate of entry of K^+ and that of the divalent cations, and the small voltage dependence of the rate constants, k_{-2} and k_{-1} .

complex (Simon and Morf, 1973). According to Fig. 41, in order to reach the blocking site, Ca^{2+} needs to jump over a barrier that is twice as high as the barrier Ba^{2+} faces, but once they are in the site the two ions should see approximately the same energy barrier to go back from the site to the solution. As shown in Table 2, this is reflected in approximately equal value for the unblocking rate constant for Ca^{2+} and Ba^{2+} .

The difference in barrier heights for these two cations can in part be due to the energy involved in the dehydration of each. We expect that, because Ba^{2+} has a larger crystal radius, it is less hydrated than Ca^{2+} and, therefore, less energy is necessary to take the water molecules solvating the former divalent cation. It is also tempting to suggest that the differences in well energies are due to cation size considerations. Ba^{2+} would make a "perfect fit" with the site, whereas Ca^{2+} , being smaller, cannot approach close enough to the chemical groups in the site that coordinate the divalent cation.

"A Channel Picture"

Based on the results presented here and on the available evidence from other channels, I propose that this Ca^{2+} -activated K^+ channel presents two wide mouths to either side of the membrane connected by a short conducting pathway that can only accommodate one ion at a time. The Ca^{2+} activating sites are located towards the cis chamber most probably not facing the conduction pathway itself. Binding sites for TEA, C_9 , Ca^{2+} and Ba^{2+} exist at different distances along the conduction pathway.

REFERENCES

- Adams, D.J., Dwyer, T.H., Hille, B. (1980) The permeability of end plate channels to monovalent and divalent metal cations. *J. Gen. Physiol.* 75:493-510.
- Adams, P.R., Constantini, A., Brown, D.A., Clark, R.B. (1982) Intracellular Ca activates a fast voltage-sensitive K current in vertebrate sympathetic neurones. *Nature* 246:746-749.
- Adrian, R.H., Chandler, W.K., Hodgkin, A.L. (1970) Slow changes in K permeability in skeletal muscle. *J. Physiol.* 208:645-668.
- Apell, H.J., Bamberg, E., Lauger, P. (1979) Effects of surface charge on the conductance of the gramicidin channel. *Biochim. Biophys. Acta* 552:369-378.
- Armstrong, C.M. (1966) Time course of TEA-induced anomalous rectification in squid giant axons. *J. Gen. Physiol.* 50:491-503.
- Armstrong, C.M. (1971) Interaction of tetraethylammonium ion derivatives with the potassium channels of giant axons. *J. Gen. Physiol.* 58:413-437.
- Armstrong, C.M. (1975a) Ionic pores, gates and gating currents. *Quart. Rev. Biophys.* 7:179-210.
- Armstrong, C.M. (1975b) Potassium pores of nerve and muscle membranes. In: Membranes, Vol. 3, edited by G. Eisenman, pp. 325-358. New York: Marcel Dekker.
- Armstrong, C.M., Bezanilla, F. (1974³) Currents related to movement of the gating particles of the sodium channels. *Nature* 242:459-461.
- Armstrong, C.M., Bezanilla, F., Rojas, E. (1973) Destruction of Na conductance inactivation in squid axons perfused with pronase. *J. Gen. Physiol.* 62:375-391.
- Armstrong, C.M., Binstock, L. (1965) Anomalous rectification in the squid giant axon injected with tetraethylammonium chloride. *J. Gen. Physiol.* 48:859-872.
- Armstrong, C.M., Gilly, W.F. (1979) Fast and slow steps in the activation of sodium channels. *J. Gen. Physiol.* 74:691-711.
- Armstrong, C.M., Hille, B. (1972) The inner quaternary ammonium ion reception in potassium channels of the node of Ranvier. *J. Gen. Physiol.* 59:388-400.
- Armstrong, C.M., Swensön, R.P., Taylor, S.R. (1982) Block of the squid axon K⁺ channels by internally and externally applied Ba²⁺ ions. *J. Gen. Physiol.* 80:663-682.

- Armstrong, C.M., Taylor, S.R. (1980) Interaction of barium ions with potassium channels in squid giant axons. *Bioophys. J.* 30:473-488.
- Barret, J.N., Barret, E.F., Dribin, L. (1981) Calcium-dependent slow potassium conductance in rat skeletal myotubes. *Devel. Biol.* 82:258-266.
- Barret, J.N., Magleby, K.L., Pallota, B.S. (1982) Properties of single calcium-activated potassium channels in cultured rat muscle. *J. Physiol.* 331:211-230.
- Bean, R., Shepherd, W.C., Chau, H., Eichner, J.T. (1969) Discrete conductance fluctuations in lipid bilayer protein membranes. *J. Gen. Physiol.* 53:741-757.
- Begenisich, T. (1975) Magnitude and location of surface charges in *Myxocolla* giant axons. *J. Gen. Physiol.* 66:47-65.
- Bell, J., Miller, C. (1983) Effects of phospholipid surface charge on ion conduction in the potassium channel of sarcoplasmic reticulum. *Bioophys. Soc. Discussions*, in press.
- Bergman, C. (1970) Increase in sodium concentration near the inner surface of nodal membrane. *Pflugers Arch.* 317:287-302.
- Bezanilla, F., Armstrong, C.M. (1972) Negative conductance caused by entry of sodium and cesium ions into the potassium channels of squid axons. *J. Gen. Physiol.* 60:588-608.
- Bezanilla, F., Vergara, J., Taylor, R. (1982a) Voltage clamping of excitable membranes. Chapter 10, In: Methods of Experimental Physics, Vol 20, pp. 445-511. New York: Academic Press.
- Bezanilla, F., White, M., Taylor, R. (1982b) Gating currents associated with potassium channel activation. *Nature* 296:657-659.
- Bezanilla, F., White, M. (1983) Properties of ionic channels in excitable membranes. In: Physiology of Membrane Disorders, 2nd Edition, edited by T.E. Andredli, J. Hoffman, and D. Fanestil, pp. New York and London: Plenum Publishing Co.
- Binstock, L., Lear, H. (1969) Ammonium ion currents in the squid giant axon. *J. Gen. Physiol.* 53:342-361.
- Blatz, A.L., Magleby, K.L. (1983) Voltage dependent chloride-selective channels of large conductance in cultured rat skeletal muscle. *Bioophys. J.* 41:62a.
- Bookris, J.O'M., Reddy, A.K.N. (1970) Modern Electrochemistry. New York: Plenum Publishing Co.
- Boneim, G., Hanke, W., Eibl, H. (1980) Lipid phase transition in planar bilayer membranes and its effect on carrier- and pore-mediated ion transport. *Proc. Natl. Acad. Sci. U.S.A.* 77:3403-3407.

- Campbell, D.T. (1976) Ionic selectivity of the sodium channel of frog skeletal muscle. *J. Gen. Physiol.* 67:295-307.
- Cecchi, X., Alvarez, O., Latorre, R. (1981) A three-barrier model for the hemocyanin channel. *J. Gen. Physiol.* 78:657-681.
- Chandler, W.K., Meves, H. (1965) Voltage clamp experiments on internally perfused giant axons. *J. Physiol.* 180:788-820.
- Chiarandini, D.I., Stefani, E. (1983) Calcium action potentials in rat fast twitch and slow twitch muscle fibers. *J. Physiol.* 335:29-40.
- Cole, K.S. (1949) Dynamic electrical characteristics of the squid axon membrane. *Arch. Sci. Physiol.* 3:253-258.
- Colquhoun, D. (1979) The link between drug binding and response: Theories and observations. In: The Receptors: A Comprehensive Treatment, Vol. 1, edited by R.D. O'Brien, pp. 93-142. New York and London: Plenum Press.
- Colquhoun, D., Hawkes, A.G. (1977) Relaxation and fluctuation of membrane currents that flow through drug operated channels. *Proc. Roy. Soc. London* 199:231-262.
- Connor, J.A. (1980) The fast K channel and repetitive firing. In: Molluscan Nerve Cells: From Biophysics to Behavior, edited by J. Koester and J. Byrne, pp. 125-133. Cold Spring Harbor, NY: Cold Spring Harbor Laboratory.
- Conti, F., Neher, E. (1980) Single channel recordings of K^+ currents in squid axons. *Nature* 285:140-143.
- Coronado, R., Latorre, R. (1983) Bilayers in patch-clamp pipettes. *Biophys. J.*, in press.
- Coronado, R., Miller, C. (1979) Voltage-dependent caesium blockade of a cation channel from fragmented sarcoplasmic reticulum. *Nature* 280:807-810.
- Coronado, R., Miller, C. (1980) Decamethonium and hexamethonium block K^+ channels of sarcoplasmic reticulum. *Nature* 288:495-497.
- Coronado, R., Miller, C. (1982) Conduction and block by organic cations in a K^+ -selective channel from sarcoplasmic reticulum incorporated into planar phospholipid bilayers. *J. Gen. Physiol.* 79:529-547.
- Coronado, R., Rosenberg, R.L., Miller, C. (1980) Ionic selectivity, saturation and block in a K^+ -selective channel from sarcoplasmic reticulum. *J. Gen. Physiol.* 76:425-446.
- De Peyer, J., Cachelin, P., Levitan, I., Reuter, H. (1982) Ca^{2+} -activated K^+ conductance in internally perfused snail neurons is enhanced by protein phosphorylation. *Proc. Natl. Acad. Sci. U.S.A.* 79:4207-4211.

- Diamond, J.M., Wright, E.M. (1969) Biological membranes: The Physical Basis of Ion and Nonelectrolyte Selectivity. *Annu. Rev. Physiol.* 31:581-649.
- Dionne, V.E., Steinbach, J.H., Stevens, C.F. (1978) An analysis of the dose response relationship at voltage clamped frog neuromuscular junction. *J. Physiol.* 281:421-444.
- Dionne, V.E., Stevens, C.F. (1975) Voltage dependence of agonist effectiveness at the frog neuromuscular junction: Resolution of a paradox. *J. Physiol.* 251:245-270.
- Eaton, D.C., Brodwick, H.S. (1980) Effect of barium on the potassium conductance of squid axons. *J. Gen. Physiol.* 75:727-750.
- Ecker, R., Lux, H.D. (1977) Calcium-dependent depression of a late outward current in snail neurones. *Science* 197:472-475.
- Ehrenstein, G., Blumenthal, R., Latorne, R., Lecar, H. (1974) Kinetics of the opening and closing of individual excitability-inducing material channels in a lipid bilayer. *J. Gen. Physiol.* 63:707-721.
- Ehrenstein, G., Lecar, H. (1972) The mechanism of signal transmission in nerve axons. *Annu. Rev. Biophys. Bioeng.* 1:347-368.
- Ehrenstein, G., Lecar, H., Nossal, R. (1970) The nature of the negative resistance in bimolecular lipid membranes containing excitability-inducing material. *J. Gen. Physiol.* 55:119-133.
- Ehrlich, B.E., Finkelstein, A., Forte, H., Kung, C. (1983) Calcium channels from Paramecium cilia incorporated in a planar lipid bilayer. *Biophys. J.* 41:293a.
- Eisenberg, R.S., Gage, P.W. (1969) Ionic conductances of the surface and transverse tubule membranes of frog sartorius fibers. *J. Gen. Physiol.* 53:325-342.
- Eisenman, G. (1962) Cation selective glass electrodes and their mode of operation. *Biophys. J.* 2:259-323.
- Eisenman, G., Horn, R. (1983) Ionic selectivity revisited. *J. Membr. Biol.*, in press.
- Elul, R.J. (1967) Fixed charge in the cell membrane. *J. Physiol.* 189:351-365.
- Eyring, H., Lumry, R., Woodbury, J.W. (1949) Some applications of modern rate theory to physiological systems. *Rec. Chem. Prog.* 10:100-114.
- Fatt, P., Katz, B. (1951) An analysis of the end plate potential recorded with an intracellular electrode. *J. Physiol.* 115:320-370.

- Fernandez, J., Roseblatt, M., Hidalgo, C. (1980) Highly purified sarcoplasmic reticulum vesicles are devoid of Ca independent (basal) ATPase activity. *Biochim. Biophys. Acta* 599:552-568.
- Fohlmeister, J.F., Adelman, W.J. (1982) Periaxonal surface calcium binding and distribution of charge on the faces of squid axon potassium channel molecules. *J. Membr. Biol.* 70:115-123.
- French, R.J., Shoukimas, J.J. (1981) Blockade of squid axon potassium conductance by internal tetra-N-alkylammonium ions of various sizes. *Biophys. J.* 34:271-291.
- Frankenhauser, B., Moore, L.E. (1963) The effect of temperature on the sodium and potassium permeability changes in myelinated fibers of *Xenopus laevis*. *J. Physiol. (London)* 169:431-437.
- French, R.J., Wells, J.B. (1977) Sodium ions as blocking agents and charge carriers in the potassium channel of the squid axon. *J. Gen. Physiol.* 70:707-724.
- Gage, P.W., Eisenberg, R.S. (1969) Action potentials, after-potentials and excitation-contraction coupling in frog sartorius fibers without transverse tubules. *J. Gen. Physiol.* 53:298-310.
- Gay, L.A., Stanfield, P. (1978) Cs^+ causes a voltage-dependent block of inward K^+ currents in resting skeletal muscle fibers. *Nature* 267:169-170.
- Gilly, W.F., Armstrong, C.M. (1980) Gating currents and potassium channels in the giant axon of the squid. *Biophys. J.* 29:485-492.
- Gilly, W.F., Armstrong, C.M. (1982) Divalent cations and the activation kinetics of potassium channels in squid giant axons. *J. Gen. Physiol.* 79:965-996.
- Görman, A.L.F., Hermann, A. (1979) Internal effects of divalent cations on K^+ permeability in molluscan neurones. *J. Physiol.* 296:393-410.
- Görman, A.L.F., Hermann, A. (1982) Quantitative differences in the currents of bursting and beating molluscan pace maker neurones. *J. Physiol.* 333:681-699.
- Görman, A.L.F., Hermann, A., Thomas, M.V. (1982) Ionic requirements for membrane oscillations and their dependence on the calcium concentration in a molluscan pacemaker cell. *J. Physiol.* 327:185-217.
- Görman, A.L.F., Woodlum, J.C., Cornwall, M.C. (1982) Selectivity of the Ca^{2+} -activated and light-dependent K^+ channels for monovalent cations. *Biophys. J.* 38:319-322.
- Gration, K.A.F., Lambert, J.J., Ramsey, R., Usherwood, P.N.R. (1981) Non random openings and concentration-dependent lifetimes of glutamate-gated channels in muscle membranes. *Nature* 291:423-425.

- Hagiwara, S. (1980) General considerations in the study of the Ca^{2+} channel. In: Molluscan Nerve Cells: From Biophysics to Behavior, edited by J. Koester and J. Byrne, pp. . Cold Spring Harbor, NY: Cold Spring Harbor Laboratory.
- Hagiwara, S., Byerly, L. (1981) Ca^{2+} channels. Annu. Rev. Neurosci. 4:69-125.
- Hagiwara, S., Eaton, D.C., Stuart, A.E., Rosenthal, N.P. (1971) Cation selectivity of the resting membrane of squid axon. J. Membr. Biol. 9:373-389.
- Hagiwara, S., Kusano, K., Saito, N. (1961) Membrane changes of Onchidium nerve cell in K^{+} -rich media. J. Physiol. 155:470-489.
- Hagiwara, S., Miyazaki, S., Krasne, S., Ciani, S. (1977) Anomalous permeability of the egg cell membrane of a starfish in K^{+} - Tl^{+} mixtures. J. Gen. Physiol. 70:269-281.
- Hagiwara, S., Miyazaki, S., Mobay, W., Patlak, J. (1978) Blocking effects of barium and hydrogen ions on the potassium current during anomalous rectification in the starfish egg. J. Physiol. 279:167-185.
- Hagiwara, S., Miyazaki, S., Rosenthal, N.P. (1976) Potassium current and the effect of cesium on this current during anomalous rectification of the egg cell membrane of a starfish. J. Gen. Physiol. 67:621-638.
- Hagiwara, S., Takahashi, K. (1974) The anomalous rectification and cation selectivity of the membrane of a starfish egg cell. J. Membr. Biol. 18:61-80.
- Hamil, O.P., Marty, A., Neher, E., Sakmann, B., Sigworth, F. (1981) Improved patch clamp techniques for high resolution current recordings from cells and cell-free membrane patches. Pflugers Arch. 391:85-100.
- Hartshorne, R.P., Catterall, W.A. (1981) Purification of the saxitoxin receptor of the Na^{+} channel from rat brain. Proc. Natl. Acad. Sci. U.S.A. 78:4620-4624.
- Hermann, A., Görman, A.L.F. (1979) Blockade of voltage and Ca^{2+} -dependent K^{+} current components by internal Ba^{2+} in molluscan pacemaker neurons. Experientia 35:229-321.
- Hermann, A., Görman, A.L.F. (1981) Effects of tetraethylammonium on potassium currents in a molluscan neuron. J. Gen. Physiol. 78:87-110.
- Hermann, A., Hartung, K. (1982) Noise and relaxation measurements of the Ca^{2+} -activated K^{+} current in *Helix* neurones. Pflugers Arch. 393:254-261.

- Hille, B. (1971) The permeability of the sodium channel to organic cations in myelinated nerve. *J. Gen. Physiol.* 58:599-619.
- Hille, B. (1972) The permeability of the sodium channel to metal cations in myelinated nerve. *J. Gen. Physiol.* 59:637-658.
- Hille, B. (1973) Potassium channels in myelinated nerve. Selective permeability to small ions. *J. Gen. Physiol.* 61:669-686.
- Hille, B. (1975) Ionic selectivity of Na⁺ and K⁺ channels of nerve membranes. In: Membranes, Vol. 3, edited by G. Eisenman, pp. 256-323. New York: Marcel Dekker.
- Hille, B., Schwartz, W. (1978) K⁺ channels as multi-ion pores. *J. Gen. Physiol.* 72:409-442.
- Hille, B., Woodhull, A.H., Shapiro, T. (1975) Negative surface charge near sodium channels of nerve; Divalent ions, monovalent ions, and pH. *Phil. Trans. R. Soc. London B* 270:301-318.
- Hodgkin, A.L. (1951) The ionic basis of electrical activity in nerve and muscle. *Biol. Rev. Cam. Phil. Soc.* 26:339-409.
- Hodgkin, A.L., Horowitz, P. (1960) The effect of sudden changes in ionic concentrations on the membrane potential of single muscle fibers. *J. Physiol.* 153:370-385.
- Hodgkin, A.L., Huxley, A.F. (1952a) Currents carried by Na⁺ and K⁺ ions through the membrane of the giant axon of Loligo. *J. Physiol.* 116:449-472.
- Hodgkin, A.L., Huxley, A.F. (1952b) The components of membrane conductance in the giant axon of Loligo. *J. Physiol.* 116:473-496.
- Hodgkin, A.L., Huxley, A.F. (1952c) The dual effect of membrane potential and sodium conductance in the giant axon of Loligo. *J. Physiol.* 116:497-506.
- Hodgkin, A.L., Huxley, A.F. (1952d) A quantitative description of membrane current and its application to conduction and excitation in nerve. *J. Physiol.* 117:500-544.
- Hodgkin, A.L., Huxley, A.F., Katz, B. (1952) Measurement of current-voltage relations in the membrane of the giant axon of Loligo. *J. Physiol.* 116L:424-448.
- Hodgkin, A.L., Katz, B. (1949) The effect of sodium ions on the electrical activity of the giant axon of the squid. *J. Physiol.* 108:37-77.
- Hodgkin, A.L., Keynes, R. (1955) The potassium permeability of a giant nerve fiber. *J. Physiol.* 128:61-88.

- Horn, R., Patlak, J. (1980) Single channel current from excised patches of muscle membranes. *Proc. Natl. Acad. Sci. U.S.A.* 77:6930-6935.
- Huganir, R.L., Schell, H.A., Raeker, E. (1979) Reconstitution of the purified acetylcholine receptor from T. californica. *FEBS Letters* 108:155-160.
- Hughes, M., Romey, G., Duval, D., Vincent, J., Lazdunski, M. (1982) Apamin as a selective blocker of the calcium-dependent potassium channel in neuroblastoma cells: Voltage clamp and biochemical characterization of the toxin receptor. *Proc. Natl. Acad. Sci. U.S.A.* 79:1308-1312.
- Huxley, A.F., Taylor, R.E. (1958) Local activation of striated muscle fibers. *J. Physiol.* 144:426-441.
- Jaimovich, E., Venosa, R.A., Shrager, P., Horowitz, P. (1976) Density and distribution of tetrodotoxin receptors in normal and detubulated frog sartorius muscle. *J. Gen. Physiol.* 67:399-416.
- Kostyuk, P.G. (1981) calcium channels in the neuronal membrane. *Biochim. Biophys. Acta* 650:128-150.
- Kostyuk, P.G., Krishtal, O.A. (1977) Effects of Ca^{2+} and Ca^{2+} chelating agents in the inward and outward currents in the membrane of molluscan neurones. *J. Physiol.* 270:569-580.
- Kostyuk, P.G., Mironov, S.L., Doroshenko, P.A. (1980) Energy profile of calcium channel in mollusk neuron membrane. *Doklad. Akad. Nauk. S.S.S.R.* 253:978-981.
- Kostyuk, P.G., Mironov, S.L., Doroshenko, P.A. (1982) Energy profile of the calcium channel in the membrane of molluscan neurons. *J. Membr. Biol.* 70:181-189.
- Krasne, S. (1978) Ion selectivity in membrane permeation. In: Physiology of Membrane Disorders, Chapter 12, edited by E. Andreoli, J. Hoffman and D. Fanestil, pp. 217-241. New York and London: Plenum Publishing Co.
- Krasne, S., Eisenman, G. (1973) In: Membranes: A Series of Advances, Vol. 2, edited by G. Eisenman, pp. 277-328. New York: Marcel Dekker.
- Krasne, S., Eisenman, G. (1976) The influence of molecular variations of ionophore and lipids on the selective ion permeability of membranes: Tetraactin and the methylation of nonactin-type carriers. *J. Membr. Biol.* 30:1-44.
- Krueger, B.K., French, R.J., Blaustein, M.B., Worley, J.F. (1982) Incorporation of Ca^{2+} -activated K^+ channels from rat brain into planar lipid bilayers. *Biophys. J.* 37:170a.

- Knueger, B., Worley, J.F., French, R.J. (1983) Sodium channels from rat brain incorporated into planar lipid bilayers. *Nature*, in press.
- Kuffler, S.W. (1960) Excitation and inhibition in single nerve cells. Harvey Lecture 1958-1959. New York: Academic Press.
- Latorne, R., Miller, C. (1983) Conduction and selectivity in potassium channels. *J. Membr. Biol.* 71:11-30.
- Latorne, R., Vergara, C., Hidalgo, C. (1982) Reconstitution in planar lipid bilayers of a Ca^{2+} -dependent K^+ channel from transverse tubule membranes isolated from rabbit skeletal muscle. *Proc. Natl. Acad. Sci. U.S.A.* 79:805-809.
- Lauger, P. (1943) Ion transport through pores. A rate theory analysis. *Biochim. Biophys. Acta* 311:423-441.
- Lauger, P., Stephan, W., Frehland, E. (1980) Fluctuations of barrier structure in ionic channels. *Biochim. Biophys. Acta* 602:167-180.
- Levitt, D.G. (1978) Electrostatic calculations for an ion channel. I. Energy and potential profiles and interactions between ions. *Biophys. J.* 22:209-219.
- Lew, V.L., Ferreira, H.G. (1978) Calcium Transport and the properties of a Ca-activated K channel in red cell membranes. In: Current Topics in Membranes and Transport, edited by F. Bonner and A. Kleinzeller, pp. 217-277. New York: Academic Press.
- Lux, H.D., Neher, E., Marty, A. (1981) Single channel activity associated with the calcium-dependent outward current in Helix pomatia. *Pflugers Arch.* 389:293-295.
- Magleby, K.L., Stevens, C.F. (1972a) The effect of voltage on the time course of end-plate currents. *J. Physiol.* 223:151-171.
- Magleby, K.L., Stevens, C.F. (1972b) A quantitative description of end-plate currents. *J. Physiol.* 223:173-197.
- Marmont, G. (1949) Studies on the axon membrane. *J. Cell Comp. Physiol.* 34:351-382.
- Marty, A. (1981) Ca^{2+} -dependent K^+ channels with large unitary conductance in chromaffin cell membranes. *Nature* 291:497-500.
- Marty, A. (1983) Blocking of large unitary calcium-dependent potassium currents by internal sodium ions. *Pflugers Arch.* 396:179-181.
- Maruyama, Y., Gallacher, D.V., Petersen, O.H. (1983) Voltage and Ca^{2+} -activated K^+ channel in basal-lateral acinar cell membranes of mammalian salivary gland. *Nature* 302:827-829.
- McLaughlin, S. (1977) Electrostatic potentials at membrane solution interfaces. In: Current Topics in Membranes and Transport, edited by F. Bonner and A. Kleinzeller, 9:71-145. New York: Academic Press.

- Meech, R.W. (1978) Ca^{2+} -dependent K^+ activation in nervous tissues. Annu. Rev. Biophys. Biogeng. 7:1-18.
- Meech, R.W. (1980) Ca^{2+} -activated K^+ conductances in molluscan nerve cells. In: Molluscan Nerve Cells: From biophysics to behavior. edited by J. Koester and J. Byrne, pp. 93-103. Cold Spring Harbor, NY: Cold Spring Harbor Laboratory.
- Meech, R.W., Standen, N.B. (1975) Potassium activation in Helix aspersa neurones under voltage clamp: A component mediated by calcium influx. J. Physiol. 249:211-239.
- Meech, R.W., Strumwasser, F. (1970) Intracellular Ca^{2+} injection activates K^+ conductance in Aplysia nerve cells. Fed. Proc. 29:834a.
- Meech, R.W., Thomas, R.C. (1980) Effect of measured calcium chloride injections on the membrane potential and internal pH of snail neurones. J. Physiol. 298:111-129.
- Methfessel, C., Böheim, G. (1982) The gating of single calcium-dependent potassium channels is described by an activation-blockage mechanism. Biophys. Struct. Mech. 9:35-60.
- Miller, C. (1982) Bis quaternary ammonium blockers as structural probes of the sarcoplasmic reticulum K^+ channel. J. Gen. Physiol. 79:869-891.
- Miller, C. (1983a) Integral membrane channels: Studies in model membranes. Physiol. Rev., in press.
- Miller, C. (1983b) Reconstitution of ion channels in planar bilayer membranes: A five year progress report. Comm. Mol. Cell Biophys., in press.
- Miller, C., Racker, E. (1976) Ca^{2+} -induced fusion of fragmented sarcoplasmic reticulum with artificial planar bilayers. J. Membr. Biol. 30:283-300.
- Moczydlowski, E., Latorre, R. (1983a) Saxitoxin and ouabain binding activity of isolated skeletal muscle membrane as indicators of surface origin and purity. J. Biol. Chem., in press.
- Moczydlowski, E., Latorre, R. (1983b) Gating kinetics of Ca^{2+} -activated K^+ channels from rat muscle incorporated into planar lipid bilayers: Evidence for two voltage-dependent Ca^{2+} binding reactions. J. Gen. Physiol., in press.
- Montal, M., Mueller, P. (1972) Formation of bimolecular membranes from lipid monolayers and a study of their electrical properties. Proc. Natl. Acad. Sci. U.S.A. 69:3561-3566.

- Moore, J.W., Blaustein, M., Anderson, C., Narahashi, T. (1967) Basis of tetrodotoxin's selectivity in blockage of squid axons. *J. Gen. Physiol.* 50:1401.
- Mudge, A.W., Leeman, S.E., Fishbach, G.D. (1979) Enkephalin inhibits release of substance P from sensory neurons in culture and decreases action potential duration. *Proc. Natl. Acad. Sci. U.S.A.* 76:526-530.
- Mueller, P., Rudin, D., Tien, H.T., Wescott, W. (1963) Methods for the formation of single bimolecular lipid membranes in aqueous solutions. *J. Phys. Chem.* 67:534-535.
- Mullins, L.J. (1961) The macromolecular properties of excitable membranes. *Ann. N.Y. Acad. Sci.* 94:390-404.
- Narahashi, T., Moore, J.W., Sobott, W.R. (1964) Tetrodotoxin blockade of Na^+ conductance increase in lobster giant axons. *J. Gen. Physiol.* 47:965-974.
- Neher, E., Sakmann, B. (1976) Single channel currents recorded from membranes of denervated frog muscle fibers. *Nature* 260:799-802.
- Neher, E., Steinbach, J.H. (1978) Local anesthetics transiently block currents through single acetylcholine-receptor channels. *J. Physiol.* 277:153-176.
- Neher, E., Stevens, C.F. (1977) Conductance fluctuations and ionic pores in membranes. *Annu. Rev. Biophys. Biog.* 6:345-381.
- Noble, D., Tsien, R.W. (1968) The kinetics and rectifier properties of the slow potassium current in cardiac purkinje fibres. *J. Physiol.* 195:185-214.
- Noda, M., Takahashi, H., Tanabe, T., Toyosato, M., Furutani, Y., Hirose, J., Asai, M., Inayama, S., Miyata, T., Numa, S. (1982) Primary structure of α -subunit precursor of Torpedo californica acetylcholine receptor deduced from cDNA sequence. *Nature* 299:793-797.
- Ohmori, H., Yoshida, S., Hagiwara, S. (1981) Single K^+ channel currents of anomalous rectification in cultured rat myotubes. *Proc. Natl. Acad. Sci. U.S.A.* 78:4960-4964.
- Oomura, Y., Oseki, S., Maeno, T. (1961) Electrical activity of a giant nerve cell under abnormal conditions. *Nature* 191:1265-1267.
- Palade, P.T., Barochi, R.L. (1977) Characteristics of the chloride conductance in muscle fibers of the rat diaphragm. *J. Gen. Physiol.* 69:325-342.
- Pallota, B.S., Magleby, K.L. (1983) Ca^{2+} dependence of open and shut interval distribution of Ca^{2+} -activated K^+ channels in cultured rat muscle. *Biophys. J.* 41:57a.

- Pallotta, B.S., Magleby, K.L., Barrett, J.N. (1981) Single channel recordings of Ca^{2+} -activated K^+ currents in rat muscle cell culture. *Nature* 293:471-474.
- Parsegian, A. (1969) Energy of an ion crossing a low dielectric membrane: Solution to four relevant electrostatic problems. *Nature* 221:844-846.
- Pauling, L. (1960) The nature of the chemical bond. Ithaca, New York: Cornell University Press.
- Pepper, K., Bradley, R.J., Dreyer, F. (1982) The acetylcholine receptor at the neuromuscular junction. *Physiol. Rev.* 62:1271-1340.
- Reuter, H., Stevens, C.F. (1980) Ion conductance and ion selectivity of potassium channels in snail neurones. *J. Membr. Biol.* 57:103-118.
- Reuter, H., Stevens, C.F., Tsien, R.W., Yellen, G. (1982) Properties of single calcium ion channels in cardiac cell culture. *Nature* 297:501-504.
- Robinson, A., Stokes, R.H. (1955) Electrolyte Solutions. New York: Academic Press.
- Rojas, E., Luxoro, M. (1963) Micro injection of trypsin into axons of squid. *Nature* 199:78-79.
- Roseblatt, M., Hidalgo, C., Vergara, C., Ikemoto, N. (1981) Immunological and biochemical properties of transverse-tubule membranes isolated from rabbit skeletal muscle. *J. Biol. Chem.* 256:8140-8148.
- Sakmann, B., Patlak, J., Neher, E. (1980) Single acetylcholine activated channels show burst-kinetics in presence of desensitizing concentrations of agonist. *Nature* 286:71-73.
- Schein, J.S., Colombini, M., Finkelstein, A. (1976) Reconstitution in planar lipid bilayers of a voltage-dependent anion-selective channel obtained from Paramecium mitochondria. *J. Membr. Biol.* 30:99-120.
- Schindler, H. (1979) Exchange and interactions between lipid bilayers at the surface of a liposome solution. *Biochim. Biophys. Acta* 555:316-336.
- Schindler, H., Rosenbusch, J.P. (1978) Matrix protein from E. coli outer membrane forms voltage-controlled channels in lipid bilayers. *Proc. Natl. Acad. Sci. U.S.A.* 75:3751-3755.
- Schindler, H., Quast, V. (1980) Functional ACh receptor from Torpedo marmorata in planar membranes. *Proc. Natl. Acad. Sci. U.S.A.* 77:3052-3056.

- Schwarz, W., Neumcke, B., Palade, P.T. (1981) K^+ current fluctuation in inward-rectifying channels of frog skeletal muscle. *J. Membr. Biol.* 63:85-92.
- Segel, J.H. (1974) Enzyme Kinetics. New York: John Wiley & Sons.
- Siegelbaum, S., Camardo, J.S., Kandel, E. (1982) Serotonin and cyclic AMP close single K^+ channels in Aplysia sensory neurons. *Nature* 299:413-417.
- Simon, W., Morf, W.E. (1973) Alkali cation specificity of carrier antibiotics and their behavior in bulk membranes. In: Membranes, A Series of Advances, Vol. 2, pp. 329-386. New York: Marcel Dekker.
- Standen, N.B., Stanfield, P.R. (1978) A potential- and time-dependent blockade of inward rectification in frog skeletal muscle by barium and strontium ions. *J. Physiol.* 280:169-191.
- Standen, N.B., Stanfield, P.R. (1980) Rubidium block and rubidium permeability of the inward rectifier of frog skeletal muscle fibers. *J. Physiol.* 304:415-435.
- Stanfield, P.R. (1970) The differential effects of tetraethylammonium and zinc ions on the resting conductance of frog skeletal muscle. *J. Physiol.* 209:231-256.
- Stefani, E., Chiarandini, D. (1982) Ionic channels in skeletal muscle. *Annu. Rev. Physiol.* 44:357-372.
- Sten-Knudsen, O. (1978) Passive transport processes. In: Membrane Transport in Biology, Vol. 1, edited by G. Giebisch, D.C. Tosteson, and H. Ussing, pp. 5-113. Berlin, Heidelberg and New York: Springer Verlag.
- Swenson, R.P. (1981) Inactivation of potassium current in squid axon by a variety of quaternary ammonium ions. *J. Gen. Physiol.* 77:255-271.
- Takenaka, T., Yamagishi, S. (1969) Morphology and electrophysiological properties of squid giant axons perfused intracellularly with protease solution. *J. Gen. Physiol.* 53:81-96.
- Takeuchi, A., Takeuchi, N. (1960) On the permeability of end-plate membrane during the action of transmitter. *J. Physiol.* 154:52-67.
- Tank, D.W., Miller, C., Webb, W.W. (1982) Isolated patch recording from liposomes containing functionally reconstituted chloride channels from Torpedo electroplax. *Proc. Natl. Acad. Sci. U.S.A.*, in press.
- Tsien, R.W. (1983) Calcium channels in excitable cell membranes. *Annu. Rev. Physiol.* 45:341-358.
- Vendisa, R.A., Hrowics, P. (1981) Density and apparent location of the sodium pump in frog sartorius muscle. *J. Membr. Biol.* 59:225-232.

- Vergara, C., Latorre, R. (1983) Kinetics of Ca^{2+} -activated K^+ channels from rabbit muscle incorporated into planar bilayers: Evidence for a Ca^{2+} and Ba^{2+} blockade. J. Gen. Physiol., in press.
- Walsh, G.V., Singer, J.J. (1983) Identification and characterization of a Ca^{2+} -activated K^+ channel in freshly dissociated vertebrate smooth muscle cells using the patch clamp technique. Biophys. J. 41:56a.
- Weigle, J.B., Barchi, R.L. (1982) Functional reconstitution of the purified Na^+ channel protein from rat sarcolemma. Proc. Natl. Acad. Sci. U.S.A. 79:3651-3655.
- Weight, F.F., Votava, J. (1970) Slow synaptic excitation in sympathetic ganglion cells: Evidence for synaptic inactivation of K^+ conductance. Science 170:755-758.
- White, M., Miller, C. (1981) Probes of the conduction process of a voltage-gated Cl^- channel from Torpedo electroplax. J. Gen. Physiol. 78:1-18.
- Wilmsen, U., Methfessel, C., Hanke, W., Boehm, G. (1983) Channel current fluctuation studies with solvent-free lipid bilayers using Neher-Sakmann pipettes. In: Physical Chemistry of Transmembrane Ion Motions, edited by C. Troyanowsky. Amsterdam: Elsevier, in press.
- Wong, B.S., Lecar, H., Adler, M. (1982) Single Ca^{2+} -dependent K^+ channels in clonal anterior pituitary cells. Biophys. J. 39:313-317.
- Woodhull, A.M. (1973) Ionic blockade of sodium channel in nerve. J. Gen. Physiol. 61:687-798.
- Zwolinski, B.I., Eyring, H., Reese, C.E. (1949) Diffusion and membrane permeability. J. Physiol. Chem. 53:1426-1453.

